Title
Regulation of crossover recombination in Caenorhabditis elegans

Author
Lee, Teresa Wei-sy

Publication Date
2014

Peer reviewed|Thesis/dissertation

Regulation of meiotic crossover recombination in *Caenorhabditis elegans*

by
Teresa Wei-sy Lee

A dissertation submitted in partial satisfaction of the
requirements for the degree of
Doctor of Philosophy
in
Molecular & Cell Biology
in the
Graduate Division
of the
University of California, Berkeley

Committee in charge:
Professor Barbara J. Meyer, Chair
Professor Doris Bachtrog
Professor W. Zacheus Cande
Professor Douglas E. Koshland, Jr.
Professor Jasper D. Rine

Fall 2014

Regulation of meiotic crossover recombination in *Caenorhabditis elegans*

by
Teresa Wei-sy Lee

Abstract

Regulation of meiotic crossover recombination in *Caenorhabditis elegans*
by
Teresa Wei-sy Lee

Doctor of Philosophy in Molecular & Cell Biology
University of California, Berkeley

Professor Barbara J. Meyer, Chair

Most eukaryotes reproduce sexually, which requires the creation of gametes through a specialized cell division known as meiosis. Crossover recombination is an essential feature of meiosis: in individuals, it facilitates proper chromosome segregation to prevent the formation of aneuploid embryos; within populations of species, it generates novel combination of alleles, to promote genetic diversity and remove deleterious mutations. Crossovers are initiated by programmed double-strand breaks (DSBs), which are a highly toxic form of DNA damage. Meiosis requires a cell to maintain an equilibrium between forming enough DSBs to generate an adequate number of crossovers, but not so many DSBs that some are left unrepaired. Therefore, recombination is subject to strict regulation at all levels, from DSB formation to crossover resolution via a certain mode of DSB repair. In this dissertation, I investigate crossover resolution pathways in the model nematode *C. elegans*.

To ensure the repair of all DSBs formed during meiosis, some organisms have multiple, compensatory repair pathways. Recent studies in *C. elegans* have identified two parallel pathways with partially overlapping resolvases, XPF-1 and MUS-81. Although XPF-1 and MUS-81 act interchangeably to resolve crossovers in wild-type animals, I show that each becomes required under conditions that threaten chromosome integrity, whether from exposure ionizing radiation or reducing the concentration of condensin, a complex required for proper chromosome structure. Conditions that independently do not create a requirement for a particular resolvase can, when combined, generate a requirement, indicating that these pathways are influenced by factors that act in a combinatorial manner. Although resolvase dependence in irradiated and condensin-depleted animals correlates with the extent of DNA damage, I demonstrate that the absolute number of DSBs is not solely responsible for invoking a requirement. Thus, DSB repair pathway choice may generate different classes of crossover depending on the DSB provenance or cellular reactions to the inducing condition. This work provides insights into the complexity of DSB repair pathways and establishes a framework for the future of pathway interactions, especially under circumstances that stress ordinary repair processes.

Table of Contents

Acknowledgements

The ideal scientist thinks like a poet and works like a bookkeeper.
E.O. Wilson

I would first like to thank my graduate advisor, Barbara Meyer, for helping me see the poetry in science. Her guidance, support, and patience have seemed inexhaustible over the years, and I truly appreciate her belief in my potential as a teacher and a scientist.

I would also like to thank my thesis committee – Doug Koshland, Zac Cande, Jasper Rine, and Doris Bachtrog – who have provided invaluable insight and helpful discussion throughout my graduate career.

I must acknowledge the role of public education in supporting my growth as a scholar, from kindergarten in North Carolina to graduate school in California. I would not be where I am today without the many teachers who cultivated my curiosity. I owe a special thanks to those at the North Carolina School of Science and Mathematics, where students were allowed to run a little wild in all the best ways.

I am indebted to the community of scholars and friends at the University of North Carolina at Chapel Hill. My undergraduate biology advisor, Shawn Ahmed, took a chance on a sophomore and opened my eyes to the beauty of *C. elegans* as a model system. Several members of the Ahmed lab – Mia Lowden, Julie Boerckel Hall, Theresa Zucchero Scocca, and Luda Shtessel – have helped me navigate the world of grad school and far beyond. My undergraduate poetry advisor, Michael McFee, was kind enough to indulge my interest in words and introduce me to the Lindanians, who always welcome me back home.

My lab mates have all in turn offered advice, an ear, or a shoulder, liberally administering coffee and yoga as needed. In particular, I'd like to thank Dave Mets and Aaron Severson for inducting me into the world of meiosis; Te-Wen Lo and Emily Crane for their indispensible mentorship; and Bayly Wheeler for being a bulwark against insanity. I am especially grateful for my co-conspirators, Will Kruesi and Christi Preston, who are friends first, and (the best of) coworkers second.

All my successes have relied on the encouragement and support I received from my parents – they had big dreams for me, and, in their wisdom, gave me every opportunity to discover my own. I cannot imagine my life in Berkeley without my friends, who, even scattered across the globe, saw me through the hard times and helped to celebrate the good times. And of course, I must thank Chris Laster, who has made the explorations of the past few years such a delight – you're still the light on the cell-phone &c.

Chapter 1

An introduction to meiosis & crossover recombination

Chapter 1.
An introduction to meiosis & crossover recombination

> You have made your way from worm to man, and much within you is still a worm.
>
> Friedrich Nietzsche, 1883

Crossover recombination is essential for meiosis – it facilitates the proper orientation of homologous chromosomes, which allows them to segregate away from each other. Crossovers are generated from double-strand breaks (DSBs), a particularly dangerous form of DNA damage. Meiosis requires a cell to maintain an equilibrium between forming enough DSBs to generate an adequate number of crossovers, but not so many DSBs that some are left unrepaired. Therefore, recombination is subject to strict regulation at all levels, from DSB formation to the mode of DSB repair. In this thesis, I have focused on understanding the repair pathways that resolve crossovers in the model nematode *C. elegans*. This introduction will review sexual reproduction, mechanisms of recombination, and the multiple layers of regulation influencing crossover resolution.

Sex: why bother?

> We do not even in the least know the final cause of sexuality; why new beings should be produced by the union of the two sexual elements, instead of by a process of parthenogenesis.
>
> Charles Darwin, 1861

<u>Sexual reproduction requires meiosis</u>

To Charles Darwin, the origins of sexual reproduction was a subject "hidden in darkness," but the popularity of sex is undisputed among eukaryotes. Despite the complications presented by this method of reproduction, most eukaryotes reproduce sexually (CHARLESWORTH 2006), generating gametes – eggs/ovules and sperm/pollen – through meiosis. This specialized cell division produces haploid daughter cells from diploid progenitors by DNA replication followed by two successive rounds of chromosome segregation (Figure 1) (PAGE and HAWLEY 2003). Most commonly, homologous chromosomes contributed from each parent are separated in the first division (meiosis I), and sister chromatids of each homolog are separated in the second division (meiosis II). The fusion of two haploid gametes, one contributed by each parent during sex, ensures that new embryos have a fully restored diploid genome.

Wilkins and Holliday have theorized that meiosis evolved from mitosis as a means of switching from a haploid to a diploid existence. After whole-genome duplication, cells must minimize recombination between non-homologous chromosomes to prevent recombination-generated damage. Homolog synapsis reduces the occurrence of ectopic pairing and subsequently, the erroneous genetic exchange between different chromosomes, while increasing the frequency of homologous recombination (WILKINS and HOLLIDAY 2009). Alternatively, Bernstein and colleagues have proposed the repair hypothesis: that sexual reproduction and the mechanisms of meiosis

evolved as a means of repairing damaged DNA, particularly DSBs (BERNSTEIN *et al.* 1987). They argue that crossover recombination is simply a by-product of the repair process, albeit a highly-beneficial one, since it generates novel combinations of alleles.

Regardless of why it evolved, meiosis itself presents many opportunities for error. Defects during meiosis result in chromosome non-disjunction and consequently, aneuploid gametes. Although some zygotic aneuploidy is tolerated in metazoans (most frequently involving the sex chromosomes), most autosomal aneuploidies cause severe developmental defects or embryonic lethality (HASSOLD and HUNT 2001). In human fetuses, only three complete autosomal trisomies survive until birth, and typically only individuals with trisomy 21 survive past infancy (HASSOLD and HUNT 2001).

The dire consequences of meiotic error make it puzzling as to why sexual reproduction and its obligatory meiosis has persisted among eukaryotes. Asexual reproduction would require less energy on the part of the organism and a simpler cell division process (OTTO and LENORMAND 2002). However, populations that reproduce asexually are essentially clonal, such that offspring are genetically identical to their parent. In asexually reproducing populations, random mutations are the only source of genetic variation (JUDSON and NORMARK 1996). Sexual reproduction thrives because it promotes the genetic diversity required for adaptation via natural selection (FELSENSTEIN 1974; GESSLER and XU 1999; GODDARD *et al.* 2005). Asexual eukaryotic populations occasionally arise from sexually-reproducing ancestors, but these populations only persist for evolutionarily short spans of time (MARK WELCH *et al.* 2004). One exception that might prove the rule is the Class Bdelloidea, or bdelloid rotifers, freshwater invertebrates in which no males and no meiosis has been discovered (MARK WELCH and MESELSON 2000). But bdelloid rotifers do undergo massive horizontal gene transfer, a mode of genetic exchange that is very rare among metazoans (GLADYSHEV *et al.* 2008). Gladyshev and colleagues theorize that the amounts of horizontal gene transfer present among rotifer populations equals the amount of genetic exchange in sexually reproducing populations, allowing bdelloid rotifers to remain both asexual and evolutionarily viable.

Meiosis provides two sources of genetic variation

Meiosis creates diversity in two ways. First, the independent assortment of homologous chromosomes ensures that each zygote will receive a combination of maternal and paternal chromosomes. Second, crossover recombination produces an exchange of genetic material between each maternal and paternal homolog that reassorts allelic combinations along a chromosome, which combines favorable alleles and prevents the accumulation of deleterious alleles (H.J. 1932; FELSENSTEIN 1974) (Maynard-smith 1968, Muller 1964). Crossovers also provide a physical connection between homologous chromosomes (cytologically visible as a chiasma), which permits their proper segregation in meiosis I (PAGE and HAWLEY 2003).

After DNA replication, homologous chromosomes must recognize each other and pair (Figure 1). Homologs maintain a lengthwise close association through the formation of a protein matrix known as the synaptonemal complex (KLECKNER 2006). Crossover recombination occurs within this context, creating physical linkages (called chiasmata) that, along with sister-chromatid cohesion, keeps homologs together after synaptonemal complex disassembly at the end of prophase

I. Chiasmata provide resistance to opposing spindle forces, which facilitates the correct orientation of homologs along the metaphase I plate (OSTERGREN 1948; PETRONCZKI *et al.* 2003).

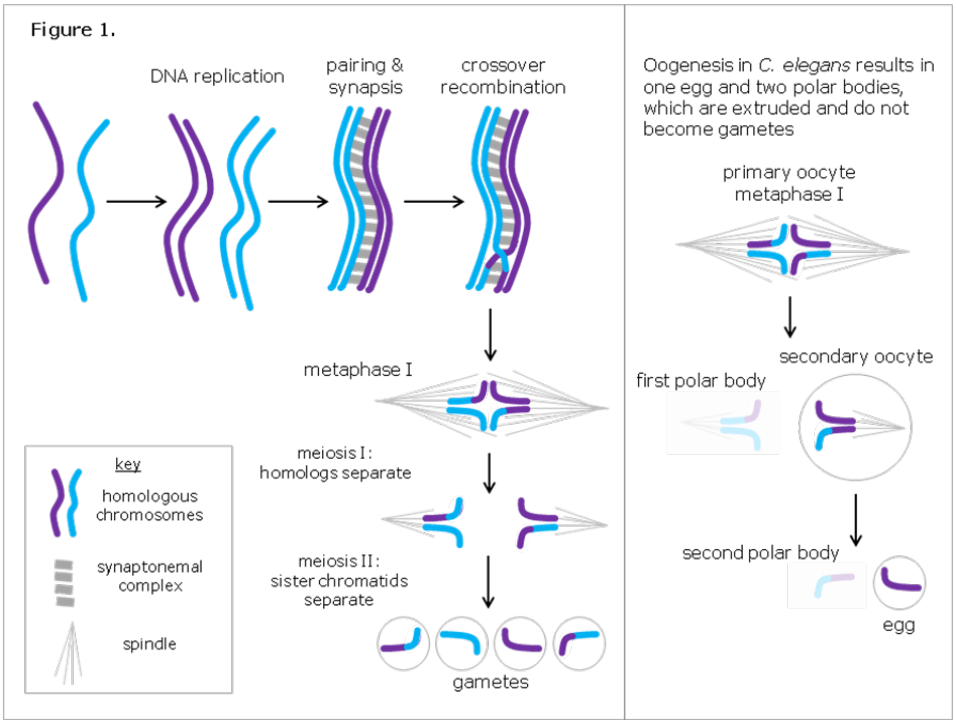

Figure 1. Summary of meiotic events in *C. elegans*. One pair of homologous chromosomes is shown, with the maternal chromosome in blue and the paternal chromosome in purple. In meiotic prophase I, homologs replicate to become 4N, then undergo pairing and synapais. Synapsed chromosomes are held together in close association by the synaptonemal complex (gray bars). Within this context, crossover recombination occurs, which allows chromosome to reorganize around the site of crossover and correctly orient on the metaphase I plate. Homologs will separate away from each other during anaphase I, and sister chromatids will separate away from each other during anaphase II. The inset demonstrates segregation during oogenesis, in which only chromatid is segregated to a gamete, and the other three are discarded as polar bodies.

Crossovers thus provide two important benefits: they allow individuals to segregate homologs properly during meiosis, and they allow populations to generate diversity, which facilitates evolution by natural selection and the culling of harmful mutations. The importance of crossovers for chromosome segregation is illustrated by the fact that many human aneuploidies have aberrations in crossover number or distribution (LAMB *et al.* 2005). A successful meiosis therefore requires that crossovers be evenly dispersed throughout the genome such that all chromosomes or chromosome arms receive at least one crossover. Organisms could easily ensure that each homolog pair receives a crossover by forming them in excess, but crossovers placed too close to chromosome ends also has an adverse effect on chromosome segregation (KOEHLER *et al.* 1996; ROCKMILL *et al.* 2006). Since crossovers are initiated from programmed DSBs (KEENEY *et al.* 1997; NEALE and KEENEY 2006), the production of excess DSBs to ensure adequate crossover numbers could be a potential source of genome instability (KOLODNER *et al.* 2002). Therefore, crossover resolution is

carefully regulated by a complex network of DSB repair pathways(LEMMENS and TIJSTERMAN 2011; KOHL and SEKELSKY 2013).

Mechanism of meiotic recombination

> Nevertheless, three aspects of recombination in meiosis remain completely obscure: first the specificity of pairing of homologues; second, the control of the initiation of genetic recombination; and third, the factors governing the interference between crossovers along the length of bivalents.
>
> Robin Holliday, 1977

Since Holliday wrote his review a few decades ago, the field has made significant progress towards addressing these points. Pairing is reviewed in detail in BHALLA and DERNBURG 2008, and the DSB initiation and crossover interference will be addressed in the remainder of this chapter.

Although DSBs are necessary for crossover formation, they pose a serious threat to meiotic cells. DSBs are a highly toxic form of DNA damage: a single unrepaired break can activate cell-cycle arrest or induce cell death (BENNETT *et al.* 1993, 1996). To preclude this possibility, DSB initiation and resolution are carefully regulated by coordinated pathways that ensure the repair of all DSBs by the end of meiosis (KOHL and SEKELSKY 2013). The molecular details of meiotic DSB repair have best been described in *S. cerevisiae*, which is summarized in this section (Figure 2.)

<u>DSB initiation and early processing</u>

DSBs are catalyzed early in prophase I by Spo11, a conserved, topopisomerase-like endonuclease (KEENEY *et al.* 1997; NEALE and KEENEY 2006). The distribution of DSBs across the genome necessarily affects the distribution of crossovers, and reflects an early manifestation of crossover regulation. Control of DSB location can be both local (through DNA sequence motifs, chromatin accessibility, or recruitment of specific pro-DSB factors) or global (by higher-order chromosome structure or chromosomal landmarks like centromeres or telomeres) (DE MASSY 2013). A high-throughput study of all recombination events during an *S. cerevisiae* meiosis revealed that DSB placement may be controlled such that one DSB could prevent the formation of another nearby DSB (MANCERA *et al.* 2008). In humans and mice, the histone methyltransferase PRDM9 globally controls nearly all DSB formation by promoting the recruitment of SPO11 to specific, rapidly evolving DNA sequence motifs (BAUDAT *et al.* 2013).

DSB formation is also temporally controlled to maximize productive repair into crossover outcomes (PADMORE *et al.* 1991; CERVANTES *et al.* 2000). We discuss a temporal feedback mechanism that regulates DSB formation in the crossover assurance section of this chapter. After formation, DSBs are resected at their 5' end by the MRX complex, consisting of Mre11, Rad50, and Xrs2 (KEENEY 2001). Resection yields a 3' single-stranded DNA overhang that is coated by RPA. RPA is then replaced, by the action of Rad51 and the Rad55-Rad57 complex, with two RecA homologs, Rad51 and Dmc1. These proteins form a nucleoprotein filament that searches for homologous regions of the genome and facilitates the single-end invasion of duplex DNA

(SHINOHARA and SHINOHARA 2004). Both Rad51 and Dmc1 are essential for meiosis, but Dmc1 is meiosis-specific (BISHOP 1994). Recent work has revealed that Rad51 acts as an accessory factor to stimulate the strand-exchange activity of Dmc1(CLOUD *et al.* 2012; LAO *et al.* 2013).

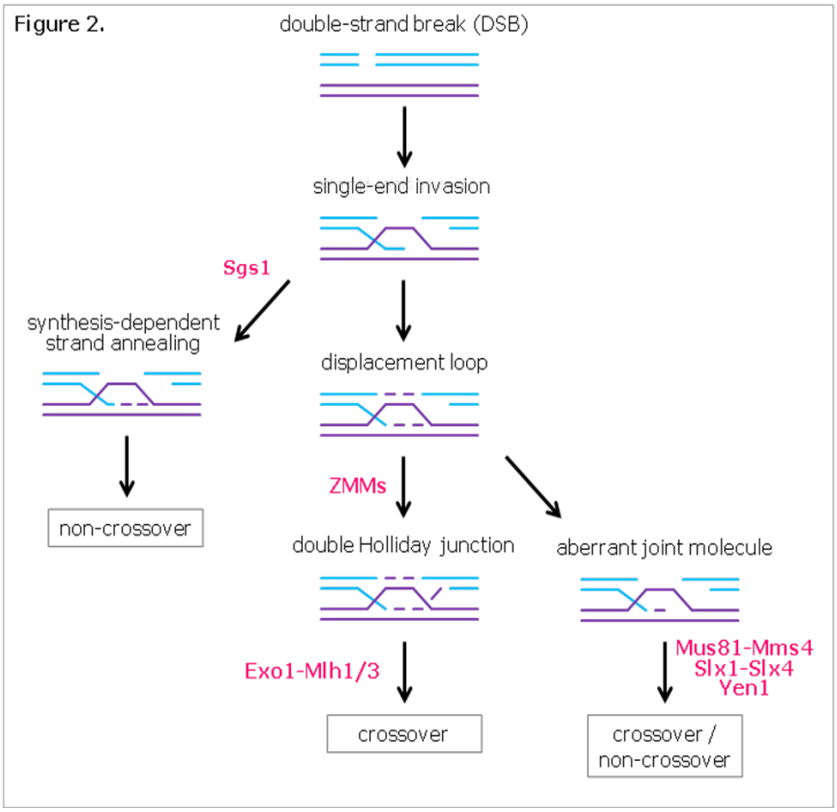

Figure 2. Model of meiotic DSB repair in *S. cerevisiae*. Two homologs are shown in blue and purple; sister chromatids are present at this stage, but are not shown. After DSB formation, one 3' end invades the other duplex DNA to form a single-end invasion intermediate. This can be dissolved by the Sgs1 helicase, to be repaired as a non-crossover via synthesis-dependent strand annealing. Alternatively, the single-end invasion intermediate can be transitioned into a displacement loop intermediate (D-loop). D-loops can be stabilized into double Holliday junctions by the ZMM family of proteins, which are exclusively resolved into crossovers by the Exo1-Mlh1/3 resolvase. In wild-type cells, a minority of D-loops are shunted to a pathway where they are resolved as either crossovers or non-crossovers by Mus81-Mms4, Slx1/4, or Yen1.

<u>DSB repair intermediates can form both non-crossovers and crossovers</u>

The invading 3' end will anneal to the complementary donor strand, displacing the other strand to form a displacement loop (HEYER *et al.* 2010). Several components of the synaptonemal complex (Red1, Hop1, Mek1, Pch2, Rad17) ensure that the homologous chromosome is invaded, rather than the sister chromatid (SCHWACHA and KLECKNER 1997; THOMPSON and STAHL 1999; ZIERHUT *et al.* 2004; CARBALLO *et al.* 2008). This single-end invasion intermediate can be sorted into both crossover and non-crossover intermediates by the Bloom helicase ortholog Sgs1 (BAUDAT and DE MASSY 2007; ZAKHARYEVICH *et al.* 2012; DE MUYT *et al.* 2012). Non-crossovers are generated by

Sgs1-mediated disassembly of the single-end invasion intermediate. After dissolution, repair proceeds by synthesis-dependent strand annealing, where the invading 3' strand captures the end on the other side of the DSB, and the remaining nicks are ligated (ALLERS and LICHTEN 2001; HEYER *et al.* 2010).

Crossovers are resolved through double Holliday junctions

Alternatively, the second DSB end can be captured and used to prime another round of DNA synthesis, which will generate a double Holliday junction (SCHWACHA and KLECKNER 1995). The ZMM family of conserved meiotic proteins – comprised of Zip1/Zip2/Zip3/Zip4, Msh4/Msh5, and Mer3 – stabilizes a subset of single-end invasion intermediates to allow replicative repair into a double Holliday junction (LYNN *et al.* 2007). At this point, multiple endonucleases can cleave the double Holliday junction in different orientations to create a crossover, with each homolog in possession of a newly-recombinant chromatid. Although it is formally possible to generate a non-crossover from cleavage of a double Holliday junction, current models place the non-crossover decision earlier in the pathway, at the step of single-end invasion dissolution (ALLERS and LICHTEN 2001; HUNTER and KLECKNER 2001; BISHOP and ZICKLER 2004; BÖRNER *et al.* 2004; MARTINI *et al.* 2006).

Multiple crossover resolvases function during meiosis

Although prokaryotic Holliday junction resolvases have been identified for decades, the discovery of eukaryotic resolvases was hindered by a focus on molecules that mechanistically resembled their prokaryotic counterparts (SCHWARTZ and HEYER 2011). Several investigations identified potential resolvases with *in vitro* Holliday junction endonuclease activities: Mus81-Mms4, Slx1-Slx4, and Yen1 (BODDY *et al.* 2001; IP *et al.* 2008; FEKAIRI *et al.* 2009). However, these resolvases are only responsible for about 20% of crossovers in *S. cerevisiae*, making it evident that the primary crossover resolvase was still to be discovered (KALIRAMAN *et al.* 2001; ARGUESO *et al.* 2004; IP *et al.* 2008). Evidence that these enzymes function as crossover resolvases in other organisms was incomplete, and suggested that a greater diversity of crossover-resolving activities exist between organisms (SCHWARTZ and HEYER 2011). *S. pombe* lack both Msh4-Msh5, and rely almost entirely on Mus-81-Mms4 to generate crossovers (BODDY *et al.* 2001; SMITH *et al.* 2003). Animals with mutations in the *Drosophila* Slx4 homolog mus312 have drastically reduced crossovers (YILDIZ *et al.* 2002). In mouse, mutations in the Mus81 gene cause meiotic defects, although *Mus81*-deficient mice are fertile and viable (HOLLOWAY *et al.* 2008). In *C. elegans*, *mus-81* mutants have no apparent meiotic defect, though *slx-4* mutants have reduced numbers of crossovers (SAITO *et al.* 2009).

Insights into the true complexity of DSB repair networks came from two studies that addressed the early role of Sgs1 in meiotic DSB repair (ZAKHARYEVICH *et al.* 2012; DE MUYT *et al.* 2012). When Sgs1 is available to dissolve single-end invasion intermediates, Mus81-Mms4, Slx1-Slx4, and Yen1 are mostly dispensable for efficient DSB resolution. However, when Sgs1 is absent, repair of strand invasion intermediates is accomplished by Mus-81-Mms4, which creates crossovers and non-crossovers in equal numbers. Yen1 is a cryptic resolvase whose activity is only evident in the

absence of Mus81-Mms4. Similarly, the activity of Slx1-Slx-4 is only evident in the absence of Yen1, Mus81-Mms4, and the primary pathway (ZAKHARYEVICH *et al.* 2012; DE MUYT *et al.* 2012).

With the early function of Sgs1 now clarified, Zakharyevich and colleagues discovered a fourth crossover resolvase, Mlh1-Mlh3, the only resolvase that exclusively forms crossovers from double Holliday junctions (ZAKHARYEVICH *et al.* 2012). Mlh1-Mlh-3 was known to localize to crossovers in mammals and was required for crossover formation in both mouse and *S. cerevisiae* (KOLAS and COHEN 2004). Working with the Exo1 nuclease, Mlh1-Mlh3 was shown to specifically promote a crossover outcome (ZAKHARYEVICH *et al.* 2012). In the quintuple mutant – *mlh3 mms4 sgs1 slx4 yen1* – crossovers are completely abrogated, indicating that when Sgs1 is present, Exo1-Mlh1-Mlh3 acts as the primary crossover resolvase (ZAKHARYEVICH *et al.* 2012). Together, these studies have exposed a robust hierarchical relationship of joint molecular resolution pathways. In wild-type cells, each pathway is subject to regulatory specialization that permits the efficient resolution of DSB repair intermediates. But in conditions that could prevent timely DSB repair, alternative crossover resolution pathways have the capacity to repair most DSBs and ensure cell survival.

Layers of crossover regulation

> …understanding the mechanism of interference remains an unrequited passion of many meiosis aficionados…
>
> Anne Villeneuve & Kenneth Hillers, 2001

It was clear from the creation of the first genetic map that crossovers are not randomly distributed (STURTEVANT 1913). In Thomas Hunt Morgan's fly room at Columbia University, Alfred Sturtevant and H.J. Muller were the first to notice that the presence of one crossover decreased the likelihood of another crossover occurring nearby – a phenomenon they called crossover interference (STURTEVANT 1915). In the century since their discovery, we have come to understand that the regulation of crossovers manifests itself in three ways. First, crossover assurance allows each homolog pair to receive its obligate crossover. Second, crossover homeostasis keeps crossover levels constant despite fluctuations in DSB number. Third, crossover interference ensures that crossovers do not form too near each other and maintain a relatively even distribution across chromosomes. It remains to be seen whether these phenomena are independent processes or whether they share regulatory mechanisms.

<u>Crossover assurance</u>

The majority of organisms create fairly few crossovers relative to their chromosome number, which, if crossovers were randomly distributed, makes the formation of one crossover per chromosome unlikely as predicted by a Poisson distribution. This observation led to the hypothesis of crossover assurance, a mechanism that specifically ensures the formation of an obligate crossover on each homolog pair (Jones 1984). It is unclear whether crossover assurance is a consequence of interference, or whether it has an independent mechanism. Work in *S. cerevisiae* supports the idea that

obligate crossover is not solely determined by a crossover interference mechanism – Shinohara and colleagues identified Spo16 mutants that retain interference but lose the requirement for an obligate crossover, indicating that these processes are functionally distinct (SHINOHARA *et al.* 2008). Conversely, a study in mice suggests that a crossover interference mechanism is fully able to account for obligate crossover formation (DE BOER *et al.* 2007).

In *C. elegans*, the formation of a single DSB on one homolog pair is sufficient to guarantee crossover formation (ROSU *et al.* 2011). When no other inhibitory DSBs are nearby, a crossover is the preferred outcome of DSB repair – therefore, an obligate crossover can be achieved by ensuring that each homolog pair receives at least one DSB (ROSU *et al.* 2011). Three studies have revealed another aspect of crossover assurance, which uses feedback loops to regulate DSB formation in response to crossover formation. The *C. elegans* meiotic proteins DSB-1 and DSB-2 are required for DSB formation (ROSU *et al.* 2013; STAMPER *et al.* 2013). By associating with chromatin, DSB-1 and DSB-2 maintain a permissive state for DSB initiation until all chromosomes have received a crossover-competent repair intermediate, at which point they are removed from chromosomes to signal a cessation of DSB formation. A study in *S. cerevisiae* examined global DSB formation in cells defective for ZMM components, a family of pro-crossover molecules that are also required for synaptonemal complex assembly (THACKER *et al.* 2014). Although ZMM proteins were thought to function after DSB formation, Thacker and colleagues discovered that they actually limit DSB formation in wild-type cells. Similar to the *C. elegans* studies, this work suggests that when chromosomes have successfully engaged their homolog (whether by synapsis or through crossover-competent repair intermediates), they undergo a ZMM-mediated change that stops DSB formation (THACKER *et al.* 2014). Taken together, these data indicate that crossover assurance mechanisms allow cells to monitor the formation of crossover-competent repair intermediates to ensure that each chromosome receives a sufficient number of DSBs; once that condition is met, cells subsequently limit DSB formation through changes in chromatin or chromosome structure.

Crossover homeostasis

All organisms studied to date create more DSBs than they do crossovers, although the ratio varies widely by species (MARTINEZ-PEREZ and COLAIÁCOVO 2009). Therefore, some level of crossover regulation must also occur after DSB formation. As discussed above, the decision between a crossover or noncrossover outcome occurs early in DSB repair. Noncrossovers are formed in a nuclease-independent manner by displacement of the invading strand through a helicase activity: Sgs1 in *S. cerevisiae* and RTEL-1 or perhaps HIM-6 in *C. elegans* (BARBER *et al.* 2008; YOUDS *et al.* 2010; ZAKHARYEVICH *et al.* 2012; DE MUYT *et al.* 2012; SCHVARZSTEIN *et al.* 2014).

To probe the crossover/noncrossover ratio in *S. cerevisiae*, Martini and colleagues used an allelic series of *spo11* hypomorphs to determine whether crossover number would be reduced in proportion to DSBs. Although they observed a dramatic reduction in DSBs, crossover number was maintained at the expense of non-crossovers – a phenomenon they called crossover homeostasis(MARTINI *et al.* 2006). Two studies suggest that homeostasis may act as a buffer to limit the number of cytologically-marked crossovers when organisms have been exposed to conditions that create artificially high numbers of DSBs. Both mice overexpressing Spo11 and *C. elegans*

exposed to ionizing radiation retain wild-type numbers of cytologically-marked crossovers (YOKOO *et al.* 2012; COLE *et al.* 2012). However, at least in *C. elegans*, not all crossovers are marked cytologically, leaving the possibility that assurance (like interference) mediates only a subset of crossovers (YOUDS *et al.* 2010; YOKOO *et al.* 2012). Additionally, in *C. elegans*, a recent study suggests that prolonging the DSB-formation period creates more DSBs without creating more crossovers (Ericca Stamper, personal communication). It is not known whether homeostasis represents a distinct mode of crossover regulation, since it could be an outcome of two mechanisms that mediate crossover interference and the formation of an obligate crossover. Conversely, the implementation of homeostasis may allow cells to promote the formation of an obligate crossover, without necessitating a separate crossover assurance mechanism.

Two classes of crossover exist: interfering and non-interfering

Over the years, several models have attempted to explain how crossover interference is communicated along the lengths of chromosomes. However, earlier models did not account for the two types of crossover that are now known to exist: those that undergo interference (class I) and those that do not undergo interference (class II). Before class II crossovers were first proposed, results in different organisms presented conflicting evidence for researchers trying to assemble a unified model of recombination. For example, the ZMM components Msh4 and Msh5 were known to be pro-crossover factors in *S. cerevisiae*, and yet Msh4 mutants still retain 30-50% of wild-type crossover levels (ROSS-MACDONALD and ROEDER 1994; HOLLINGSWORTH *et al.* 1995; POCHART *et al.* 1997). However, loss of Msh4 and Msh5 in *C. elegans* eliminates all crossovers (ZALEVSKY *et al.* 1999; KELLY *et al.* 2000), while crossovers in *S. pombe* are completely independent of Msh4-Msh-5 and instead dependent on Mus81-Mms4 homologs (BODDY *et al.* 2001; SMITH *et al.* 2003).

To account for these differences between organisms, Zalevsky and colleagues proposed a dual-pathway model: one pathway utilizes Msh4-Msh5 and other ZMM components to produce class I interfering crossovers, while the second pathway produces class II non-interfering crossovers independent of Msh4-Msh-5 (ZALEVSKY *et al.* 1999). In support of this model, mutants lacking both pathways have fewer crossovers than mutants only lacking one of the two pathways (SANTOS *et al.* 2003; BERCHOWITZ *et al.* 2007). Additionally, crossovers that remain in mutants lacking ZMM components are non-interfering (NOVAK *et al.* 2001; BÖRNER *et al.* 2004; HIGGINS *et al.* 2004; ARGUESO *et al.* 2004; LU *et al.* 2008), while those that remain in mutants lacking Mus81-Mms4 are interfering (SANTOS *et al.* 2003; BERCHOWITZ *et al.* 2007). Finally, statistical analyses of crossover distributions in some organisms also supports a model in which both interfering and non-interfering crossovers exist(COPENHAVER *et al.* 2002; GETZ *et al.* 2008). *S. cerevisiae, Arabidopsis,* mice, and humans have both crossover classes. In these systems, the primary pathway for crossover formation is the interfering pathway, which accounts for 60-90% of all crossovers, depending on the system (BERCHOWITZ and COPENHAVER 2010). Conversely, *S. pombe* only has non-interfering crossovers, and all crossovers in this organism are dependent on Mus81-Eme1 (CROMIE and SMITH 2007). At the other extreme, untreated wild-type *C. elegans* has only interfering crossovers, which will be discussed in depth below.

Multiple models for crossover interference

Crossover interference requires that one crossover is able to communicate its location in *cis* to inhibit the formation of other crossovers nearby. Interference could be related to the mechanisms that ensure an obligate crossover, but the underlying basis for both remains largely mysterious. Early models proposed that interference was transmitted by the synaptonemal complex, which is assembled between homologs in a two-step process (PAGE and HAWLEY 2003). Before synapsis, two lateral elements (also known as axial elements) are formed on each homolog. Central element components are then loaded between homologs in a zipper-like structure, which in *S. cerevisiae*, occurs at the same time as DSB initiation. In mice and *S. cerevisiae*, DSBs are required for synaptonemal complex formation (ROEDER 1997; BAUDAT *et al.* 2000; ROMANIENKO and CAMERINI-OTERO 2000), while in *Drosophila* and *C. elegans*, chromosome synapsis occurs independent from DSB formation (DERNBURG *et al.* 1998; MCKIM and HAYASHI-HAGIHARA 1998; LIU *et al.* 2002). Although components of the synaptonemal complex have undergone rapid sequence divergence, a striking conservation exists for overall synaptonemal structure among eukaryotes (ZICKLER and KLECKNER 1999). In support of the synaptonemal complex mediating interference, *S. cerevisiae* cells lacking components of the central element also lack crossover interference (NOVAK *et al.* 2001; BÖRNER *et al.* 2004; HIGGINS *et al.* 2004; ARGUESO *et al.* 2004; LU *et al.* 2008). Additionally, two organisms that do not have synaptonemal complexes also lack interfering crossovers: *Aspergillus nidulans* and *S. pombe* (EGEL-MITANI *et al.* 1982; MUNZ 1994).

Further support comes from experiments performed in *C. elegans,* which has holocentric chromosomes that can stably propagate end-to-end chromosome fusions (HILLERS and VILLENEUVE 2003). Interference is mostly maintained along fusion chromosomes that have an unbroken synaptonemal complex, even though these chromosomes can be up to three times the length of a normal chromosome. In male *C. elegans*, a fusion chromosome that consists of two autosomes on either end of the X chromosome will synapse with each terminal autosome. Since males only have one X, the central region of the fusion chromosome will remain unpartnered and thus break the continuity of the synaptonemal complex. On this fusion chromosome, each autosome will receive one crossover, indicating that interference is not transmitted across the center of the fusion, where there is no synapsis (HILLERS and VILLENEUVE 2003). A recent study has depleted a central element by attenuated RNAi in a manner that permits a limited amount of synaptonemal complex to form but weakens the overall structure, causing an increase in the number of cytologically-marked crossovers (LIBUDA *et al.* 2013). This work specifically implicates central element proteins as some of the mediators of interference.

However, some studies in *S. cerevisiae* provide evidence that crossover interference is present before formation of the synaptonemal complex. Synapsis initiation sites have a non-random distribution that indicates they interfere with each other, and these are present in cells that have yet to form synaptonemal complexes (FUNG *et al.* 2004). This observation corresponds with a genome-wide analysis of DSB repair outcomes that discovered interference also operates at the level of DSB formation (MANCERA *et al.* 2008). In addition, mutations that prevent the loading of central elements in the synaptonemal complex reduce crossover number without reducing interference between the remaining crossovers (SHINOHARA *et al.* 2008). This situation is also true in mice, where disruption

of synaptonemal complex components did not prevent crossover interference between cytologically-marked crossovers (DE BOER *et al.* 2007).

An alternative model for interference relies on the intrinsic mechanical properties of the chromosome itself. Kleckner and colleagues argue that chromosomes are under mechanical stress from interactions between chromatin, chromosome structure proteins, and axial element components (KLECKNER *et al.* 2003). If regions subject to high stress promote crossover formation, the formation of a crossover would release stress at that site. A local change in stress would cause a natural redistribution for a certain distance along the length of the chromosome, both communicating the formation of a crossover and inhibiting any nearby crossovers.

The placement of DSBs is also regulated

We have been discussing interference only in terms of crossovers, but earlier recombination intermediates also influence the distribution of their neighbors. There is evidence that DSBs may also prevent the formation of nearby DSBs, and therefore play a role in shaping the overall crossover landscape (BERCHOWITZ and COPENHAVER 2010). Like crossovers, DSB placement is not random, as they tend to be less prevalent near centromeres and telomeres (ZENVIRTH *et al.* 1992; BAUDAT and NICOLAS 1997; GERTON *et al.* 2000). Ectopic insertion of a region that often receives a DSB (a DSB hotspot) can reduce the formation of a DSB in nearby regions (OHTA *et al.* 1999).

A study using high-resolution microarray analysis in *S. cerevisiae* uncovered genome-wide correlations between all DSB repair outcomes. The authors saw that non-crossovers exert a positive interference on nearby crossovers, strongly implying that some amount of interference occurs on their common precursor, the DSB (MANCERA *et al.* 2008). Researchers have also demonstrated that, at a single DSB initiation site, DSBs only ever occurred once per chromatid pair, which they assume to be sister chromatids (ZHANG *et al.* 2011). They most commonly observed one DSB occurring per all four chromatids, which indicates the presence of a DSBs communicates a *trans*-inhibition to prevent DSB formation on the other homolog. Additionally, in *C. elegans*, conditions known to alter crossover distribution also correspondingly alter DSB distribution (METS and MEYER 2009).

In mammals, several groups identified a single component able to enact genome-wide changes in DSB distribution, and therefore crossover distribution (COOP *et al.* 2008; GREY *et al.* 2009; PARVANOV *et al.* 2009). The histone methyltransferase PRDM9 contains a DNA-binding zinc finger domain that recognizes specific DNA motifs (MYERS *et al.* 2010). PRDM9 catalyzes the addition of a tri-methyl group to H3K4 in regions of the genome near its DNA-binding targets, which recruit or activate SPO11 to form DSBs at those locations (HAYASHI *et al.* 2010). In support of this, changes to PRDM9's zinc finger domain created correlating changes in genome-wide DSB activity, H3K4me3 levels, and CO distribution (GREY *et al.* 2011). In mice lacking PRDM9, DSBs still occur, but their distribution is severely altered towards promoters and other regions with PRDM9-independent H3K4me3 (BRICK *et al.* 2012).

Recombination in *C. elegans*

> As a more long term possibility, I would like to tame a small metazoan organism to study development directly…
>
> Sydney Brenner, 1963

A few years after he wrote those words, Sydney Brenner chose the nematode *C. elegans* to use as a model for genetic, developmental, and molecular studies (BRENNER 1974). This animal has made an effective system to understand the dynamics of meiosis and meiotic DSB repair: partly because its short generation time and ease of maintenance allows efficient forward and reverse genetic screening to identify new meiotic components, and partly because its sequenced genome permits an in-depth analysis of known meiotic factors. Additionally, the germlines of *C. elegans* function like a production line with meiocytes traveling from the distal end of the gonad to the proximal end as they developmentally progress through the stages of prophase I. This feature is particularly useful for cytological studies, as it creates a snapshot of multiple meiotic stages within one fixed specimen.

Unique features of *C. elegans* meiosis

Meiosis in *C. elegans* has several unique features. First, unlike in *S. cerevisiae*, plants, and mammals, the initiation of synapsis can occur without DSB formation (which is also the case in *Drosophila*) (DERNBURG *et al.* 1998; MCKIM and HAYASHI-HAGIHARA 1998), permitting the functional separation of components required for synaptonemal complex formation and those required for recombination. Second, chromosomes are holocentric, which necessitates some differences in segregation machinery compared to monocentric organisms (HERMAN *et al.* 1982). Finally, recombination in *C. elegans* oocytes undergoes an extreme form of crossover interference, in which only one crossover forms on each homolog pair (BARNES *et al.* 1995; MENEELY *et al.* 2002; NABESHIMA *et al.* 2004; HAMMARLUND *et al.* 2005). In wild-type animals, this crossover is cytologically marked by COSA-1, a conserved meiotic protein that shares homology with cyclin (YOKOO *et al.* 2012).

Crossovers tend to form on both terminal thirds of a chromosome, dividing it into a long and a short arm (ALBERTSON and THOMSON 1993; BARNES *et al.* 1995; ROCKMAN and KRUGLYAK 2009). As meiocytes enter late prophase I, chromosomes are remodeled around the site of crossover into a highly condensed cruciform structure (NABESHIMA *et al.* 2004). One feature of diakinesis reorganization is that at the end of prophase I, certain synaptonemal complex components are specifically maintained on the short arm and others are removed from the long arm. This differential localization protects the association of sister chromatids and ensures that homologs segregate away from each other (MARTINEZ-PEREZ and COLAIÁCOVO 2009; SEVERSON *et al.* 2009).

Two crossover resolving pathways in *C. elegans*

In *C. elegans*, three recent studies have identified two parallel and partially redundant pathways responsible for crossover formation in wild-type animals – one dependent on MUS-81 and

one dependent on XPF-1 (AGOSTINHO *et al.* 2013; O'NEIL *et al.* 2013; SAITO *et al.* 2013). XPF-1 is a homolog of *Drosophila* MEI-9*,* which is required for most meiotic crossovers in *Drosophila* (SEKELSKY *et al.* 1995). The endonuclease SLX-1 had previously been shown to be required for some meiotic crossovers in *C. elegans*, and these studies demonstrated that it functions in the same pathway as MUS-81 (SAITO *et al.* 2009, 2013; AGOSTINHO *et al.* 2013). The XPF-1 pathway also includes the Bloom helicase ortholog HIM-6 (AGOSTINHO *et al.* 2013). And finally, the Slx4 ortholog HIM-18 functions in both pathways, perhaps as a scaffold that brings pathway components in close proximity (AGOSTINHO *et al.* 2013; SAITO *et al.* 2013). The meiotic functions of XPF-1 and MUS-81 went previously undetected because single mutations in either gene did not reduce crossovers from wild-type levels – components in both pathways must be perturbed before crossover number is reduced. *mus-81* single mutants have wild-type levels of crossovers, as do *xpf-1* single mutants, while *mus-81; xpf-1* double mutants have 35-60% fewer crossovers than wild-type animals (AGOSTINHO *et al.* 2013; SAITO *et al.* 2013). However, at least one other resolvase must also function during meiosis, as none of the groups identified a condition in which crossovers were completely abolished, and the remaining crossovers in the *mus-81; xpf-1* double mutant must be resolved by this unidentified resolvase or resolvases. These studies, along with those in *S. cerevisiae*, reveal the previously unsuspected complexity of possible interactions between meiotic crossover resolvases.

Although XPF-1 can completely compensate for the absence of MUS-81 (and vice versa), it is not clear whether both are used in a wild-type meiosis or whether one is preferred over the other. It has been previously shown that MUS-81 was required for crossover resolution in animals exposed to high levels of ionizing radiation (YOUDS *et al.* 2010). In a wild-type animal, irradiation increases the number of meiotic DSBs and crossovers in a dose-dependent manner (KIM and ROSE 1987; METS and MEYER 2009). Intriguingly, irradiated animals retain wild-type levels of COSA-1 foci – one per chromosome – even though extra crossovers are detected by genetic assays (YOKOO *et al.* 2012). This result indicates that cells are capable of producing two types of crossovers, distinguished by whether they are marked by COSA-1 at late meiotic prophase.

The network of crossover resolvases and other DSB repair pathways in *S. cerevisiae* and *C. elegans* highlights the interconnected nature of these components. In this dissertation, I investigate whether threats to chromosome integrity affect the relative involvement of the two known resolvases in generating crossovers. In Chapter 2, I use two conditions – ionizing radiation and condensin-depletion – that create more of DSBs and crossovers without affecting the numbers of COSA-1 foci. Although MUS-81 and XPF-1 are each sufficient on their own during a wild-type meiosis, both resolvases become required for forming crossovers in animals when the threat reaches a certain level of severity. In the case of exposure to radiation, doses of 2.5 grays and higher invoke a requirement for MUS-81, while all doses examined invoke a requirement for XPF-1. For condensin-depleted animals, both meiotic condensins need to be depleted before a requirement for XPF-1 and MUS-81 is invoked. We present evidence that the requirement for MUS-81 is not solely invoked by the absolute number of DSBs, but rather by the presence of DNA damage. Finally, a combination of insults can generate resolvase-dependent crossovers through conditions that, on their own, create crossovers that not dependent on any one resolvase. These data are the first indication that in *C. elegans*, some crossovers may be matured differently depending on the provenance of the DSB or

external factors like radiation that damage the meiotic cell. This study establishes a framework for further investigations into the interdependence of different crossover resolvases in meiosis. In Appendix I, I revisit work previously performed in our lab using cytological methods to estimate the total number of DSBs formed during meiosis. In Appendix II, I summarize the meiotic defects of animals lacking the SUMO peptide. In Appendix III, I discuss a preliminary analysis of ChIP-seq against the chromosome axis components REC-8 and COH-3/4.

References

AGOSTINHO A., MEIER B., SONNEVILLE R., JAGUT M., WOGLAR A., BLOW J., JANTSCH V., GARTNER A., 2013 Combinatorial regulation of meiotic holliday junction resolution in *C. elegans* by HIM-6 (BLM) helicase, SLX-4, and the SLX-1, MUS-81 and XPF-1 nucleases. PLoS Genet. **9**: e1003591.

ALBERTSON D. G., THOMSON J. N., 1993 Segregation of holocentric chromosomes at meiosis in the nematode, *Caenorhabditis elegans*. Chromosome Res. **1**: 15–26.

ALLERS T., LICHTEN M., 2001 Differential timing and control of noncrossover and crossover recombination during meiosis. Cell **106**: 47–57.

ARGUESO J. L., WANAT J., GEMICI Z., ALANI E., 2004 Competing crossover pathways act during meiosis in *Saccharomyces cerevisiae*. Genetics **168**: 1805–16.

BARBER L. J., YOUDS J. L., WARD J. D., MCILWRAITH M. J., O'NEIL N. J., PETALCORIN M. I. R., MARTIN J. S., COLLIS S. J., CANTOR S. B., AUCLAIR M., TISSENBAUM H., WEST S. C., ROSE A. M., BOULTON S. J., 2008 RTEL1 maintains genomic stability by suppressing homologous recombination. Cell **135**: 261–71.

BARNES T. M., KOHARA Y., CODSON A., HEKIMI S., 1995 Meiotic Recombination, Noncoding DNA and Genomic Organization in *Caenorhabditis elegans*. Genetics **179**: 159–179.

BAUDAT F., IMAI Y., MASSY B. DE, 2013 Meiotic recombination in mammals: localization and regulation. Nat. Rev. Genet. **14**: 794–806.

BAUDAT F., MANOVA K., YUEN J. P., JASIN M., KEENEY S., 2000 Chromosome synapsis defects and sexually dimorphic meiotic progression in mice lacking Spo11. Mol. Cell **6**: 989–98.

BAUDAT F., MASSY B. DE, 2007 Regulating double-stranded DNA break repair towards crossover or non-crossover during mammalian meiosis. Chromosome Res. **15**: 565–77.

BAUDAT F., NICOLAS A, 1997 Clustering of meiotic double-strand breaks on yeast chromosome III. Proc. Natl. Acad. Sci. U. S. A. **94**: 5213–8.

BENNETT C. B., LEWIS A. L., BALDWIN K. K., RESNICK M. A., 1993 Lethality induced by a single site-specific double-strand break in a dispensable yeast plasmid. Proc. Natl. Acad. Sci. U. S. A. **90**: 5613–7.

BENNETT C. B., WESTMORELAND T. J., SNIPE J. R., RESNICK M. A., 1996 A double-strand break within a yeast artificial chromosome (YAC) containing human DNA can result in YAC loss , deletion or cell lethality . Mol. Cell. Biol. **16**: 4414–4425.

BERCHOWITZ L. E., COPENHAVER G. P., 2010 Genetic Interference: Don't Stand So Close to Me. Curr. Genomics **11**: 91–102.

BERCHOWITZ L. E., FRANCIS K. E., BEY A. L., COPENHAVER G. P., 2007 The role of AtMUS81 in interference-insensitive crossovers in *A. thaliana*. PLoS Genet. **3**: e132.

BERNSTEIN H., HOPF F. A., MICHOD R. E., 1987 The molecular basis of the evolution of sex. Adv. Genet. **24**: 323–370.

BHALLA N., DERNBURG A. F., 2008 Prelude to a division. Annu. Rev. Cell Dev. Biol. **24**: 397–424.

BISHOP D. K., 1994 RecA homologs Dmc1 and Rad51 interact to form multiple nuclear complexes prior to meiotic chromosome synapsis. Cell **79**: 1081–92.

BISHOP D. K., ZICKLER D., 2004 Early Decision: Meiotic Crossover Interference prior to Stable Strand Exchange and Synapsis. Cell **117**: 9–15.

BODDY M. N., GAILLARD P. H., MCDONALD W. H., SHANAHAN P., YATES J. R., RUSSELL P., 2001 Mus81-Eme1 are essential components of a Holliday junction resolvase. Cell **107**: 537–48.

BOER E. DE, DIETRICH A. J. J., HÖÖG C., STAM P., HEYTING C., 2007 Meiotic interference among MLH1 foci requires neither an intact axial element structure nor full synapsis. J. Cell Sci. **120**: 731–6.

BÖRNER G. V., KLECKNER N., HUNTER N., 2004 Crossover/noncrossover differentiation, synaptonemal complex formation, and regulatory surveillance at the leptotene/zygotene transition of meiosis. Cell **117**: 29–45.

BRENNER S., 1974 The Genetics of *Caenorhabditis elegans*. Genetics **77**: 71–94.

BRICK K., SMAGULOVA F., KHIL P., CAMERINI-OTERO R. D., PETUKHOVA G. V, 2012 Genetic recombination is directed away from functional genomic elements in mice. Nature **485**: 642–5.

CARBALLO J. a, JOHNSON A. L., SEDGWICK S. G., CHA R. S., 2008 Phosphorylation of the axial element protein Hop1 by Mec1/Tel1 ensures meiotic interhomolog recombination. Cell **132**: 758–70.

CERVANTES M. D., FARAH J. A., SMITH G. R., 2000 Meiotic DNA Breaks Associated with Recombination in *S . pombe*. Mol. Cell **5**: 883–888.

CHARLESWORTH B., 2006 The evolutionary biology of sex. Curr. Biol. **16**: R693–5.

CLOUD V., CHAN Y.-L., GRUBB J., BUDKE B., BISHOP D. K., 2012 Rad51 is an accessory factor for Dmc1-mediated joint molecule formation during meiosis. Science **337**: 1222–5.

COLE F., KAUPPI L., LANGE J., ROIG I., WANG R., KEENEY S., JASIN M., 2012 Homeostatic control of recombination is implemented progressively in mouse meiosis. Nat. Cell Biol. **14**: 424–30.

COOP G., WEN X., OBER C., PRITCHARD J. K., PRZEWORSKI M., 2008 High-resolution mapping of crossovers reveals extensive variation in fine-scale recombination patterns among humans. Science **319**: 1395–8.

COPENHAVER G. P., HOUSWORTH E. A., STAHL F. W., 2002 Crossover Interference in *Arabidopsis*. Genetics **1639**: 1631–1639.

CROMIE G., SMITH G. R., 2007 Meiotic Recombination in *Schizosaccharomyces pombe*: A Paradigm for Genetic and Molecular Analysis. Genome.

DERNBURG A. F., MCDONALD K., MOULDER G., BARSTEAD R., DRESSER M., VILLENEUVE A. M., 1998 Meiotic recombination in *C. elegans* initiates by a conserved mechanism and is dispensable for homologous chromosome synapsis. Cell **94**: 387–98.

EGEL-MITANI M., OLSON L. W., EGEL R., 1982 Meiosis in *Aspergillus nidulans*: Another example for lacking synaptonemal complexes in the absence of crossover interference. Heriditas **187**: 179–187.

FEKAIRI S., SCAGLIONE S., CHAHWAN C., TAYLOR E. R., TISSIER A., COULON S., DONG M.-Q., RUSE C., YATES J. R., RUSSELL P., FUCHS R. P., MCGOWAN C. H., GAILLARD P.-H. L., 2009 Human SLX4 is a Holliday junction resolvase subunit that binds multiple DNA repair/recombination endonucleases. Cell **138**: 78–89.

FELSENSTEIN J., 1974 The evolutionary advantage of recombination. Genetics **78**: 737–756.

FUNG J. C., ROCKMILL B., ODELL M., ROEDER G. S., HAVEN N., 2004 Imposition of Crossover Interference through the Nonrandom Distribution of Synapsis Initiation Complexes. Cell **116**: 795–802.

GERTON J. L., DERISI J., SHROFF R., LICHTEN M., BROWN P. O., PETES T. D., 2000 Global mapping of meiotic recombination hotspots and coldspots in the yeast *Saccharomyces cerevisiae*. Proc. Natl. Acad. Sci. U. S. A. **97**: 11383–90.

GESSLER D. D., XU S., 1999 On the evolution of recombination and meiosis. Genet. Res. **73**: 119–31.

GETZ T. J., BANSE S. a, YOUNG L. S., BANSE A. V, SWANSON J., WANG G. M., BROWNE B. L., FOSS H. M., STAHL F. W., 2008 Reduced mismatch repair of heteroduplexes reveals "non"-interfering crossing over in wild-type *Saccharomyces cerevisiae*. Genetics **178**: 1251–69.

GLADYSHEV E. A., MESELSON M., ARKHIPOVA I. R., 2008 Massive horizontal gene transfer in bdelloid rotifers. Science **320**: 1210–3.

GODDARD M. R., GODFRAY H. C. J., BURT A., 2005 Sex increases the efficacy of natural selection in experimental yeast populations. Nature **434**: 636–640.

GREY C., BARTHÈS P., CHAUVEAU-LE FRIEC G., LANGA F., BAUDAT F., MASSY B. DE, 2011 Mouse PRDM9 DNA-Binding Specificity Determines Sites of Histone H3 Lysine 4 Trimethylation for Initiation of Meiotic Recombination (M Lichten, Ed.). PLoS Biol. **9**: e1001176.

GREY C., BAUDAT F., MASSY B. DE, 2009 Genome-wide control of the distribution of meiotic recombination. PLoS Biol. **7**: e35.

H.J. M., 1932 Some Genetic Aspects of Sex. Am. Nat. **66**: 118–138.

HAMMARLUND M., DAVIS M. W., NGUYEN H., DAYTON D., JORGENSEN E. M., 2005 Heterozygous insertions alter crossover distribution but allow crossover interference in *Caenorhabditis elegans*. Genetics **171**: 1047–56.

HASSOLD T., HUNT P., 2001 To err (meiotically) is human: the genesis of human aneuploidy. Nat. Rev. Genet. **2**: 280–91.

HAYASHI M., MLYNARCZYK-EVANS S., VILLENEUVE A. M., 2010 The synaptonemal complex shapes the crossover landscape through cooperative assembly, crossover promotion and crossover inhibition during *Caenorhabditis elegans* meiosis. Genetics **186**: 45–58.

HERMAN R. K., KARI C. K., HARTMAN P. S., 1982 Dominant X-chromosome nondisjunction mutants of *Caenorhabditis elegans*. Genetics **102**: 379–400.

HEYER W.-D., EHMSEN K. T., LIU J., 2010 Regulation of homologous recombination in eukaryotes. Annu. Rev. Genet. **44**: 113–39.

HIGGINS J. D., ARMSTRONG S. J., FRANKLIN F. C. H., JONES G. H., 2004 The *Arabidopsis MutS* homolog *AtMSH4* functions at an early step in recombination: evidence for two classes of recombination in *Arabidopsis*. Genes Dev. **18**: 2557–70.

HILLERS K. J., VILLENEUVE A. M., 2003 Chromosome-Wide Control of Meiotic Crossing over in *C. elegans*. Curr. Biol. **13**: 1641–1647.

HOLLIDAY R., LEWIS K. R., HULTEN M., 1977 Recombination and Meiosis [and Discussion]. Philos. Trans. R. Soc. B Biol. Sci. **277**: 359–370.

HOLLINGSWORTH N. M., PONTE L., HALSEY C., 1995 MSH5, a novel MutS homolog, facilitates meiotic reciprocal recombination between homologs in *Saccharomyces cerevisiae* but not mismatch repair. Genes Dev. **9**: 1728–1739.

HOLLOWAY J. K., BOOTH J., EDELMANN W., MCGOWAN C. H., COHEN P. E., 2008 MUS81 generates a subset of MLH1-MLH3-independent crossovers in mammalian meiosis. PLoS Genet. **4**: e1000186.

HUNTER N., KLECKNER N., 2001 The single-end invasion: an asymmetric intermediate at the double-strand break to double-Holliday junction transition of meiotic recombination. Cell **106**: 59–70.

IP S. C. Y., RASS U., BLANCO M. G., FLYNN H. R., SKEHEL J. M., WEST S. C., 2008 Identification of Holliday junction resolvases from humans and yeast. Nature **456**: 357–61.

JUDSON O. P., NORMARK B. B., 1996 Ancient asexual scandals. Trends Ecol. Evol. **11**: 41–6.

KALIRAMAN V., MULLEN J. R., FRICKE W. M., BASTIN-SHANOWER S. a, BRILL S. J., 2001 Functional overlap between Sgs1-Top3 and the Mms4-Mus81 endonuclease. Genes Dev. **15**: 2730–40.

KEENEY S., 2001 Mechanism and Control of Meiotic Recombination Initiation. Curr. Top. Dev. Biol. **52**: 1–53.

KEENEY S., GIROUX C. N., KLECKNER N., 1997 Meiosis-Specific DNA Double-Strand Breaks Are Catalyzed by Spo11 , a Member of a Widely Conserved Protein Family. Cell **88**: 375–384.

KELLY K. O., DERNBURG A. F., STANFIELD G. M., VILLENEUVE A. M., 2000 Caenorhabditis elegans msh-5 is required for both normal and radiation-induced meiotic crossing over but not for completion of meiosis. Genetics **156**: 617–30.

KIM J. S., ROSE A. M., 1987 The effect of gamma radiation on recombination frequency in *Caenorhabditis elegans*. Genome **29**: 457–462.

KLECKNER N., 2006 Chiasma formation: chromatin/axis interplay and the role(s) of the synaptonemal complex. Chromosoma **115**: 175–94.

KLECKNER N., STORLAZZI A., ZICKLER D., 2003 Coordinate variation in meiotic pachytene SC length and total crossover/chiasma frequency under conditions of constant DNA length. Trends Genet. **19**: 623–628.

KOEHLER K. E., BOULTON C. L., COLLINS H. E., FRENCH R. L., HERMAN K. C., LACEFIELD S. M., MADDEN L. D., SCHUETZ C. D., HAWLEY R. S., 1996 Spontaneous X Chromosome MI and MII nondisjunction events in *Drosophila melanogaster* oocytes have different recombinational histories. Nat. Genet. **14**: 406–414.

KOHL K. P., SEKELSKY J., 2013 Meiotic and mitotic recombination in meiosis. Genetics **194**: 327–34.

KOLAS N. K., COHEN P. E., 2004 Novel and diverse functions of the DNA mismatch repair family in mammalian meiosis and recombination. Cytogenet. Genome Res. **107**: 216–31.

KOLODNER R. D., PUTNAM C. D. ., MYUNG K., 2002 Maintenance of Genome Stability in *Saccharomyces cerevisiae*. Science (80-.). **297**: 552–557.

LAMB N. E., SHERMAN S. L., HASSOLD T. J., 2005 Effect of meiotic recombination on the production of aneuploid gametes in humans. Cytogenet. Genome Res. **111**: 250–5.

LAO J. P., CLOUD V., HUANG C.-C., GRUBB J., THACKER D., LEE C.-Y., DRESSER M. E., HUNTER N., BISHOP D. K., 2013 Meiotic crossover control by concerted action of Rad51-Dmc1 in homolog template bias and robust homeostatic regulation. PLoS Genet. **9**: e1003978.

LEMMENS B. B. L. G., TIJSTERMAN M., 2011 DNA double-strand break repair in *Caenorhabditis elegans*. Chromosoma **120**: 1–21.

LIBUDA D. E., UZAWA S., MEYER B. J., VILLENEUVE A. M., 2013 Meiotic chromosome structures constrain and respond to designation of crossover sites. Nature **502**: 703–6.

LIU H., JANG J. K., KATO N., MCKIM K. S., 2002 *mei-P22* encodes a chromosome-associated protein required for the initiation of meiotic recombination in *Drosophila melanogaster*. Genetics **162**: 245–58.

LU X., LIU X., AN L., ZHANG W., SUN J., PEI H., MENG H., FAN Y., ZHANG C., 2008 The *Arabidopsis MutS* homolog *AtMSH5* is required for normal meiosis. Cell Res. **18**: 589–99.

LYNN A., SOUCEK R., BÖRNER G. V., 2007 ZMM proteins during meiosis: crossover artists at work. Chromosome Res. **15**: 591–605.

MANCERA E., BOURGON R., BROZZI A., HUBER W., STEINMETZ L. M., 2008 High-resolution mapping of meiotic crossovers and non-crossovers in yeast. Nature **454**: 479–85.

MARK WELCH J. L., MARK WELCH D. B., MESELSON M., 2004 Cytogenetic evidence for asexual evolution of bdelloid rotifers. Proc. Natl. Acad. Sci. U. S. A. **101**: 1618–21.

MARK WELCH D. B., MESELSON M., 2000 Evidence for the Evolution of Bdelloid Rotifers Without Sexual Reproduction or Genetic Exchange. Science (80-.). **288**: 1211–1215.

MARTINEZ-PEREZ E., COLAIÁCOVO M. P., 2009 Distribution of meiotic recombination events: talking to your neighbors. Curr. Opin. Genet. Dev. **19**: 105–12.

MARTINI E., DIAZ R. L., HUNTER N., KEENEY S., 2006 Crossover homeostasis in yeast meiosis. Cell **126**: 285–95.

MASSY B. DE, 2013 Initiation of meiotic recombination: how and where? Conservation and specificities among eukaryotes. Annu. Rev. Genet. **47**: 563–99.

MCKIM K. S., HAYASHI-HAGIHARA A., 1998 *mei-W68* in *Drosophila melanogaster* encodes a Spo11 homolog: evidence that the mechanism for initiating meiotic recombination is conserved. Genes Dev. **12**: 2932–2942.

MENEELY P. M., FARAGO A. F., KAUFFMAN T. M., 2002 Crossover distribution and high interference for both the X chromosome and an autosome during oogenesis and spermatogenesis in *Caenorhabditis elegans*. Genetics **162**: 1169–77.

METS D. G., MEYER B. J., 2009 Condensins regulate meiotic DNA break distribution, thus crossover frequency, by controlling chromosome structure. Cell **139**: 73–86.

MUNZ P., 1994 An Analysis of Interference in the Fission Yeast *Schizosaccharomyces pombe*. Genetics **137**: 701–707.

MUYT A. DE, JESSOP L., KOLAR E., SOURIRAJAN A., CHEN J., DAYANI Y., LICHTEN M., 2012 BLM helicase ortholog Sgs1 is a central regulator of meiotic recombination intermediate metabolism. Mol. Cell **46**: 43–53.

MYERS S., BOWDEN R., TUMIAN A., BONTROP R. E., FREEMAN C., MACFIE T. S., MCVEAN G., DONNELLY P., 2010 Drive against hotspot motifs in primates implicates the PRDM9 gene in meiotic recombination. Science **327**: 876–9.

NABESHIMA K., VILLENEUVE A. M., HILLERS K. J., 2004 Chromosome-wide regulation of meiotic crossover formation in *Caenorhabditis elegans* requires properly assembled chromosome axes. Genetics **168**: 1275–92.

NEALE M. J., KEENEY S., 2006 Clarifying the mechanics of DNA strand exchange in meiotic recombination. Nature **442**: 153–8.

NOVAK J. E., ROSS-MACDONALD P. B., ROEDER G. S., 2001 The Budding Yeast Msh4 Protein Functions in Chromosome Synapsis and the Regulation of Crossover Distribution. Genetics **158**: 1013–1025.

O'NEIL N. J., MARTIN J. S., YOUDS J. L., WARD J. D., PETALCORIN M. I. R., ROSE A. M., BOULTON S. J., 2013 Joint molecule resolution requires the redundant activities of MUS-81 and XPF-1 during *Caenorhabditis elegans* meiosis. PLoS Genet. **9**: e1003582.

OHTA K., WU T. C., LICHTEN M., SHIBATA T., 1999 Competitive inactivation of a double-strand DNA break site involves parallel suppression of meiosis-induced changes in chromatin configuration. Nucleic Acids Res. **27**: 2175–80.

OSTERGREN G., 1948 The mechanism of co-orientation in bivalents and multivalents: the theory of orientation by pulling. Hereditas **37**: 85–156.

OTTO S. P., LENORMAND T., 2002 Resolving the paradox of sex and recombination. Nat. Rev. Genet. **3**: 252–61.

PADMORE R., CAO L., KLECKNER N., 1991 Temporal comparison of recombination and synaptonemal complex formation during meiosis in *S. cerevisiae*. Cell **66**: 1239–56.

PAGE S. L., HAWLEY R. S., 2003 Chromosome choreography: the meiotic ballet. Science **301**: 785–9.

PARVANOV E. D., NG S. H. S., PETKOV P. M., PAIGEN K., 2009 Trans-regulation of mouse meiotic recombination hotspots by Rcr1. PLoS Biol. **7**: e36.

PETRONCZKI M., SIOMOS M. F., NASMYTH K., CORRENS C., VRIES H. De, TSCHER- E., 2003 Un Menage a Quatre: The Molecular Biology of Chromosome Segregation in Meiosis. **112**: 423–440.

POCHART P., WOLTERING D., HOLLINGSWORTH M., HOLLINGSWORTH N. M., 1997 Nucleic Acids, Protein Synthesis, and Molcular Genetics: Conserved Properties between Functionally Distinct MutS Homologs in Yeast Conserved Properties between Functionally Distinct MutS Homologs in Yeast. J. Biol. Chem. **272**: 30345–30349.

ROCKMAN M. V, KRUGLYAK L., 2009 Recombinational landscape and population genomics of *Caenorhabditis elegans*. PLoS Genet. **5**: e1000419.

ROCKMILL B., VOELKEL-MEIMAN K., ROEDER G. S., 2006 Centromere-proximal crossovers are associated with precocious separation of sister chromatids during meiosis in *Saccharomyces cerevisiae*. Genetics **174**: 1745–54.

ROEDER G. S., 1997 Meiotic chromosomes: it takes two to tango. Genes Dev. **11**: 2600–2621.

ROMANIENKO P. J., CAMERINI-OTERO R. D., 2000 The mouse Spo11 gene is required for meiotic chromosome synapsis. Mol. Cell **6**: 975–87.

ROSS-MACDONALD P., ROEDER G. S., 1994 Mutation of a meiosis-specific MutS homolog decreases crossing over but not mismatch correction. Cell **79**: 1069–80.

ROSU S., LIBUDA D. E., VILLENEUVE A. M., 2011 Robust crossover assurance and regulated interhomolog access maintain meiotic crossover number. Science **334**: 1286–9.

ROSU S., ZAWADZKI K. A., STAMPER E. L., LIBUDA D. E., REESE A. L., DERNBURG A. F., VILLENEUVE A. M., 2013 The *C. elegans* DSB-2 protein reveals a regulatory network that controls competence for meiotic DSB formation and promotes crossover assurance. PLoS Genet. **9**: e1003674.

SAITO T. T., LUI D. Y., KIM H.-M., MEYER K., COLAIÁCOVO M. P., 2013 Interplay between structure-specific endonucleases for crossover control during *Caenorhabditis elegans* meiosis. PLoS Genet. **9**: e1003586.

SAITO T. T., YOUDS J. L., BOULTON S. J., COLAIÁCOVO M. P., 2009 *Caenorhabditis elegans* HIM-18/SLX-4 interacts with SLX-1 and XPF-1 and maintains genomic integrity in the germline by processing recombination intermediates. PLoS Genet. **5**: e1000735.

SANTOS T. D. L., HUNTER N., LEE C., LARKIN B., LOIDL J., HOLLINGSWORTH N. M., 2003 Junction Resolution to Promote a Distinct Subset of Crossovers During Meiosis in Budding Yeast. Genetics **94**: 81–94.

SCHVARZSTEIN M., PATTABIRAMAN D., LIBUDA D. E., RAMADUGU A., TAM A., MARTINEZ-PEREZ E., ROELENS B., ZAWADZKI K. A., YOKOO R., ROSU S., SEVERSON A. F., MEYER B. J., NABESHIMA K., VILLENEUVE A. M., 2014 DNA Helicase HIM-6/BLM Both Promotes MutS

γ-Dependent Crossovers and Antagonizes MutS γ-Independent Inter-homolog Associations during *Caenorhabditis elegans* meiosis. Genetics.

SCHWACHA A., KLECKNER N., 1995 Identification of double Holliday junctions as intermediates in meiotic recombination. Cell **83**: 783–91.

SCHWACHA A., KLECKNER N., 1997 Interhomolog bias during meiotic recombination: meiotic functions promote a highly differentiated interhomolog-only pathway. Cell **90**: 1123–35.

SCHWARTZ E. K., HEYER W.-D., 2011 Processing of joint molecule intermediates by structure-selective endonucleases during homologous recombination in eukaryotes. Chromosoma **120**: 109–27.

SEKELSKY J. J., MCKIM K. S., CHIN G. M., HAWLEY R. S., 1995 The *Drosophila* Meiotic Recombination Gene mei-9 Encodes a Homologue of the Yeast Excision Repair Protein Rad1. Genetics **627**: 619–627.

SEVERSON A. F., LING L., ZUYLEN V. VAN, MEYER B. J., 2009 The axial element protein HTP-3 promotes cohesin loading and meiotic axis assembly in *C. elegans* to implement the meiotic program of chromosome segregation. Genes Dev. **23**: 1763–78.

SHINOHARA M., OH S. D., HUNTER N., SHINOHARA A., 2008 Crossover assurance and crossover interference are distinctly regulated by the ZMM proteins during yeast meiosis. Nat. Genet. **40**: 299–309.

SHINOHARA a, SHINOHARA M., 2004 Roles of RecA homologues Rad51 and Dmc1 during meiotic recombination. Cytogenet. Genome Res. **107**: 201–7.

SMITH G. R., BODDY M. N., SHANAHAN P., RUSSELL P., 2003 Fission yeast Mus81.Eme1 Holliday junction resolvase is required for meiotic crossing over but not for gene conversion. Genetics **165**: 2289–93.

STAMPER E. L., RODENBUSCH S. E., ROSU S., AHRINGER J., VILLENEUVE A. M., DERNBURG A. F., 2013 Identification of DSB-1, a protein required for initiation of meiotic recombination in *Caenorhabditis elegans*, illuminates a crossover assurance checkpoint. PLoS Genet. **9**: e1003679.

STURTEVANT A. H., 1913 The Linear Arrangement of Six Sex-Linked Factors in *Drosophila*, as Shown by Their Mode of Association. J. Exp. Zool. **14**: 43–59.

STURTEVANT A. H., 1915 The Behavior of the Chromosomes as Studied through Linkage. Zeitschrift fur Indukt. Abstammungs-und Vererbungslehre **13**: 234–287.

THACKER D., MOHIBULLAH N., ZHU X., KEENEY S., 2014 Homologue engagement controls meiotic DNA break number and distribution. Nature **510**: 241–246.

THOMPSON D. A., STAHL F. W., 1999 Genetic control of recombination partner preference in yeast meiosis: Isolation and characterization of mutants elevated for meiotic unequal sister-chromatid recombination. Genetics **153**: 621–41.

WILKINS A. S., HOLLIDAY R., 2009 The evolution of meiosis from mitosis. Genetics **181**: 3–12.

YILDIZ O., MAJUMDER S., KRAMER B., SEKELSKY J. J., 2002 *Drosophila* MUS312 Interacts with the Nucleotide Excision Repair Endonuclease MEI-9 to Generate Meiotic Crossovers. Mol. Cell **10**: 1503–1509.

YOKOO R., ZAWADZKI K. A., NABESHIMA K., DRAKE M., ARUR S., VILLENEUVE A. M., 2012 COSA-1 reveals robust homeostasis and separable licensing and reinforcement steps governing meiotic crossovers. Cell **149**: 75–87.

YOUDS J. L., METS D. G., MCILWRAITH M. J., MARTIN J. S., WARD J. D., ONEIL N. J., ROSE A. M., WEST S. C., MEYER B. J., BOULTON S. J., 2010 RTEL-1 enforces meiotic crossover interference and homeostasis. Science **327**: 1254–8.

ZAKHARYEVICH K., TANG S., MA Y., HUNTER N., 2012 Delineation of Joint Molecule Resolution Pathways in Meiosis Identifies a Crossover-Specific Resolvase. Cell **149**: 334–347.

ZALEVSKY J., MACQUEEN a J., DUFFY J. B., KEMPHUES K. J., VILLENEUVE a M., 1999 Crossing over during *Caenorhabditis elegans* meiosis requires a conserved MutS-based pathway that is partially dispensable in budding yeast. Genetics **153**: 1271–83.

ZENVIRTH D., ARBEL T., SHERMAN A., GOLDWAY M., KLEIN S., SIMCHEN G., 1992 Multiple sites for double-strand breaks in whole meiotic chromosomes of *Saccharomyces cerevisiae*. EMBO J. **11**: 3441–7.

ZHANG L., KLECKNER N. E., STORLAZZI A., KIM K. P., 2011 Meiotic double-strand breaks occur once per pair of (sister) chromatids and, via Mec1/ATR and Tel1/ATM, once per quartet of chromatids. Proc. Natl. Acad. Sci. U. S. A.: 1–6.

ZICKLER D., KLECKNER N., 1999 Integrating Structure and Function. Annu. Rev. Genet. **33**: 603–754.

ZIERHUT C., BERLINGER M., RUPP C., SHINOHARA A., KLEIN F., 2004 Mnd1 Is Required for Meiotic Interhomolog Repair. Curr. Biol. **14**: 752–762.

Chapter 2

Disrupting crossover regulation affects resolvase preference

Chapter 2.
Disrupting crossover regulation affects resolvase preference

Abstract

Crossover recombination provides a physical link between homologous chromosomes that is essential for meiotic chromosome segregation. Crossovers are initiated by SPO-11-dependant double-strand breaks (DSBs), which, if unrepaired, pose a hazard to genome stability. Thus, some organisms have multiple, compensatory repair pathways that ensure the repair of all DSBs formed during meiosis. Recent studies in *C. elegans* have identified two parallel pathways with partially overlapping resolvases that are each sufficient for crossover resolution in wild-type animals – one pathway uses XPF-1 and the other uses MUS-81. In this study, we investigate whether resolvase preference can be distinguished. We show that while XPF-1 and MUS-81 act interchangeably to resolve crossovers in wild-type animals, they become required under conditions that threaten chromosome integrity, whether from exposure ionizing radiation or reducing the concentration of condensin, a complex required for proper chromosome structure. We also show that two conditions which independently do not create a requirement for a particular resolvase can, when combined, generate a requirement. This indicates that crossover resolution pathways are influenced by factors that act in a combinatorial manner. Although resolvase dependence in irradiated and condensin-depleted animals correlates with the extent of DNA damage, the absolute number of DSBs is not solely responsible for invoking a requirement. Thus, DSB repair pathway choice may generate different classes of crossover depending on the DSB provenance or cellular reactions to the inducing condition.

Introduction

Crossover recombination is an essential feature of meiosis, the specialized cell division that creates haploid gametes from diploid progenitor cells. Crossovers – a reciprocal exchange of DNA between homologous chromosomes – are necessary for proper chromosome segregation (HEYER *et al.* 2010). Failure to form a crossover results in gametes that produce aneuploid embryos, which are usually inviable. Within sexual species, crossovers serve to promote genetic diversity while permitting the removal of deleterious mutations. Due to their importance, crossovers undergo strict regulation, from initiation to resolution, but the factors that dictate preferences for specific crossover resolution pathways remain incompletely understood. Crossover are consequences of programmed DNA double-strand breaks (DSBs), which are a highly toxic form of DNA damage – an unrepaired DSB can activate cell-cycle arrest or induce cell death (BENNETT *et al.* 1993). Therefore, viability requires that meiotic cells maintain an equilibrium between producing enough DSBs to ensure at least one crossover per chromosome, but not so many DSBs that some are left unrepaired to threaten genome integrity.

Meiotic DSBs are catalyzed by the conserved meiotic protein SPO-11, a type II-like topoisomerase (KEENEY *et al.* 1997; DERNBURG *et al.* 1998). SPO-11 is removed from the site of DSB initiation by DNA cleavage of the SPO-11-DNA oligo complex (NEALE *et al.* 2005). DSBs are then resected to produce a 3' stretch of single-stranded DNA, where the RecA-like recombinase RAD-51 binds and promotes invasion of the homologous chromosome. These joint-molecule intermediates can become non-crossovers through dissolution by a helicase (in *S. cerevisiae*, this is performed by Sgs1, an ortholog to Bloom helicase) or resolution through synthesis-dependent strand annealing; alternatively, they can be stabilized by the ZMM family of proteins in the form of double Holliday junctions and resolved as crossovers by crossover resolvases (HOLLIDAY 1964; SUN *et al.* 1989; PÂQUES and HABER 1999; HEYER *et al.* 2010). Most organisms studied to date create more DSBs than they do crossovers, although the ratio varies widely by species (MARTINEZ-PEREZ and COLAIÁCOVO 2009). *C. elegans* represents one extreme of the DSB to crossover ratio: although chromosomes may receive an average of three to eight DSBs, only one of these is resolved as a crossover in wild-type animals (HILLERS and VILLENEUVE 2003; NOTTKE *et al.* 2011; ROSU *et al.* 2011; SAITO *et al.* 2012). This single crossover is destined to become a chiasma, a physical connection that holds two homologous chromosomes together after desynapsis, facilitating their correct orientation on the metaphase I plate (PAGE and HAWLEY 2003).

Because unresolved DSBs pose a hazard to genome stability, many organisms have multiple and compensating DSB repair pathways to ensure the repair of all breaks induced during meiosis (YOUDS and BOULTON 2011; KOHL and SEKELSKY 2013). In *S. cerevisiae*, two extensive studies revealed a series of coordinated DSB repair pathways, several of which are able to achieve a crossover outcome (ZAKHARYEVICH *et al.* 2012; DE MUYT *et al.* 2012). The primary crossover resolvase in *S. cerevisiae* is the Mlh1-Mlh3 heterodimer, which acts in conjunction with the Exo1 exonuclease to generate only crossovers from double Holliday junctions (ZAKHARYEVICH *et al.* 2012). In *S. cerevisiae*, a minority of crossovers are resolved by the Mus81-Mms4 heterodimer, which acts on joint-molecule intermediates in an unbiased manner to generate an equal number of crossovers and non-crossovers (BODDY *et al.* 2001; CROMIE *et al.* 2006; JESSOP and LICHTEN 2008;

OH *et al.* 2008; ZAKHARYEVICH *et al.* 2012; DE MUYT *et al.* 2012). In the absence of the primary crossover resolving pathway and the Mus81-Mms4 pathway, the cryptic resolvase activity of Yen1 is revealed, while the cryptic activity of Slx1-Slx-4 is only revealed in the absence of Yen1, Mus81-Mms4, and the primary pathway (ZAKHARYEVICH *et al.* 2012; DE MUYT *et al.* 2012). These studies exposed a robust hierarchical relationship between DSB repair pathways. In wild-type cells, each pathway is subject to regulatory utilization that permits the efficient resolution of DSB repair intermediates, but under conditions that prevent timely DSB repair, alternative crossover resolution pathways have the capacity to repair most DSBs and ensure cell survival.

Though DSB repair pathways are conserved between diverse taxa, the relative involvement of different components in each pathway varies between species. Although Mus81 is only responsible for a minority of crossovers in *S. cerevisiae, Arabidopsis*, *Drosophila,* and mice, it generates most of the crossovers in *S. pombe* (BODDY *et al.* 2001; MATOS *et al.* 2011; KOHL and SEKELSKY 2013; HOLLOWAY *et al.* 2014). In *Drosophila*, MEI-9 (a homolog of the yeast excision repair protein Rad1) resolves most meiotic crossovers (SEKELSKY *et al.* 1995). Recent work has shown that crossovers in *C. elegans* are resolved by at least two parallel and overlapping pathways, dependent on either the MUS-81 nuclease or the XPF-1 nuclease (a homolog of MEI-9) (AGOSTINHO *et al.* 2013; O'NEIL *et al.* 2013; SAITO *et al.* 2013). The endonuclease SLX-1 functions in the same pathway as MUS-81 (SAITO *et al.* 2009, 2013; AGOSTINHO *et al.* 2013), while the XPF-1 pathway includes the Bloom helicase and Sgs1 ortholog HIM-6 (AGOSTINHO *et al.* 2013). And finally, the Slx4 ortholog HIM-18 was shown to function in both pathways, perhaps acting as a scaffold to keep pathway components in close proximity (AGOSTINHO *et al.* 2013; SAITO *et al.* 2013). In *C. elegans*, resolvases in both pathways must be perturbed before crossover number is reduced: *mus-81* single mutants have wild-type levels of crossovers, as do *xpf-1* single mutants, while *mus-81; xpf-1* double mutants have fewer crossovers than wild-type animals (AGOSTINHO *et al.* 2013; SAITO *et al.* 2013). Remaining crossovers in the *mus-81; xpf-1* double mutant must be resolved by a third, as yet unidentified resolvase. These studies, along with those in *S. cerevisiae*, reveal the previously unsuspected complexity of meiotic crossover resolvases.

In *C. elegans*, there are two classes of crossover that are distinguished cytologically. COSA-1 is a conserved meiotic protein that localizes to crossovers in wild-type animals, making a convenient cytological marker for crossovers in late prophase I (YOKOO *et al.* 2012). *C. elegans* animals known to have multiple crossovers per chromosome have only one COSA-1 focus per homolog pair (YOKOO *et al.* 2012). Therefore, animals with excessive numbers of DSBs create two types of crossover: those marked by COSA-1, and those not marked by COSA-1. This result corroborates an earlier finding that crossovers in conditions of excess DSB formation are not associated with ZHP-3, an earlier cytological marker of COSA-1-marked crossovers (YOUDS *et al.* 2010). It is not known whether COSA-1 only marks crossovers generated by a specific resolvase, or whether it can mark crossovers generated by any resolvase. However, these data suggest that conditions creating multiple crossovers might also create opportunities for cryptic crossover resolving pathways, or create a requirement for both wild-type crossover pathways.

In this study, we have tested whether crossover pathway preference can be influenced by exposure to chromosomal insults. In *C. elegans*, certain conditions create more DSBs and

subsequently, more crossovers. These conditions also perturb crossover regulation to generate multiple crossovers on a single chromosome. The first condition, ionizing radiation, induces DSBs in a dose-dependent manner, and irradiated animals have a corresponding increase in crossovers (YOKOO *et al.* 2012). Previously, MUS-81 was shown to be required for a crossover increase in a region of Chromosome V induced by a high dose of radiation, and we have tested the generality of this observation using a higher-resolution, chromosome-wide analysis (YOUDS *et al.* 2010). The second condition we examined was depletion of condensin, a highly-conserved member of the SMC (Structural Maintenance of Chromosome) family that restructures chromosomes in preparation for segregation. *C. elegans* has three condensin complexes: condensin I and condensin II have roles during mitosis and meiosis, while the third functions in the dosage compensation complex to mediate gene expression during embryogenesis (CSANKOVSZKI *et al.* 2009; METS and MEYER 2009). Reducing the concentrations of either condensin I or condensin II during meiosis disrupts chromosome structure as reflected by lengthened chromosome axes (METS and MEYER 2009). This change in structure correlates with an increase in meiotic DSBs, which also correlates with an increase in crossovers and a shift in their distribution along Chromosome X (TSAI *et al.* 2008; METS and MEYER 2009)

By examining the involvement of each known resolvase in irradiated and condensin-depleted animals, we show that XPF-1 and MUS-81 have a differential usage that is not apparent in untreated wild-type animals. Although both are sufficient for wild-type crossovers, we describe conditions in which both XPF-1 and MUS-81 become essential, and showed that their requirement correlated with the severity of the chromosomal insult: XPF-1 and MUS-81 both become required for crossovers in animals exposed to doses of radiation above 2.5 grays and in animals depleted of both condensin complexes. We present evidence that the requirement for MUS-81 is not solely invoked by the absolute number of DSBs, but rather by the presence of DNA damage or an altered chromosome structure. Additionally, we found that combining two conditions that did not independently create a requirement for a particular resolvase could create a requirement for MUS-81 or XPF-1. These results are the first indication that in *C. elegans*, some DSBs may be resolved into crossovers by different pathways, perhaps depending on their provenance or specific threats against the meiotic cell.

Results

Both MUS-81 and XPF-1 are required for crossovers induced by ionizing radiation

Ionizing radiation creates germline DSBs in a dose-dependent manner (YOKOO *et al.* 2012), leading to an increase in crossovers. An animal exposed to a dose of 7.5 grays has nearly twice the number of crossovers s on both Chromosome X and Chromosome II as untreated control animal (Figures 1 and 2) (METS and MEYER 2009). Neither XPF-1 nor MUS-81 are required for crossover formation in untreated wild-type animals (AGOSTINHO *et al.* 2013; O'NEIL *et al.* 2013; SAITO *et al.* 2013), and we first investigated whether irradiation could change the dependence on these resolvases. A previous study showed that, within a genetic interval spanning nearly a fifth of Chromosome V, MUS-81 is required to resolve crossovers induced by 20 grays of irradiation (YOUDS *et al.* 2010). We tested the generality of this observation using a higher-resolution, chromosome-wide analysis.

To determine whether MUS-81 is required for crossover formation at lower levels of DNA damage, we conducted a higher-resolution, chromosome-wide analysis of crossover formation on the X chromosome and an autosome. We exposed animals to doses ranging from 0.5 to 10 grays, a dose that creates twice as many DSBs in wild-type animals as untreated controls (Figures 1-4) (YOKOO *et al.* 2012). Using six single nucleotide polymorphisms that are also restriction fragment length polymorphisms (snip-SNPs), we assayed crossover formation in five genetic intervals spanning approximately 80% of Chromosome X and 78% of Chromosome II. This analysis allowed us to measure both the frequency of crossovers in any given interval (which sum to the map length), as well as the incidence of multiple crossovers on a single chromosome. Since *C. elegans* chromosomes typically have just one crossover, a chromosome that receives two crossovers represents a noteworthy disruption of crossover regulation (NABESHIMA *et al.* 2004; HAMMARLUND *et al.* 2005). In determining whether two genotypes receive significantly different numbers of crossovers, we sort chromosomes into classes based on the number of crossovers they receive (from zero to four) and compare the full distribution of chromosome classes between both genotypes.

We first examined crossovers on Chromosome X and II at different doses of radiation in wild-type animals, as well as *mus-81* and *xpf-1* single mutants. In wild-type animals, crossover number increases linearly with dose (Figures 1-4). At the two highest doses examined, we observe a decrease in the class of chromosomes that receive no crossovers (the products of oocytes that received non-recombinant chromatids). This observation may suggest that, as more crossovers are formed on a chromosome, more chromatids are involved in strand-exchange. Chromatid interference, which prevents chromatids from being used to generate a crossover if they have already been involved in strand exchange, is another aspect of crossover interference that has previously been theorized (ZHAO *et al.* 1995; TEUSCHER *et al.* 2000). Recent empirical support for chromatid interference has been discovered in human oocytes (HOU *et al.* 2013).

In *mus-81* mutants irradiated with 0.5 or 1 gray, map length increased by a similar amount as that in comparably irradiated wild-type animals (Figures 1 and 2), and the distribution of chromosome classes did not differ significantly between the two genotypes (Figures 3 and 4). At

these low doses, both wild-type animals and *mus-81* mutants have a low number of multiple-crossover chromosomes. However, at doses of 2.5 grays and higher, map length in irradiated *mus-81* mutants is similar to that observed in unirradiated *mus-81* mutants. Consistent with this observation, at these higher does, chromosome classes in irradiated *mus-81* animals differed significantly from those in comparably irradiated wild-type animals ($P < 0.01$, Fisher's exact test), though we still observe infrequent double crossovers (Figures 3 and 4). Thus, while MUS-81 was not required for crossover formation at doses below 1 gray, higher amounts of radiation invoke a dependence on MUS-81. The dose-dependent requirement for MUS-81 could be invoked by the amount of DNA damage, perhaps as measured by DSB number. Alternatively, MUS-81 may become required as a response to irradiation, and not necessarily to the number of DSBs created. We investigate these possibilities later in this study.

In contrast, in *xpf-1* mutants, we observe a complete suppression of extra crossovers induced by 1 gray, 2.5 grays, and 7.5 grays of radiation (Figures 5 and 6). At these doses, map length in *xpf-1* mutants is similar to that in unirradiated wild-type animals. Consistent with this observation, chromosome classes differ significantly from those in comparably irradiated wild-type animals ($P < 0.03$ for all three doses). Therefore, in animals exposed to low levels of radiation, MUS-81 is not required to generate crossovers, while XPF-1 is necessary for the increase in crossovers induced by low levels of radiation. The comparable number of crossovers between unirradiated wild-type animals and irradiated *xpf-1* single mutants suggests that XPF-1 is the predominant resolvase used for the radiation-induced increase in crossovers.

Consistent with prior studies, we observed that crossover number is reduced but not eliminated in unirradiated *mus-81; xpf-1* double mutants (Figures 5 and 6) (AGOSTINHO *et al.* 2013; SAITO *et al.* 2013). When compared to wild-type animals, map lengths in *mus-81; xpf-1* double mutants are reduced on both chromosomes (Figure 5 and 6). At all doses, map length in irradiated *mus-81; xpf-1* double mutants remained similar to that in unirradiated *mus-81; xpf-1* double mutants, and multiple-crossover chromosomes were never observed (Figures 5 and 6). Thus, unlike crossovers in wild-type animals, the extra radiation-induced crossovers are completely dependent on both XPF-1 and MUS-81. These data indicate that, in addition to creating crossovers that are not marked by GFP:COSA-1, radiation-induced crossovers differ from those in wild-type animals because they require XPF-1 and, depending on dose, MUS-81 for their resolution.

Apoptosis does not account for the loss of radiation-induced crossovers in *mus-81* mutants

In female germlines, damaged nuclei are removed by apoptosis, which is triggered by a checkpoint that recognizes unrepaired DSBs (GARTNER *et al.* 2000; BHALLA and DERNBURG 2005). We have shown that radiation increases crossovers in a MUS-81- and XPF-1-dependent manner – but if oocytes with higher numbers of DSBs (and therefore potential crossovers) are preferentially removed, the suppression observed in irradiated *mus-81* and *xpf-1*single mutants could be due to apoptosis of the most damaged nuclei. To distinguish between suppression by mutations in *mus-81* or an apparent suppression by apoptotic culling, we examined crossover formation in *mus-81; ced-4* double mutants (Figures 7 and 8). The *ced-4* gene is required to initiate apoptosis, and damaged

nuclei are not removed in a *ced-4* mutant (ELLIS and HORVITZ 1986; GARTNER *et al.* 2000). The map length of irradiated *mus-81; ced-4* double mutants is similar to that of *mus-81* single mutants, and chromosome classes do not differ significantly. These data indicate that abrogating apoptosis in a *mus-81* mutant background does not increase crossover numbers, making it unlikely that suppression is due to apoptosis.

Mutations that disrupt crossover resolution create chromosome non-disjunction, resulting in aneuploid embryos which will eventually die. Defects in both apoptosis and DSB repair should increase the number of embryos with unrepaired meiotic DSBs, thereby causing an increase in embryonic lethality. If the suppression of crossovers observed in *mus-81* mutants at 2.5 grays or higher is primarily due to culling of damaged oocytes, we expect to see a decoupling between embryonic lethality and irradiation dose, especially between 1 and 2.5 grays. To test this hypothesis, we assayed embryonic lethality in irradiated animals with defects in apoptosis.

In accordance with previous reports, we observed 7.8% embryonic lethality in *mus-81* mutants and 26.6% embryonic lethality in *ced-4* mutants (Figure 9) (O'NEIL *et al.* 2013). In *mus-81; ced-4* double mutants, we observed a comparable amount of lethality as in *ced-4* single mutants (17.5% in *mus-81; ced-4*). In *mus-81; ced-4* double mutants, embryonic lethality increased in a linear manner relative to radiation dose ($R^2 = 0.95$, Figure 9). Lethality did not differ significantly until animals have been exposed to 7.5 grays, at which point *mus-81; ced-4* double mutants had more lethality than *ced-4* single mutants. These data support a decoupling between the transition to MUS-81-dependent crossovers from 1 gray to 2.5 grays and the linear increase in embryonic lethality, suggesting that the suppression of crossovers by a *mus-81* mutant background is not due solely to apoptotic culling of nuclei with the most crossovers.

In the absence of SPO-11-induced DSBs, *mus-81* is required to resolve radiation-induced DSBs

We have shown that MUS-81 is required for a radiation-induced increase in crossovers, but the animals we examined received DSBs from two sources: ectopic breaks from radiation and endogenous breaks from SPO-11. Therefore, we do not know whether MUS-81 is required specifically for DSBs induced by radiation, by SPO-11, or for both. To differentiate between the repair of SPO-11-induced DSBs and radiation-induced DSBs, we used a *spo-11* genetic background, which cannot form DSBs and therefore has no crossovers. Radiation generates artificial DSBs that can partially rescue the nearly complete lethality of *spo-11* mutants (Figure 10) (DERNBURG *et al.* 1998). In *spo-11* single mutants, we observe 96% embryonic lethality, which is reduced to 64% in animals exposed to 7.5 grays (Figure 10). To see whether the absence of MUS-81 affects the radiation-induced rescue of animals lacking SPO-11, we examined embryonic lethality in *spo-11; mus-81*double mutants. In both irradiated and unirradiated *spo-11; mus-81* double mutants, we observe complete embryonic lethality (Figure 10). Therefore, in irradiated animals, we see a complete dependence on MUS-81 for crossover formation in the absence of SPO-11.

Oocytes lacking *spo-11*-induced DSBs need to receive at least one DSB on each autosome to produce a viable embryo. The X chromosome does not need to receive a DSB or crossover, since in

C. elegans, embryos with one X develop into male. An X chromosome non-disjunction would generate an oocyte that lacks X, which, when fertilized by a sperm with an X, becomes an XO male embryo. Therefore, assays of embryonic survival are a stringent measure of crossover formation, requiring an oocyte to receive at least five crossovers. As a more sensitive assay able to detect crossovers that may form in oocytes that do not reach this level of DSB formation, we counted DAPI-stained bodies in diakinesis oocytes of animals lacking SPO-11 and either MUS-81 or XPF-1 (Figure 11). Diakinesis nuclei in wild-type animals have six DAPI bodies, one for each homolog pair. Because no crossovers form in *spo-11* mutants, homolog pairs are not held together during diakinesis and create twelve DAPI bodies, one for each homolog (Figure 11) (DERNBURG *et al.* 1998). Irradiated *spo-11* mutants had a reduction in DAPI bodies to 7.8, indicating that at least four chromosomes per nucleus received a crossover. Like unirradiated *spo-11* mutants, unirradiated *mus-81; spo-11* and *xpf-1; spo-11* double mutants have nearly twelve DAPI bodies. At 7.5 grays, each double mutant had 8.9 DAPI bodies, which is fewer than seen in unirradiated double mutants, but still higher than seen in comparable irradiated *spo-11* single mutants (Figure 11a).

As observed when crossovers were assayed in irradiated animals lacking MUS-81 or XPF-1, a mutation in the *xpf-1* gene has a stronger defect in rescue from radiation than a mutation in the *mus-81* gene. The average number of DAPI bodies in irradiated *xpf-1; spo-11* double mutants is only slightly higher than seen in irradiated *spo-11* single mutants, but the distribution of nuclei with specific numbers of DAPI bodies is significantly different between the two genotypes ($p < 0.02$, Student's t-Test). Though we observe a similar distribution in *mus-81; spo-11* double mutants as in *xpf-1; spo-11* double mutants, nuclei distributions in *mus-81; spo-11* animals is not significantly different than *spo-11* single mutants. Therefore, in irradiated animals lacking SPO-11-induced DSBs, both MUS-81 and XPF-1 are required for the formation of some crossovers. However, at 7.5 grays, we did not see a complete rescue of DAPI body number in *spo-11* mutants, which makes it difficult to interpret DAPI body distributions in *mus-81; spo-11*and *xpf-1; spo-11* double mutants. A more definitive comparison could be made by repeating this analysis at 10 grays, a dose at which nearly complete rescue is observed in *spo-11* single mutants.

In the *spo-11* single mutant and *mus-81; spo-11* or *xpf-1; spo-11* double mutants, radiation reduced the number of DAPI bodies, indicating the formation of radiation-induced crossovers. In irradiated *spo-11* mutants, we observed a corresponding rescue of embryonic lethality, but we saw no rescue of embryonic lethality in irradiated *mus-81; spo-11* double mutants, despite the apparent formation of rescuing crossovers as indicated by lower numbers of DAPI bodies. Nuclei with six DAPI bodies should have received a sufficient number of crossovers to create a viable embryo, and both double mutants had nuclei that met this requirement (17% in irradiated *mus-81; spo-11* and 13% in irradiated *xpf-1; spo-11* double mutants) (Figure 11a). However, the complete lethality observed in *mus-81; spo-11* indicates that chromosome segregation still fails. During diakinesis, chromosomes rearrange themselves around the site of crossovers to form the characteristic compact DAPI bodies called bivalents, consisting of homolog pairs; chromosomes that do not receive a crossover condense into univalents, one for each homolog. At this stage of meiosis, crossovers manifest as physical linkages called chiasmata (ZICKLER and KLECKNER 1999). Some DAPI bodies in *mus-81; spo-11* and *xpf-1; spo-11* double mutants are held in close proximity by DNA linkages, and were

therefore scored as one DAPI body. However, examination of chromosome axis staining reveals that some of these DAPI bodies lack a true chiasmata, which makes them disassociated bivalents (Figure 11b) (AGOSTINHO *et al.* 2013). Although these DAPI bodies are held together in closer proximity than univalents, they are incapable of correctly orienting homologs for proper segregation. This observation may explain why we only see a mild DAPI bodies increase in *xpf-1; spo-11*and *mus-81; spo-11* double mutants; because we only counted the total number of DAPI bodies and did not score the numbers of diassociated bivalents versus true bivalents. When we repeat the analysis at 10 grays, in addition to the number of DAPI bodies, we will assay the incidence of bivalents, disassociated bivalent, and univalents. It is also possible that the loss of MUS-81 or XPF-1 in *spo-11* mutants may impair repair of DSBs induced by radiation, as our assay does not allow us to distinguish between unrepaired DSB intermediates or crossovers that do not form a chiasma. An experiment that would determine whether the increase in disassociated bivalents corresponds to a decrease in COSA-1-marked chiasmata is a comparison of COSA-1foci in irradiated *spo-11* mutants to foci numbers in *spo-11; mus-81* or *spo-11; xpf-1* double mutants.

Radiation creates chiasmata that require COSA-1

To determine whether chiasmata in irradiated animals, like those in wild-type animals, require COSA-1, we examined diakinesis DAPI bodies in irradiated *cosa-1* mutants (Figure 12). At 7.5 grays, we observed twelve DAPI bodies in *cosa-1* mutants (Figure 12). Therefore, although radiation creates crossovers that differ from wild-type in that they are dependent on MUS-81 and XPF-1 and are not marked by COSA-1, they still require COSA-1 for their formation. An experiment that would determine whether *cosa-1* is also required for chiasmata in the absence of SPO-11-dependent DSBs, is to examine DAPI bodies in irradiated *cosa-1; spo-11* double mutants.

Examining the involvement of other crossover resolvases

GEN-1 is another enzyme that can resolve double Holliday junctions *in vitro,* and acts in *S. cerevisiase* in the absence of Mus81 and the primary crossover resolving pathway (ZAKHARYEVICH *et al.* 2012; DE MUYT *et al.* 2012). However, in *C. elegans*, *gen-1* single mutants have no obvious meiotic phenotype and no evidence suggests that GEN-1 acts in the absence of either MUS-81 or XPF-1 (BAILLY *et al.* 2010; AGOSTINHO *et al.* 2013; SAITO *et al.* 2013). To determine whether GEN-1 has a role in resolving radiation-induced crossovers, we exposed *gen-1* single mutants to 7.5 grays of radiation (Figure 13). Map lengths in irradiated and unirradiated *gen-1* single mutants were nearly the same as in similarly-treated wild-type animals, and multiple-crossover chromosome classes did not differ significantly from those of wild-type animals. Therefore, radiation-induced crossovers, like those in wild-type animals, do not require GEN-1 for their resolution.

In contrast, the Bloom helicase ortholog HIM-6 was found to act in the same crossover-resolving pathway as XPF-1 (AGOSTINHO *et al.* 2013). To determine whether HIM-6 has a similar role as XPF-1 in irradiated animals, we assessed whether HIM-6 is required for a radiation-induced increase in crossovers (Figure 14). In accordance with previous studies, unirradiated *him-6* single

mutants had a 20% decrease in map length compared to wild-type animals (Figure 14) (WICKY *et al.* 2004; SCHVARZSTEIN *et al.* 2014). At 7.5 grays, map length is higher in *him-6* single mutants than in unirradiated *him-6* animals, but still lower than in comparably irradiated wild-type animals. Additionally, irradiated *him-6* single mutants had a significantly different distribution of chromosome classes than irradiated wild-type animals ($P < 0.001$). These data indicate that HIM-6 is required for some irradiation-induced crossovers, but not to the same extent as XPF-1, since irradiated *him-6* mutants still had significantly more multiple-crossover chromosomes than irradiated *xpf-1*single mutants ($P < 0.01$). We conclude that HIM-6 plays a role in resolving radiation-induced crossovers, but is not required in the same manner as XPF-1. In wild-type animals, XPF-1 and HIM-6 act in the same pathway, and we are examining crossovers in irradiated *xpf-1; him-6* double mutants to see if both components also act in the same pathway for radiation-induced crossovers.

Establishing condensin depletion as a condition to query resolvase requirement for SPO-11-induced crossovers

We have shown that ionizing radiation, a condition that creates artificial DSBs, and therefore extra crossovers, creates a dependence on both MUS-81 and XPF-1. We next examined another condition that also creates extra DSBs and crossovers, but does so in a SPO-11-dependent manner: condensin depletion. Reducing the concentrations of meiotic condensin increases DSB and crossover number, and this increase correlates with extended chromosome axes; in condensin-depleted animals, the increase in DSBs, but not the axis extension, requires SPO-11 (TSAI *et al.* 2008; METS and MEYER 2009). Condensin complexes have well-conserved roles in chromosome dynamics, repression of gene expression, and development (WOOD *et al.* 2010). *C. elegans* has three condensins, each with separate functions in dosage compensation, chromosome segregation, and crossover control (CSANKOVSZKI *et al.* 2009; METS and MEYER 2009). The two meiotic condensins, condensin I and condensin II, share SMC subunits but differ in their CAP (chromosome-associated protein) paralogs. Condensins are essential, and disruption of condensin complexes causes embryonic lethality. Mutations in genes encoding condensin I and condensin II components have a dominant effect on crossover frequency, which permits us to examine recombination in animals with heterozygous mutations and avoid the complication of recessive lethality (METS and MEYER 2009)

Condensin depletion provides another opportunity to test whether this condition, which affects DSB and crossover number, also affect crossover resolution pathways. To prepare for an analysis of resolvase requirement, we first characterized chromosome axis length and DSB number in animals with two different levels of condensin disruption. Condensin's role in higher-order chromosome structure suggest a means by which its depletion might affect DSB formation and the pathways used for their repair. Mets and Meyer reasoned that changes in chromosome structure might also affect the length of a chromosome axis, the protinaceous core around which meiotic chromatin is organized (BHALLA and DERNBURG 2008; METS and MEYER 2009). They demonstrated that chromosome axis length is extended in condensin I and condensin II single mutants, reflecting an alteration of overall chromosome structure (METS and MEYER 2009). They

also showed that exposure to radiation does not affect chromosome axis length, indicating that the increase in DSBs does not necessarily cause axis changes; therefore, condensin-depletion creates more DSBs in correlation to axis extension (METS and MEYER 2009). In early pachytene, consistent with the results of Mets and Meyer, we observe nearly 50% longer X chromosome axes in *dpy-26/+* mutants (henceforth called condensin I mutants) and in *kle-2/+* mutants (henceforth called condensin II mutants) when compared to wild-type (Figure 15). When both paralogs are depleted in *kle-2/+; dpy-26/+* double trans-heterozygotes (henceforth called condensin double mutants), X-chromosome axis length is longer than in wild-type animals, but not significantly longer than in either single mutant.

We next assayed DSB formation in both condensin single mutants and in the condensin double mutant using an antibody against RAD-51, a RecA homolog that binds to nascent DSBs (ALPI *et al.* 2003). During the course of meiosis, RAD-51 appears as discrete foci on chromosomes in transition zone nuclei (which corresponds to the meiotic stage of leptotene-zygotene), reaches a peak in mid-pachytene nuclei, and is nearly absent from nuclei by the end of pachytene. In wild-type animals, we observe an average of 5.1 RAD-51 foci per nucleus at mid-pachytene, consistent with prior reports (Figure 16a) (ALPI *et al.* 2003; METS and MEYER 2009; NOTTKE *et al.* 2011; ROSU *et al.* 2011; SAITO *et al.* 2012). In condensin I mutants, we observe an increase to 7.1 foci per nucleus, and in condensin II mutants, to 6.9 foci per nucleus. In condensin double mutants, we observed an average of 7.5 foci per nucleus, which is comparable to the increase observed in either condensin single mutant when compared to wild-type animals (Figure 16a). At med-pachytene, the distribution of nuclei in either condensin single mutant did not significantly differ from the distribution of nuclei in the condensin single mutants (Figure 16b, Mann-Whitney U). Therefore, condensin disruption changes the number of DSBs in both condensin single mutants and the condensin double mutant, but depleting both condensins does not increase DSB number more than depleting just one condensin. These data correlate with the observation that depleting condensin disrupts chromosome axes (Figure 15) (METS and MEYER 2009). However, this assay only captures a subset of DSBs at the time of sample fixation, since DSB repair is an ongoing process throughout meiosis (ALPI *et al.* 2003).

In our analyses of chromosome axis length and DSB number, we did not observe a striking difference between condensin double mutants and condensin single mutants. However, we did observe a qualitative difference in the chromosome axes of condensin double mutants, where immunostaining against a chromosome axis component was sometimes less continuous than we observed in condensin single mutants, indicating a further disruption of chromosome structure that was not reflected by axis length. Therefore, condensin depletion, like radiation, may allow us to query resolvase dependence in a condition with multiple levels of chromosomal insult (depending on whether one condensin is disrupted or both are disrupted).

Depleting condensins does not increase COSA-1 foci

To further characterize the extra crossovers created by condensin depletion, we assessed whether they have the same cytological properties as those generated by radiation. COSA-1 localizes

to crossovers in late pachytene, and make a convenient cytological marker for crossovers at this stage (YOKOO *et al.* 2012). Irradiated *spo-11* single mutants have only one COSA-1 focus per chromosome, even at very high doses that create excessive numbers of DSBs (YOKOO *et al.* 2012). Previously, Yokoo and colleagues examined COSA-1 foci in the condensin I mutant *dpy-28 (s939)*, and showed that X chromosomes only had one COSA-1 focus, despite the genetic observation of double crossovers in this background (METS and MEYER 2009; YOKOO *et al.* 2012). To extend this observation, we have examined COSA-1 foci in both condensin single mutants and the condensin double mutant (Figures 17). In all cases, we observe levels of COSA-1 foci that do not differ significantly from the six foci observed in wild-type animals. Therefore, as in irradiated animals, condensin disruption increases crossover frequency without increasing COSA-1 foci. Condensin mutants might also have DSBs that are being resolved by a different pathway than those in wild-type animals.

cosa-1 is required for both crossovers and chiasmata in condensin-depleted animals

Since condensin depletion creates extra crossovers that are not marked by COSA-1, we investigated whether these crossovers were dependent on *cosa-1* like those in wild-type animals by examining both crossover and chiasmata formation in *cosa-1* mutants depleted of condensin. In addition to cytologically marking wild-type crossovers at the end of meiotic prophase I, COSA-1 also plays an earlier role in the formation of crossovers: *cosa-1* mutants have a severe reduction in crossovers and lack chiasmata (YOKOO *et al.* 2012). To determine whether some crossovers in condensin-depleted animals might form independently of COSA-1, we assayed crossovers in *cosa-1/+; dpy-26/+* double mutants. The map length of *cosa-1/+; dpy-26/+* double mutants was reduced in comparison to *dpy-26/+* mutants, though not to the levels observed in *cosa-1/+* mutants (Figure 18). This indicates that some crossovers in *dpy-26/+* animals require COSA-1. Surprisingly, the classes of multiple-crossover chromosomes in the *cosa-1/+; dpy-26/+* double mutant did not differ significantly from those in the *dpy-26/+* single mutant. Therefore, although crossovers in condensin mutants require COSA-1, the remaining crossovers in a *cosa-1/+* mutant can have their regulation perturbed by condensin depletion, as evidenced by the presence of multiple-crossover chromosomes.

We cannot examine crossovers in the complete absence of COSA-1 (since *cosa-1* homozygotes are sterile), but we can examine DAPI body number, since this assay does not require animals to complete a successful meiosis. We have shown that radiation and condensin depletion create extra crossovers that are not marked by COSA-1, and in the case of condensin depletion, require COSA-1. Since a subset of crossovers in condensin mutants require COSA-1, we expect to see no chiasmata in *cosa-1* mutants that are also depleted for condensin. We examined diakinesis DAPI bodies in *cosa-1; dpy-26* double mutants and irradiated *cosa-1* mutants as a proxy for chiasmata formation. Consistent with prior reports, in untreated *cosa-1* mutants, we observe an average of nearly twelve DAPI bodies in diakinesis nuclei (Figure 19a) (YOKOO *et al.* 2012). In *dpy-26* mutants, we see an average of 6.2 diakinesis DAPI bodies; *dpy-26* causes increased X chromosome non-disjunction, which is reflected in a slightly higher average than seen in wild-type animals (HODGKIN

1983; PLENEFISCH *et al.* 1989). *dpy-26* mutants form 19% more crossovers than wild-type animals (Figure 18), which could lead to a comparable frequency of chiasmata formation if these crossovers are *cosa-1*-independent. In *cosa-1; dpy-26* double mutants, we observed an average of 10.6 DAPI bodies, which is significantly lower than *cosa-1* single mutants ($P < .0001$, Student's t-Test) (Figure 19a). Although we see fewer than twelve DAPI bodies in *cosa-1; dpy-26* double mutants, a closer cytological examination reveals that some DAPI bodies which were scored as bivalents are actually disassociated bivalents (Figure 19b). Therefore, crossovers in condensin-depleted animals, like those in irradiated animals, are dependent on COSA-1, even though they are not cytologically marked by COSA-1.

Depletion of both condensins creates an increase in crossovers that requires *mus-81* and *xpf-1*

Condensin depletion creates SPO-11-dependent and COSA-1-dependent crossovers, and we next investigated whether these crossovers also require MUS-81 or XPF-1. To first determine the effects of depleting one condensin or two condensins, we analyzed crossovers in condensin double mutants and each condensin single mutant. Consistent with prior reports, map length of Chromosome X in both condensin single mutants was increased over that in wild-type animals, and both single mutants had a significant increase in multiple-crossover chromosomes ($P < .0001$) (Figure 20) (METS and MEYER 2009). We also observed the previously reported changes in crossover distribution: condensin I mutants had a drastic crossover increase on the right end of Chromosome X, whereas condensin II mutants displayed a crossover increase on the left end (Figure 5a) (METS and MEYER 2009). The differential placement of extra crossovers induced by condensin depletion indicates that both complexes act independently, though they may share an underlying mechanism for regulating crossover formation (Figure 20) (METS and MEYER 2009).

We have taken two different genetic approaches to depleting both condensin complexes to assay crossover formation. MIX-1 is a shared SMC component of both condensin I and condensin II. Consistent with prior reports, in *mix-1/+* single mutants, map length on the X chromosome was increased over wild-type animals (more than seen in either condensin single mutant) and *mix-1/+* mutants had significantly more multiple-crossover chromosomes than wild-type animals ($P < 0.00001$) (Figure 20) (METS and MEYER 2009). The condensin double mutant (the *kle-2/+; dpy-26/+* double trans-heterozygote) had a longer X chromosome map length than observed in *mix-1/+* mutants and nearly a quarter more multiple-crossover chromosomes than wild-type animals ($P < 0.00001$), an increase which exceeds that observed in either single condensin mutant, as well as that observed in *mix-1/+* mutants (Figure 20). This observation corresponds with previously reported axis lengths in *mix-1/+* mutants, which were longer than seen in condensin single mutants, but less than reported in condensin double mutants (Figure 17) (METS and MEYER 2009). Because we are examining trans-heterozygotes, each condensin double mutant still has a half dose of both paralogs. The significant increase in crossover frequency in the condensin double mutant indicates that either these paralogs are unable to substitute for each other either because they are present in limiting quantities, or because they are functionally distinct.

Condensin depletion is a condition that, like radiation, creates more DSBs and crossovers that are not marked by COSA-1, but require COSA-1 for their formation. We next investigated whether the increase in crossovers caused by condensin depletion also require MUS-81 or XPF-1, like that in irradiated animals. Neither a *mus-81* nor a *xpf-1* mutation suppressed crossover formation in either condensin single mutant (Figures 20 and 21). Map length in *mus-81; dpy-26/+* double mutants is comparable to that in *dpy-26/+* single mutants, and map length in *mus-81; kle-2/+* double mutants is comparable to that in *kle-2/+* single mutants. Chromosome classes in either double mutant are not significantly different from those in condensin single mutant (Figure 20). Likewise, map length in *xpf-1; dpy-26/+* is comparable to *dpy-26/+* single mutants, and chromosome classes do not differ significantly between the two backgrounds (Figure 21).

To examine whether MUS-81 and XPF-1 are required when both condensin complexes are disrupted, we assayed crossover formation on the X chromosome in both *mix-1/+* animals and condensin double mutants (Figures 20 and 21). Map length in *mus-81; mix-1/+* double mutants is less than in *mix-1/+* single mutants, and multiple-crossover chromosomes are reduced ($P < .001$) (Figure 20). MUS-81 was also required for the increase in crossovers observed in condensin double mutants. Map length in *mus-81; kle-2/+; dpy-26/+* triple mutants is reduced with compared to the condensin double mutant (nearly to the length observed in condensin single mutants), and multiple-crossover chromosomes are significantly reduced in the absence of MUS-81 ($P < .000001$) (Figure 20). An *xpf-1* mutation similarly reduces crossover number on Chromosome X in condensin double mutants (Figure 21). Map length in the triple mutant *xpf-1; kle-2/+; dpy-26/+* was much less than observed in condensin double mutants and nearly equivalent to that observed in condensin single mutants, and multiple-crossover chromosomes were significantly reduced in the triple mutant ($P <.0001$). Therefore, MUS-81 and XPF-1 are both required for the large increase in crossovers that result from depleting both condensin complexes. To see whether condensin depletion can generate a requirement on other chromosomes in the same manner as irradiation, we are extending this analysis to Chromosome II. A mutation in *mus-81* only partially suppresses the crossover increases, since both genetic backgrounds still have chromosomes with double crossovers. Although crossovers in wild-type animals can be generated using either MUS-81 or XPF-1, the lack of one resolvase does not affect crossover formation. In contrast, depletion of both condensin complexes reveals three different types of crossover: some that require neither XPF-1 nor MUS-81, some that require MUS-8, and others that require XPF-1.

A resolvase requirement can be invoked by combining insults that do not independently cause a requirement

The difference in requirement for XPF-1 or MUS-81 between depleting one condensin and depleting both condensins resembles the threshold of MUS-81-dependency observed between 1 gray and 2.5 grays in irradiated animals. Together, these data suggest that certain conditions must be met before crossovers become dependent on both resolvases. To invoke a requirement for MUS-81, animals must be depleted of both condensins or expose to doses of radiation higher than 2.5 grays. To become dependent on XPF-1, animals must be depleted of both condensins or exposed to any

dose of radiation. Therefore, we have identified two conditions in which MUS-81 is not required for crossover formation: depletion of one condensin complex and radiation at doses below 1 gray. A requirement for MUS-81 is invoked by intensifying either of these conditions, whether by depleting both condensins or increasing the dose of radiation. Therefore, we theorized that combining two insults which, on their own, do not create a requirement for MUS-81, might generate a new condition in which crossovers do require MUS-81. To test this possibility, we exposed condensin I single mutants to 1 gray of radiation (Figures 22-25).

At 1 gray, *mus-81; dpy-26/+* double mutants had a smaller X chromosome map length and fewer multiple-crossover chromosomes than irradiated *dpy-26/+* single mutants ($P < 0.05$) (Figure 22). Map length in *mus-81; dpy-26/+* double mutants exposed to 1 gray is comparable to unirradiated *mus-81; dpy-26/+* double mutants. At a higher dose of 7.5 grays – which was sufficient to generate a requirement for MUS-81 in wild-type animals – *mus-81; dpy-26/+* double mutants have a more drastic suppression of map length than at the 1 gray dose (Figure 22) - when compared to irradiated condensin I single mutants, map length on Chromosome X was reduced. At this dose, multiple-crossover chromosomes were also suppressed in double mutants ($P < 0.002$). Reflecting the higher suppression observed at 7.5 grays, map length in irradiated *mus-81; dpy-26/+* double mutants is even lower than in unirradiated *mus-81; dpy-26/+* double mutants, and is comparable to that observed in unirradiated wild-type animals.

One difference between the radiation-induced requirement for XPF-1 and MUS-81 is that XPF-1 was required at all irradiation doses, while MUS-81 was required at doses above 2.5 grays. In contrast, both MUS-81 and XPF-1 were not required for the extra crossovers observed in a condensin single mutant. As expected, when we combined two DNA damaging conditions in an *xpf-1* mutant background, we also observe suppression (Figures 23 and 24). The map lengths of Chromosome X and Chromosome II in *xpf-1; dpy-26/+* double mutants exposed to 1 gray was less than in irradiated condensin I single mutants, and multiple-crossover chromosomes were reduced in the irradiated double mutant ($P < 0.02$). At the high dose of 7.5 grays, the map lengths of both chromosomes in *xpf-1; dpy-26/+* double mutants was less than in irradiated condensin I single mutants, and we did not observe any multiple-crossover chromosomes in the double mutant ($P < .02$). At all doses, map length in *xpf-1; dpy-26/+* double mutants was comparable to similarly irradiated *xpf-1* single mutants and to unirradiated wild-type animals (Figures 23 and 24). These data demonstrate that the combination of two DSB-inducing conditions can generate resolvase-dependent crossovers via damaging conditions that, on their own, create crossovers that are not dependent on any one resolvase.

Depleting condensin without increasing DSB number affects the requirement for MUS-81 in irradiated animals

To determine whether a resolvase requirement is invoked by the presence of DNA damage, we used a genetic background that depletes condensin without increasing the numbers of DSBs or crossovers. DPY-28 is a component of condensin I, and its partial loss-of-function allele *y283* does not increase DSB number or create extra crossovers on the X chromosome, but still alters crossover

distribution in the same way as mutations in other condensin I components (TSAI *et al.* 2008; METS and MEYER 2009). Map length in *dpy-28 (y283)* mutants is comparable to that in wild-type animals, and consistent with prior reports, we did not observe multiple-crossover chromatids in this background (Figure 25) (TSAI *et al.* 2008; METS and MEYER 2009). As was observed in other condensin single mutants (*dpy-26/+* and *kle-2/+*) MUS-81 is not required for crossover formation in *dpy-28 (y283)* mutants: map length in *mus-81; dpy-28 (y283)* double mutants is comparable to that in *dpy-28 (y283)* mutants, and chromatid classes in these backgrounds do not significantly differ.

Exposing *dpy-28 (y283)* mutants to radiation allows us to separate the presence of DNA damage from the number of DSBs created, since depletion of condensin by the *y283* allele does not create excess DSBs. At a high dose of 7.5 grays (which generates a requirement for MUS-81 in wild-type animals), map length in *mus-81; dpy-28 (y283)* double mutants was smaller and there were significantly fewer multiple-crossover chromosomes than observed in comparably irradiated *dpy-28 (283)* mutants ($P < 0.01$) (Figure 25). Therefore, a mutation in *mus-81* can suppress part of the radiation-induced increase in crossovers in *dpy-28 (y293)* mutants, indicating that irradiation of *dpy-28 (y283)* mutants does generate a requirement for MUS-81. However, we do not observe the level of suppression by a mutation in *mus-81* as we do in other irradiated condensin single mutants (like *dpy-26/+* mutants, which depletes another component of condensin I). This result indicates that, although the increase in crossovers we observe in irradiated *dpy-28 (y283)* mutants requires MUS-81, a mutation in the *dpy-28 (y283)* gene can partially suppress the radiation-induced requirement for MUS-81. When DPY-26 is depleted from condensin I in irradiated animals, most extra crossovers (that presumably arise from extra DSBs caused both by condensin depletion and radiation) require MUS-81. However, when DPY-28 is depleted by the partial-loss-of-function allele *y283*, extra crossovers (presumably arising from extra DSBs caused only by radiation), and only a subset of these extra crossovers require MUS-81.

We next examined crossovers in *mus-81; dpy-28 (y283)* double mutants at 1 gray, a level that does not generate a MUS-81 requirement in wild-type animals. Map length in *mus-81;dpy-28 (y283)* double mutants exposed to 1 gray is similar to that of comparably irradiated *dpy-28 (y283)* mutants, and classes of multiple-crossover chromosomes do not significantly differ between the two genotypes (Figure 25). Therefore, *dpy-28 (y283)* completely suppresses the requirement for MUS-81 at this dose, which differs from what we observed in *mus-81; dpy-26* animals exposed to 1 gray, where MUS-81 was required for the increase in crossovers. Although it is not clear what effect the *y283* allele has on the DPY-28 protein, we know that *dpy-28 (y283)* affects chromosome structure to the same extent as other condensin I mutants (METS and MEYER 2009). *dpy-28 (y283)* single mutants chromosome axes that are the same length as other condensin mutants, but they only form wild-type levels of DSBs (Mets and Meyer 2009). In *dpy-28 (y283)* animals, irradiation generates crossovers that are MUS-81-independent. We are currently examining whether another allele of the *dpy-28* gene (*s939,* which is genetically null), can also generate radiation-dependent but MUS-81-independent crossovers.

Discussion

In wild-type animals, both XPF-1 and MUS-81 function as parallel and overlapping crossover resolvases, where both are sufficient for crossover formation. In this study, we have described conditions that demonstrate that XPF-1 and MUS-81 cannot in fact substitute for each other: ionizing radiation and condensin depletion. Both conditions perturb DSB number, chromosome structure, and crossover regulation, and we show that these conditions create crossovers dependent on MUS-81 and XPF-1. Exposing animals to any amount of radiation generates crossovers that require XPF-1, and exposing animals to doses of radiation higher than 1 gray generates crossovers that also require MUS-81. In a similar manner, when the concentrations of both meiotic condensins are reduced, XPF-1 and MUS-81 are both required for crossovers. In both irradiated and condensin-depleted animals lacking MUS-81, we observed a residual amount of multiple-crossover chromosomes, whereas in animals lacking XPF-1, we almost never observed multiple-crossover chromosomes; we therefore infer that XPF-1 is the predominant resolvase under these conditions. We also show that two conditions which, acting alone, do not create crossovers that depend on a particular resolvase, can, when combined, induce a resolvase dependence. This indicates that crossover resolution pathways are influenced by factors that act in a combinatorial manner. Although resolvase requirement under these conditions correlates with the extent of DNA damage, we find that the absolute number of DSBs is not the only factor that invokes a requirement. These data suggest that threats to chromosome integrity may influence the usage of DSB repair pathways and affect the type of crossover generated in meiotic cells.

What creates a resolvase requirement under certain conditions? In irradiated animals, a requirement for MUS-81 correlated with the extent of the damage inflicted upon chromosomes – MUS-81-dependent crossovers were only induced at higher doses of radiation. Ionizing radiation creates extra DSBs in correlation to dose severity (YOKOO *et al.* 2012), so the possibility exists that absolute numbers of DSBs act to generate a resolvase dependence. When we examined the resolvase requirement in condensin single mutants exposed to 1 gray of radiation, we saw that both conditions together induced a requirement, even though each alone did not. Therefore, MUS-81 became more important for crossover resolution in situations where a further threat has been added to one that didn't create a requirement for MUS-81 on its own. This results suggests that DSB repair pathway choice is influenced by factors that act in a combinatorial manner. We assessed whether different levels of DNA, damage as measured by DSBs, or whether the insults themselves (whether radiation or condensin-depletion) act to create a resolvase dependence, and demonstrated that DSB number is not the sole determining factor that establishes a resolvase requirement. In animals that lack SPO-11-induced DSBs, exposure to 7.5 grays of radiation produces an amount of DSBs comparable to that observed in unirradiated wild-type animals, but *mus-81; spo-11* and *xpf-1; spo-11* double mutants displayed a slight defect in generating chiasmata when compared to irradiated *spo-11* single mutants (Figure 11) (YOKOO *et al.* 2012). Our results suggest that MUS-81 and XPF-1 become essential for some radiation-induced crossovers, even when the total number of DSBs is at a wild-type level. It seems likely that the presence of DNA damage from radiation induced a requirement for both resolvases. To test this observation more completely, we are repeating these experiments using a

dose that fully rescues chiasmata formation in *spo-11* mutants; this will allow us to definitively assess whether the lack of MUS-81 or XPF-1 hinders crossover formation in the absence of SPO-11-dependent crossovers.

How could DNA-damaging agents affect the pathways of DSB resolution? One possibility is that both irradiation and condensin depletion alter chromosome structure in different ways. Disrupting condensin lengthens entire chromosome axes in a global fashion, whereas IR has a more local effect on axis synapsis: high levels of radiation causes the separation of chromosome axes in late-pachytene nuclei, which may be linked to a DNA damage response induced by the presence of artificial DSBs (COUTEAU and ZETKA 2011). Although the dose used by Couteau and Zetka was tenfold higher than that used in this study, small numbers of extra breaks could still alter chromosome axes in a way that impairs ordinary meiotic repair. Disruption of condensin also affects chromosome structure, as reflected in lengthened chromosome axes (Figure 15) (METS and MEYER 2009). These gross chromosomal changes could shunt DSB repair to pathways that are usually suppressed in meiotic cells, like those used during mitosis. For example, in mitosis, both of the known crossover resolvases in *C. elegans* repair DNA damage in somatic and mitotic cells. Additionally, in *S. cerevisiae*, Mus81 generates mitotic crossovers (HO *et al.* 2010), and mammalian and *S. cerevisiae* homologs of XPF-1 function during nucleotide excision repair and homologous recombination (CICCIA *et al.* 2008).

We have shown that XPF-1 and MUS-81 are required to resolve crossovers in certain conditions, but our crossover assay only examined resolvase requirement in animals that still received endogenous DSBs (and presumably crossovers) formed by SPO-11. To see whether the absence of SPO-11-induced crossovers could influence resolvase dependence, we examined DAPI bodies in diakinesis nuclei as a proxy for chiasmata formation. We show that the loss of either resolvase in animals that also lack SPO-11-dependent crossovers affects the repair of IR-induced DSBs into chiasmata, leading to an increase in DAPI body number. By counting DAPI bodies, we have likely underestimated chiasmata formation in *spo-11; mus-81* and *spo-11; xpf-1*double mutants, because we observed a higher incidence of apparent bivalents that did not have true chiasmata. These DAPI-stained bodies, held together by non-chiasma DNA linkages and therefore scored as one unit, are classified as disassociated bivalents, to distinguish them from bivalents held together by chiasmata and sister chromatid cohesin (AGOSTINHO *et al.* 2013). Therefore, although some radiation-induced breaks were competent to form chiasmata in the absence of MUS-81 or XPF-1, our results suggest that the remaining resolvases are not fully able to resolve radiation-induced breaks as crossovers. This indicates that in irradiated *spo-11* mutants, meiotic cells do not license other cryptic repair pathways than those that have already been reveled in irradiated wild-type animals.

This study adds to our understanding of the complex, interdependent relationships between DSB repair pathways. Perturbations against chromosomes or meiotic cells may activate alternative pathways, which could allow cells to repair most meiotic DSBs and ensure gametic survival. We have described conditions that disrupt the network of DSB repair, creating a dependence on specific crossover resolvases to generate crossovers that are not marked by COSA-1. This establishes a framework for further study of the interactions between different DSB repair pathways, especially in

circumstances that stress the ordinary repair processes. It will be interesting to see how chromosome structure or other local properties at potential crossover sites affects DSB repair pathway choice. These data are the first indication that in *C. elegans*, some DSBs may be resolved into crossovers by different pathways, perhaps depending on their provenance or specific threats against the meiotic cell.

Figure 1.

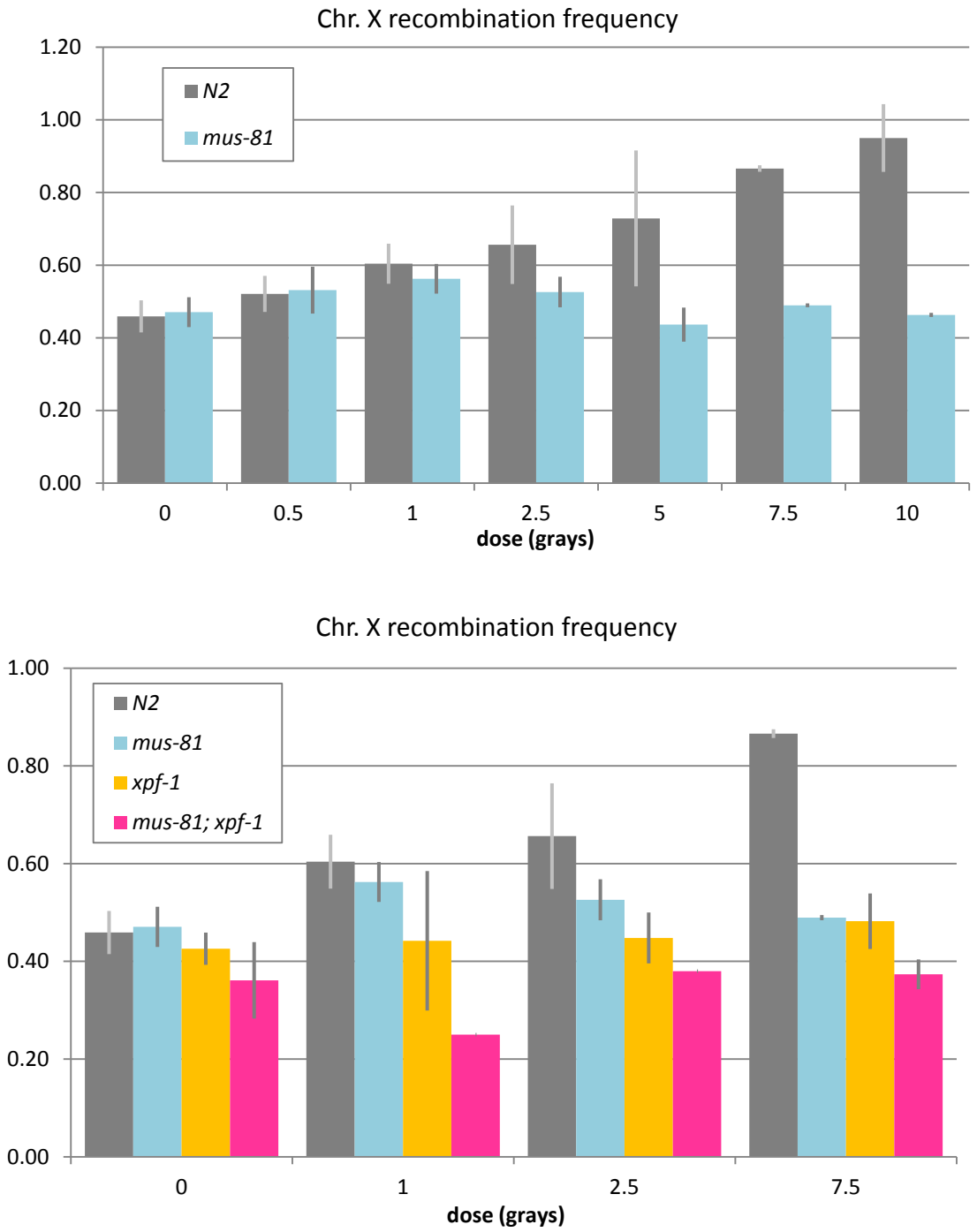

Figure 1. Ionizing radiation generates an increase in genetic map length dependent on *mus-81* and *xpf-1*. Animals were exposed to doses of ionizing radiation ranging from 0 to 10 grays, and crossovers were scored in six intervals on Chromosome X to calculate total map distance. Error bars are standard error of the mean.

Figure 2.

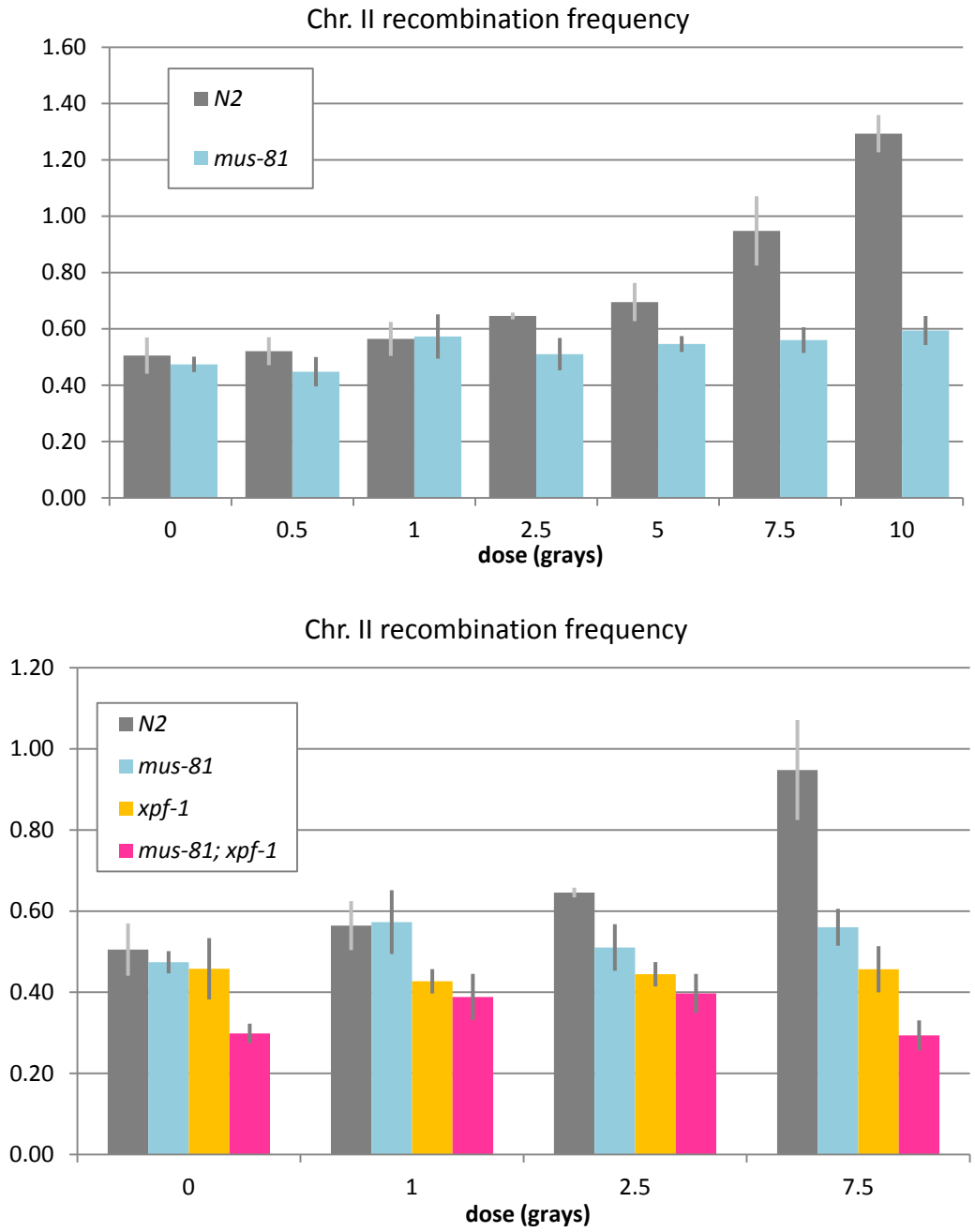

Figure 2. Ionizing radiation generates an increase in genetic map length dependent on *mus-81* and *xpf-1*. Animals were exposed to doses of ionizing radiation ranging from 0 to 10 grays, and crossovers were scored in six intervals on Chromosome II to calculate total map distance. Error bars are standard error of the mean.

Figure 3a.

Chr. X genotype	dose (Gy)	recomb	SEM	chromosomes with indicated number of crossovers: raw values 4	3	2	1	0	N (mothers)	frequencies 4	3	2	1	0
WT	0	0.46	0.04	0	0	0	168	200	368 (10)	0.00	0.00	0.00	0.46	0.55
mus-81	*	0.47	0.04	0	0	3	144	125	272 (6)	0.00	0.00	0.01	0.53	0.46
WT	0.5	0.52	0.05	0	0	4	42	50	96 (4)	0.00	0.00	0.04	0.44	0.52
mus-81		0.53	0.06	0	0	3	45	48	96 (4)	0.00	0.00	0.03	0.47	0.50
WT	1	0.58	0.06	0	1	7	39	49	96 (4)	0.00	0.01	0.07	0.31	0.49
mus-81		0.56	0.04	0	0	8	92	92	192 (7)	0.00	0.00	0.04	0.48	0.48
WT	2.5	0.66	0.11	0	2	12	33	49	96 (4)	0.00	0.02	0.13	0.34	0.51
mus-81	****	0.53	0.04	0	0	1	99	92	192 (4)	0.00	0.00	0.01	0.52	0.48
WT	5	0.73	0.19	0	11	18	70	92	191 (4)	0.00	0.06	0.09	0.37	0.48
mus-81	****	0.44	0.05	0	0	0	80	104	184 (4)	0.00	0.00	0.00	0.43	0.57
WT	7.5	0.87	0.01	0	5	36	69	70	180 (5)	0.00	0.03	0.20	0.38	0.39
mus-81	****	0.49	0.01	0	0	3	87	100	190 (4)	0.00	0.00	0.02	0.46	0.53
WT	10	0.95	0.09	2	10	42	94	68	216 (4)	0.01	0.05	0.19	0.44	0.31
mus-81	****	0.46	0.01	0	0	2	84	104	190 (5)	0.00	0.00	0.01	0.44	0.55

p values between N2 and *mus-81*

Figure 3b.

Chr. X

genotype	dose (Gy)	A - B	B - C	C -D	D -E	E -F	recomb	SEM
WT	0	0.07	0.07	0.13	0.09	0.10	0.46	0.04
mus-81		0.10	0.11	0.09	0.10	0.08	0.47	0.04
WT	0.5	0.06	0.05	0.17	0.08	0.16	0.52	0.05
mus-81		0.07	0.02	0.11	0.18	0.15	0.53	0.06
WT	1	0.08	0.08	0.16	0.16	0.10	0.58	0.06
mus-81		0.09	0.17	0.16	0.07	0.07	0.56	0.04
WT	2.5	0.17	0.15	0.11	0.10	0.13	0.66	0.11
mus-81		0.10	0.09	0.10	0.13	0.11	0.53	0.04
WT	5	0.15	0.17	0.22	0.14	0.06	0.73	0.19
mus-81		0.10	0.05	0.10	0.13	0.06	0.44	0.05
WT	7.5	0.23	0.24	0.21	0.12	0.07	0.87	0.01
mus-81		0.10	0.07	0.11	0.11	0.11	0.49	0.01
WT	10	0.22	0.23	0.24	0.18	0.08	0.95	0.09
mus-81		0.14	0.08	0.07	0.08	0.10	0.46	0.01

relative recombination frequency

4.50+
3.50-4.49
2.50-3.49
1.50-2.49
.50-1.49
0-.49

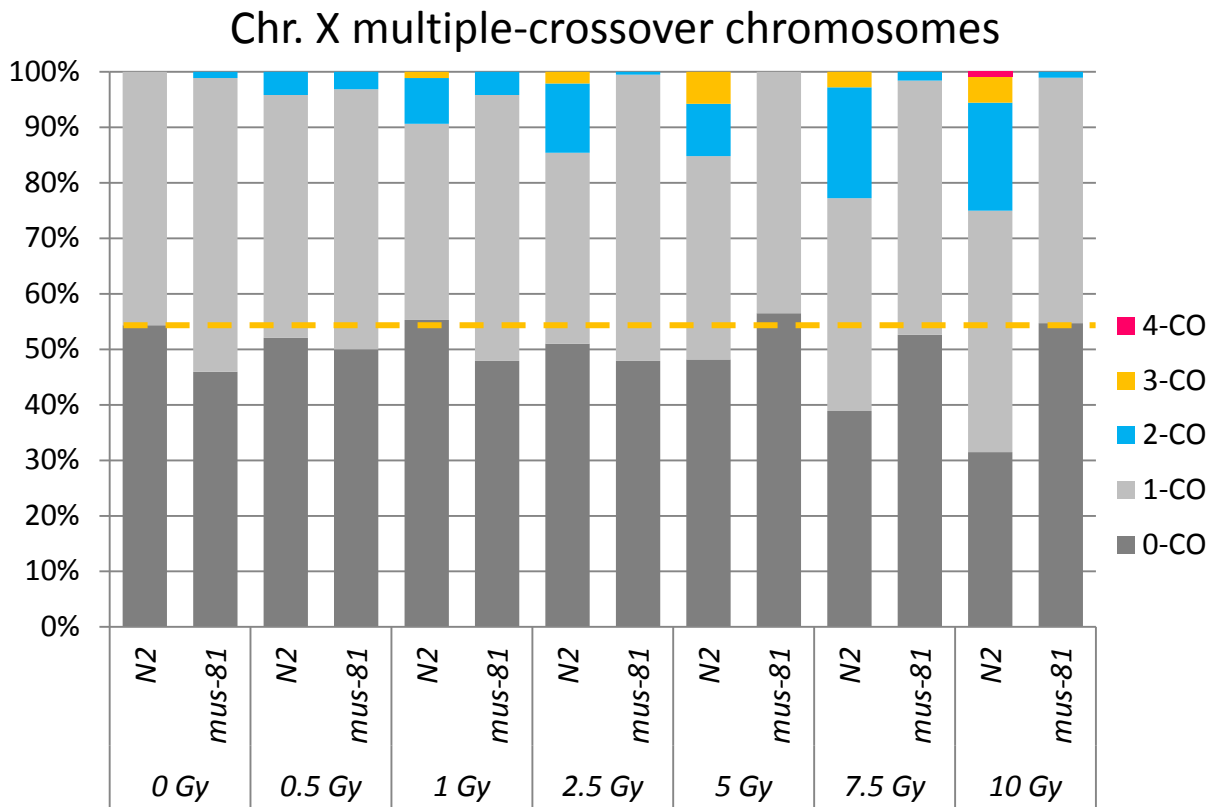

Figure 3. Ionizing radiation creates crossovers that require *mus-81* on Chromosome X. (a) Crossover frequency for *mus-81* mutants using six genetic markers on Chromosome X. Shown are map distance (with standard error of the mean); chromosomes that received either four, three, two, one, or no crossovers; and N values for meiotic products assayed and, in parentheses, meioses assayed. Frequencies were calculated by the formula (number of crossovers in each class)/(total meiotic products assayed). Asterisks indicate statistical significance of chromosome class distribution between *mus-81* mutants and wild-type animals: *$P<0.05$, **$P<0.01$, ***$P<0.001$, and ****$P<0.0001$ by the Fisher's exact test. (b) Two visual representations of crossovers formed: crossover frequencies for each interval assayed and a stacked histogram of chromosomes that received the indicated number of crossovers. For each genotype, crossover frequencies (numbers in the colored boxes) were calculated by the formula (number of crossovers in each class)/(total meiotic products assayed). Box colors indicate the relative recombination frequency compared to untreated wild-type animals; key is shown to the right. The histogram of multiple-crossover chromosomes has each class of crossovers represented by the color in the key shown to the right. Dashed orange line represents the percentage of chromosomes receiving no crossovers in untreated wild-type animals.

Figure 4a.

Chr. II genotype	dose (Gy)	recomb	SEM	chromosomes with indicated number of crossovers: raw values 4	3	2	1	0	N (mothers)	frequencies 4	3	2	1	0
WT	0 *	0.51	0.06	0	0	1	95	96	192 (4)	0.00	0.00	0.01	0.49	0.50
mus-81		0.47	0.03	0	0	1	89	102	192 (4)	0.00	0.00	0.01	0.46	0.53
WT	0.5	0.52	0.05	0	0	3	44	49	96 (4)	0.00	0.00	0.03	0.46	0.51
mus-81		0.45	0.05	0	0	1	41	54	96 (4)	0.00	0.00	0.01	0.43	0.56
WT	1	0.56	0.06	0	0	6	41	47	94 (4)	0.00	0.00	0.06	0.44	0.50
mus-81		0.57	0.08	0	0	4	47	45	96 (4)	0.00	0.00	0.04	0.49	0.47
WT	2.5 *	0.65	0.01	0	0	8	46	42	96 (3)	0.00	0.00	0.08	0.48	0.44
mus-81		0.51	0.06	0	0	0	49	47	96 (4)	0.00	0.00	0.00	0.51	0.49
WT	5 ****	0.70	0.07	0	1	33	71	86	191 (4)	0.00	0.01	0.17	0.37	0.45
mus-81		0.55	0.03	0	0	3	100	89	192 (3)	0.00	0.00	0.02	0.52	0.46
WT	7.5 ****	0.95	0.12	1	1	24	36	34	96 (4)	0.01	0.01	0.25	0.38	0.35
mus-81		0.56	0.05	0	0	6	94	92	192 (3)	0.00	0.00	0.03	0.49	0.48
WT	10 ****	1.29	0.07	2	22	35	63	43	165 (5)	0.01	0.13	0.21	0.38	0.26
mus-81		0.59	0.05	0	0	5	103	82	190 (2)	0.00	0.00	0.03	0.54	0.43

p values between N2 and *mus-81*

Figure 4. Ionizing radiation creates crossovers that require *mus-81* on Chromosome II. (a) Crossover frequency for *mus-81* mutants using six genetic markers on Chromosome II. Shown are map distance (with standard error of the mean); chromosomes that received either four, three, two, one, or no crossovers; and N values for meiotic products assayed and, in parentheses, meioses assayed. Frequencies were calculated by the formula (number of crossovers in each class)/(total meiotic products assayed). Asterisks indicate statistical significance of chromosome class distribution between *mus-81* mutants and wild-type animals: *$P<0.05$, **$P<0.01$, ***$P<0.001$, and ****$P<0.0001$ by the Fisher's exact test. (b) Two visual representations of crossovers formed: crossover frequencies for each interval assayed and a stacked histogram of chromosomes that received the indicated number of crossovers. For each genotype, crossover frequencies (numbers in the colored boxes) were calculated by the formula (number of crossovers in each class)/(total meiotic products assayed). Box colors indicate the relative recombination frequency compared to untreated wild-type animals; key is shown to the right. The histogram of multiple-crossover chromosomes has each class of crossovers represented by the color in the key shown to the right. Dashed orange line represents the percentage of chromosomes receiving no crossovers in untreated wild-type animals.

Figure 5a.

Chr. X genotype	dose (Gy)	recomb	SEM	chromosomes with indicated number of crossovers: raw values 4	3	2	1	0	N (mothers)	frequencies 4	3	2	1	0
WT	0 *	0.46	0.04	0	0	0	168	200	368 (10)	0.00	0.00	0.00	0.46	0.55
mus-81		0.47	0.04	0	0	3	144	125	272 (6)	0.00	0.00	0.01	0.53	0.46
xpf-1		0.43	0.03	0	0	0	68	89	157 (5)	0.00	0.00	0.00	0.43	0.57
mus-81; xpf-1		0.36	0.08	0	0	0	52	92	144 (3)	0.00	0.00	0.00	0.36	0.64
WT	1 ****	0.58	0.06	0	1	7	39	49	96 (4)	0.00	0.01	0.07	0.31	0.49
mus-81		0.56	0.04	0	0	8	92	92	192 (7)	0.00	0.00	0.04	0.48	0.48
xpf-1		0.44	0.14	0	0	0	42	53	95 (2)	0.00	0.00	0.00	0.44	0.56
mus-81; xpf-1		0.28	0.05	0	0	0	57	133	190 (3)	0.00	0.00	0.00	0.28	0.72
WT	2.5 ****	0.66	0.11	0	2	12	33	49	96 (4)	0.00	0.02	0.13	0.34	0.51
mus-81		0.53	0.04	0	0	1	99	92	192 (4)	0.00	0.00	0.01	0.52	0.48
xpf-1		0.45	0.05	0	0	0	43	53	96 (2)	0.00	0.00	0.00	0.45	0.55
mus-81; xpf-1		0.38	0.00	0	0	0	54	89	143 (3)	0.00	0.00	0.00	0.38	0.62
WT	7.5 ****	0.87	0.01	0	5	36	69	70	180 (5)	0.00	0.03	0.20	0.38	0.39
mus-81		0.49	0.01	0	0	3	87	100	190 (4)	0.00	0.00	0.02	0.46	0.53
xpf-1		0.48	0.06	0	0	0	81	87	168 (5)	0.00	0.00	0.00	0.48	0.52
mus-81; xpf-1		0.37	0.03	0	0	0	52	90	142 (3)	0.00	0.00	0.00	0.37	0.63

p values between N2 and *mus-81; xpf-1*

Figure 5b.

Chr. X genotype	dose (Gy)	Chr. X A to B	B to C	C to D	D to E	E to F	recomb	SEM
WT	0	0.07	0.07	0.13	0.09	0.10	0.46	0.04
mus-81		0.10	0.11	0.09	0.10	0.08	0.47	0.04
xpf-1		0.09	0.08	0.07	0.11	0.08	0.43	0.03
mus-81; xpf-1		0.08	0.08	0.07	0.06	0.06	0.36	0.08
WT	1	0.08	0.08	0.16	0.16	0.10	0.58	0.06
mus-81		0.09	0.17	0.16	0.07	0.07	0.56	0.04
xpf-1		0.04	0.11	0.12	0.07	0.11	0.44	0.14
mus-81; xpf-1		0.05	0.03	0.06	0.07	0.07	0.28	0.05
WT	2.5	0.17	0.15	0.11	0.10	0.13	0.66	0.11
mus-81		0.10	0.09	0.10	0.13	0.11	0.53	0.04
xpf-1		0.09	0.09	0.07	0.06	0.13	0.45	0.05
mus-81; xpf-1		0.06	0.10	0.08	0.07	0.07	0.38	0.00
WT	7.5	0.23	0.24	0.21	0.12	0.07	0.87	0.01
mus-81		0.10	0.07	0.11	0.11	0.11	0.49	0.01
xpf-1		0.08	0.08	0.11	0.13	0.08	0.48	0.06
mus-81; xpf-1		0.06	0.05	0.10	0.08	0.08	0.37	0.03

relative recombination frequency

4.50+
3.50-4.49
2.50-3.49
1.50-2.49
.50-1.49
0-.49

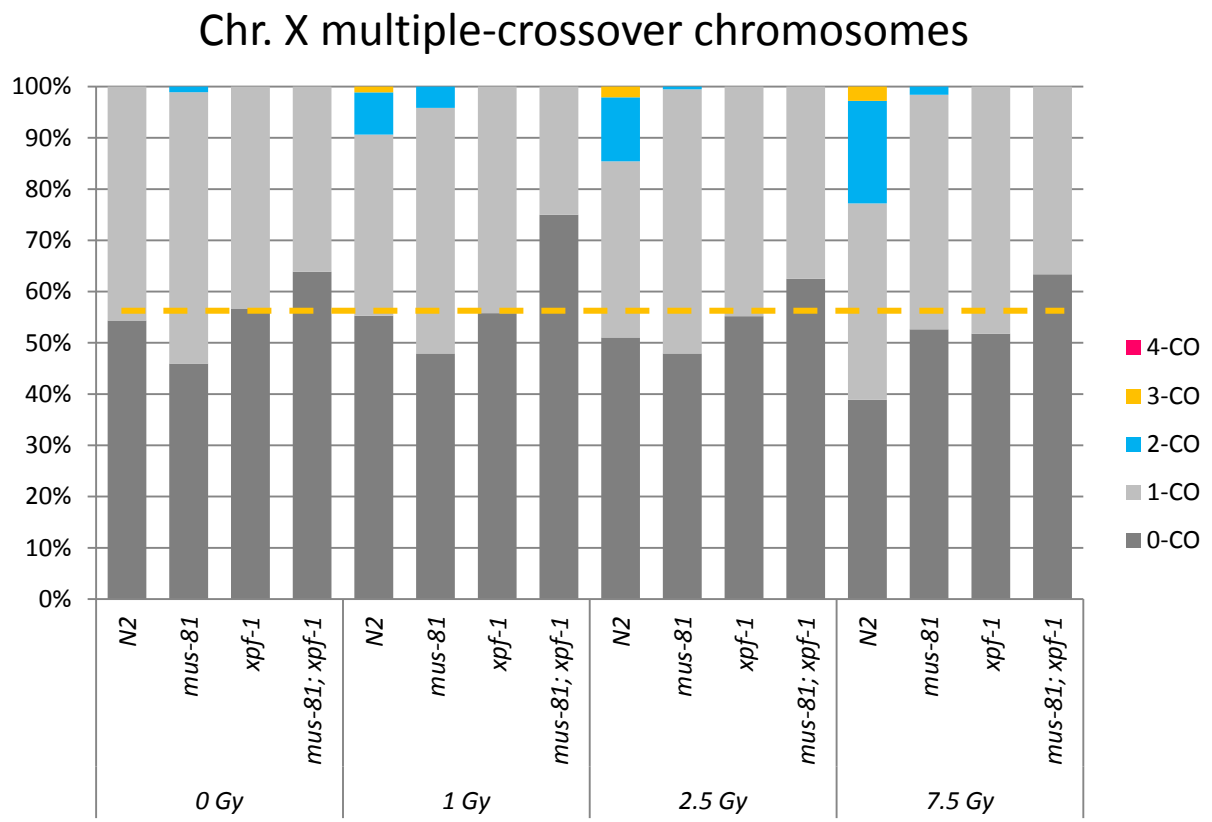

Figure 5. Ionizing radiation creates crossovers that require *mus-81* and *xpf-1* on Chromosome X. (a) Crossover frequency for *mus-81, xpf-1,* and *mus-81; xpf-1* mutants using six genetic markers on Chromosome X. Shown are map distance (with standard error of the mean); chromosomes that received either four, three, two, one, or no crossovers; and N values for meiotic products assayed and, in parentheses, meioses assayed. Frequencies were calculated by the formula (number of crossovers in each class)/(total meiotic products assayed). Asterisks indicate statistical significance of chromosome class distribution between *mus-81; xpf-1* mutants and wild-type animals: *$P<0.05$, **$P<0.01$, ***$P<0.001$, and ****$P<0.0001$ by the Fisher's exact test. (b) Two visual representations of crossovers formed: crossover frequencies for each interval assayed and a stacked histogram of chromosomes that received the indicated number of crossovers. For each genotype, crossover frequencies (numbers in the colored boxes) were calculated by the formula (number of crossovers in each class)/(total meiotic products assayed). Box colors indicate the relative recombination frequency compared to untreated wild-type animals; key is shown to the right. The histogram of multiple-crossover chromosomes has each class of crossovers represented by the color in the key shown to the right. Dashed orange line represents the percentage of chromosomes receiving no crossovers in untreated wild-type animals.

Figure 6a.

Chr. II				chromosomes with indicated number of crossovers										
				raw values					N	frequencies				
genotype	dose (Gy)	recomb	SEM	4	3	2	1	0	(mothers)	4	3	2	1	0
WT	0 *	0.51	0.06	0	0	1	95	96	192 (4)	0.00	0.00	0.01	0.49	0.50
mus-81		0.47	0.03	0	0	1	89	102	192 (4)	0.00	0.00	0.01	0.46	0.53
xpf-1		0.46	0.08	0	0	0	109	129	238 (6)	0.00	0.00	0.00	0.46	0.54
mus-81; xpf-1		0.30	0.02	0	0	0	79	185	264 (3)	0.00	0.00	0.00	0.30	0.70
WT	1 *	0.56	0.06	0	0	6	41	47	94 (4)	0.00	0.00	0.06	0.44	0.50
mus-81		0.57	0.08	0	0	4	47	45	96 (4)	0.00	0.00	0.04	0.49	0.47
xpf-1		0.43	--	0	0	0	41	55	96 (1)	0.00	0.00	0.00	0.43	0.57
mus-81; xpf-1		0.42	--	0	0	0	40	56	96 (1)	0.00	0.00	0.00	0.42	0.58
WT	2.5 **	0.65	0.01	0	0	8	46	42	96 (3)	0.00	0.00	0.08	0.48	0.44
mus-81		0.51	0.06	0	0	0	49	47	96 (4)	0.00	0.00	0.00	0.51	0.49
xpf-1		0.44	--	0	0	0	32	40	72 (1)	0.00	0.00	0.00	0.44	0.56
mus-81; xpf-1		0.40	0.08	0	0	0	38	58	96 (2)	0.00	0.00	0.00	0.40	0.60
WT	7.5 ****	0.95	0.12	1	1	24	36	34	96 (4)	0.01	0.01	0.25	0.38	0.35
mus-81		0.56	0.05	0	0	6	94	92	192 (3)	0.00	0.00	0.03	0.49	0.48
xpf-1		0.46	0.06	0	0	0	79	94	173 (5)	0.00	0.00	0.00	0.46	0.54
mus-81; xpf-1		0.29	0.04	0	0	0	74	177	251 (8)	0.00	0.00	0.00	0.29	0.71

p values between N2 and *mus-81; xpf-1*

Figure 6b.

Chr. II genotype	dose (Gy)	Chr. II A to B	B to C	C to D	D to E	E to F	recomb	SEM
WT	0	0.08	0.15	0.07	0.11	0.10	0.51	0.06
mus-81		0.10	0.09	0.06	0.09	0.14	0.47	0.03
xpf-1		0.06	0.10	0.09	0.11	0.09	0.46	0.08
mus-81; xpf-1		0.04	0.07	0.06	0.06	0.06	0.30	0.02
WT	1	0.10	0.17	0.14	0.13	0.03	0.56	0.06
mus-81		0.09	0.10	0.11	0.08	0.18	0.57	0.08
xpf-1		0.10	0.08	0.06	0.08	0.09	0.43	0.03
mus-81; xpf-1		0.05	0.13	0.05	0.06	0.10	0.39	0.06
WT	2.5	0.17	0.11	0.19	0.11	0.06	0.65	0.01
mus-81		0.06	0.14	0.09	0.09	0.13	0.51	0.06
xpf-1		0.01	0.10	0.17	0.14	0.03	0.44	0.03
mus-81; xpf-1		0.06	0.09	0.07	0.07	0.11	0.40	0.05
WT	7.5	0.21	0.13	0.25	0.15	0.22	0.95	0.12
mus-81		0.07	0.10	0.10	0.10	0.19	0.56	0.05
xpf-1		0.08	0.09	0.12	0.12	0.04	0.46	0.06
mus-81; xpf-1		0.10	0.04	0.04	0.06	0.05	0.29	0.04

relative recombination frequency

4.50+
3.50-4.49
2.50-3.49
1.50-2.49
.50-1.49
0-.49

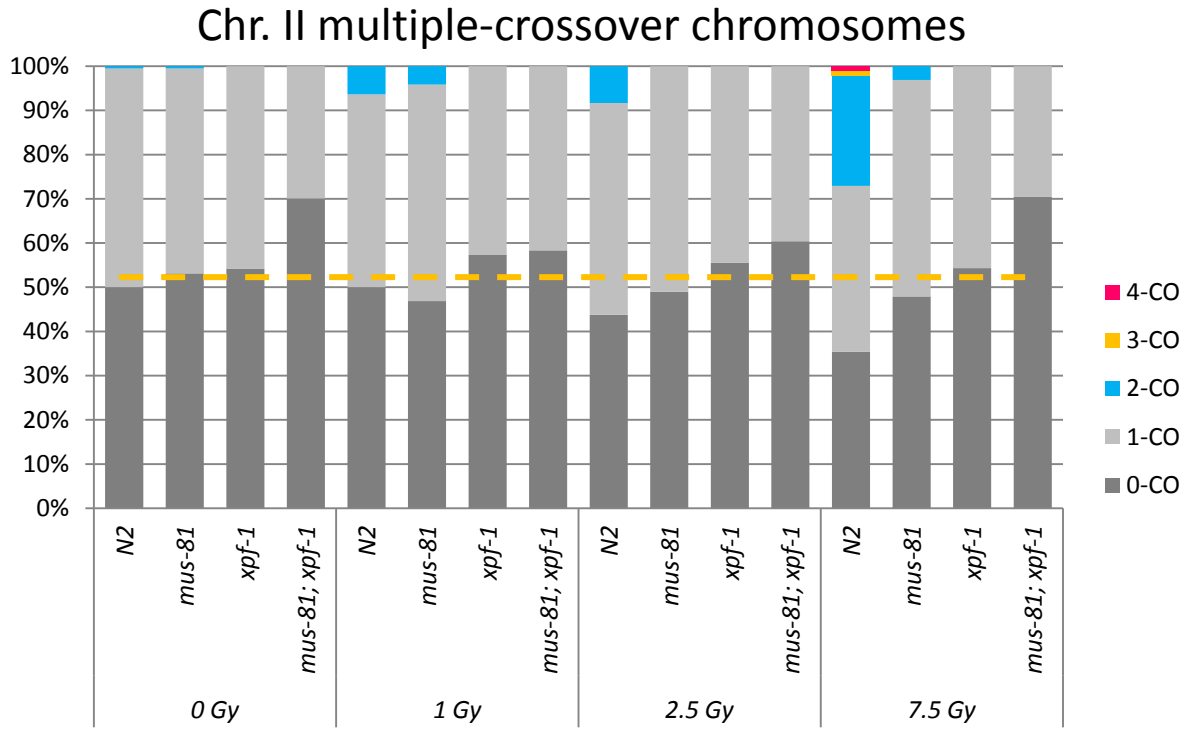

Figure 6. Ionizing radiation creates crossovers that require *mus-81* and *xpf-1* on Chromosome II. (a) Crossover frequency for *mus-81, xpf-1,* and *mus-81; xpf-1* mutants using six genetic markers on Chromosome II. Shown are map distance (with standard error of the mean); chromosomes that received either four, three, two, one, or no crossovers; and N values for meiotic products assayed and, in parentheses, meioses assayed. Frequencies were calculated by the formula (number of crossovers in each class)/(total meiotic products assayed). Asterisks indicate statistical significance of chromosome class distribution between *mus-81; xpf-1* mutants and wild-type animals: *$P<0.05$, **$P<0.01$, ***$P<0.001$, and ****$P<0.0001$ by the Fisher's exact test. (b) Two visual representations of crossovers formed: crossover frequencies for each interval assayed and a stacked histogram of chromosomes that received the indicated number of crossovers. For each genotype, crossover frequencies (numbers in the colored boxes) were calculated by the formula (number of crossovers in each class)/(total meiotic products assayed). Box colors indicate the relative recombination frequency compared to untreated wild-type animals; key is shown to the right. The histogram of multiple-crossover chromosomes has each class of crossovers represented by the color in the key shown to the right. Dashed orange line represents the percentage of chromosomes receiving no crossovers in untreated wild-type animals.

Figure 7.

Chr. X genotype	dose (Gy)	recomb	SEM	chromosomes with indicated number of crossovers: raw values 4	3	2	1	0	N (mothers)	frequencies 4	3	2	1	0
WT	0	0.46	0.04	0	0	0	168	200	368 (10)	0.00	0.00	0.00	0.46	0.55
mus-81		0.47	0.04	0	0	3	144	125	272 (6)	0.00	0.00	0.01	0.53	0.46
mus-81; ced-4		0.48	0.02	0	0	0	46	50	96 (2)	0.00	0.00	0.00	0.48	0.52
WT	1	0.58	0.06	0	1	7	39	49	96 (4)	0.00	0.01	0.07	0.31	0.49
mus-81		0.56	0.04	0	0	8	92	92	192 (7)	0.00	0.00	0.04	0.48	0.48
mus-81; ced-4		0.48	0.01	0	0	2	42	52	96 (3)	0.00	0.00	0.02	0.44	0.54
WT	7.5	0.87	0.01	0	5	36	69	70	180 (5)	0.00	0.03	0.20	0.38	0.39
mus-81		0.49	0.01	0	0	3	87	100	190 (4)	0.00	0.00	0.02	0.46	0.53
mus-81; ced-4		0.49	0.02	0	0	0	46	48	94 (3)	0.00	0.00	0.00	0.49	0.51

p values between N2 and *mus-81; ced-4*

Figure 7. Apoptosis does not account for the loss of radiation-induce crossovers in *mus-81* mutants on Chromosome X. (a) Crossover frequency for *mus-81* and *mus-81; ced-4* mutants using six genetic markers on Chromosome X. Shown are map distance (with standard error of the mean); chromosomes that received either four, three, two, one, or no crossovers; and N values for meiotic products assayed and, in parentheses, meioses assayed. Frequencies were calculated by the formula (number of crossovers in each class)/(total meiotic products assayed). Asterisks indicate statistical significance of chromosome class distribution between *mus-81; ced-4* mutants and wild-type animals: **P*<0.05, ***P*<0.01, ****P*<0.001, and *****P*<0.0001 by the Fisher's exact test. (b) Crossover frequencies in each interval assayed. For each genotype, crossover frequencies (numbers in the colored boxes) were calculated by the formula (number of crossovers in each class)/(total meiotic products assayed). Box colors indicate the relative recombination frequency compared to untreated wild-type animals; key is shown to the right.

Figure 7b.

Chr. X genotype	dose (Gy)	Chr. X A to B	B to C	C to D	D to E	E to F	recomb	SEM
WT	0	0.07	0.07	0.13	0.09	0.10	0.46	0.04
mus-81		0.10	0.11	0.09	0.10	0.08	0.47	0.04
mus-81; ced-4		0.13	0.09	0.09	0.09	0.07	0.48	0.02
WT	1	0.08	0.08	0.16	0.16	0.10	0.58	0.06
mus-81		0.09	0.17	0.16	0.07	0.07	0.56	0.04
mus-81; ced-4		0.06	0.11	0.13	0.08	0.09	0.48	0.01
WT	7.5	0.23	0.24	0.21	0.12	0.07	0.87	0.01
mus-81		0.10	0.07	0.11	0.11	0.11	0.49	0.01
mus-81; ced-4		0.10	0.11	0.13	0.07	0.09	0.49	0.02

relative recombination frequency

4.50+
3.50-4.49
2.50-3.49
1.50-2.49
.50-1.49
0-.49

Figure 8a.

Chr. II genotype	dose (Gy)	recomb	SEM	chromosomes with indicated number of crossovers: raw values 4	3	2	1	0	N (mothers)	frequencies 4	3	2	1	0
WT	0	0.51	0.06	0	0	1	95	96	192 (4)	0.00	0.00	0.01	0.49	0.50
mus-81		0.47	0.03	0	0	1	89	102	192 (4)	0.00	0.00	0.01	0.46	0.53
mus-81; ced-4		0.46	--	0	0	0	11	13	24 (1)	0.00	0.00	0.00	0.46	0.54
WT	7.5	0.95	0.12	1	1	24	36	34	96 (4)	0.01	0.01	0.25	0.38	0.35
mus-81		0.56	0.05	0	0	6	94	92	192 (4)	0.00	0.00	0.03	0.49	0.48
mus-81; ced-4		0.44	0.06	0	0	3	27	42	72 (2)	0.00	0.00	0.04	0.38	0.58

p values between N2 and *mus-81; ced-4*

Figure 8b.

Chr. II genotype	dose (Gy)	Chr. II A to B	B to C	C to D	D to E	E to F	recomb	SEM
WT	0	0.08	0.15	0.07	0.11	0.10	0.51	0.06
mus-81		0.10	0.09	0.06	0.09	0.14	0.47	0.03
mus-81; ced-4		0.04	0.08	0.17	0.13	0.04	0.46	--
WT	7.5	0.21	0.13	0.25	0.15	0.22	0.95	0.12
mus-81		0.07	0.10	0.10	0.10	0.19	0.56	0.05
mus-81; ced-4		0.08	0.07	0.08	0.07	0.13	0.44	0.06

relative recombination frequency

4.50+
3.50-4.49
2.50-3.49
1.50-2.49
.50-1.49
0-.49

Figure 8. Apoptosis does not account for the loss of radiation-induce crossovers in *mus-81* mutants on Chromosome II. (a) Crossover freq for *mus-81* and *mus-81; ced-4* mutants using six genetic markers on Chromosome II. Shown are map distance (with standard error of the mean); chromosomes that received either four, three, two, one, or no crossovers; and N values for meiotic products assayed and, in parentheses, meioses assayed. Frequencies were calculated by the formula (number of crossovers in each class)/(total meiotic products assayed). Asterisks indicate statistical significance of chromosome class distribution between *mus-81; ced-4* mutants and wild-type animals: **P*<0.05, ***P*<0.01, ****P*<0.001, and *****P*<0.0001 by the Fisher's exact test. (b) Crossover frequencies in each interval assayed. For each genotype, crossover frequencies (numbers in the colored boxes) were calculated by the formula (number of crossovers in each class)/(total meiotic products assayed). Box colors indicate the relative recombination frequency compared to untreated wild-type animals; key is shown to the right.

Figure 9a.

	Lethality calculated from 0-48 hours post-irradiation				
	% lethality	SEM	average brood	SEM	broods
WT *(0 Gy)*	0.33	0.14	177.8	3.2	5
WT *(.5 Gy)*	9.53	4.57	162.7	2.9	3
WT *(1 Gy)*	9.42	1.85	183.3	18.6	3
WT *(2.5 Gy)*	10.95	0.90	150.7	30.8	3
WT *(5 Gy)*	11.20	3.89	105.0	14.0	3
WT *(7.5 Gy)*	9.30	4.97	109.0	21.2	3
mus-81 (0 Gy)	7.80	1.53	90.8	8.3	5
mus-81 (.5 Gy)	6.07	0.10	74.0	7.0	2
mus-81 (1 Gy)	13.26	1.59	76.2	9.7	9
mus-81 (2.5 Gy)	21.89	3.58	65.1	9.7	9
mus-81 (5 Gy)	18.63	6.51	65.8	8.4	5
mus-81 (7.5 Gy)	27.46	5.13	77.0	17.6	3
ced-4 (0 Gy)	24.63	2.61	89.5	3.2	4
ced-4 (1 Gy)	27.74	2.21	95.3	14.0	4
ced-4 (2.5 Gy)	40.24	2.87	105.3	10.7	3
ced-4 (5 Gy)	42.03	4.04	164.4	8.9	5
ced-4 (7.5 Gy)	52.17	8.55	121.3	22.1	3
mus-81; ced-4 (0 Gy)	17.49	3.27	53.3	2.4	8
mus-81; ced-4 (.5 Gy)	23.47	5.21	61.3	3.0	4
mus-81; ced-4 (1 Gy)	32.93	3.28	34.0	2.3	9
mus-81; ced-4 (2.5 Gy)	34.66	7.77	65.3	7.4	8
mus-81; ced-4 (5 Gy)	57.51	19.08	65.0	7.9	4
mus-81; ced-4 (7.5 Gy)	64.33	7.64	41.0	5.3	7

Figure 9b.

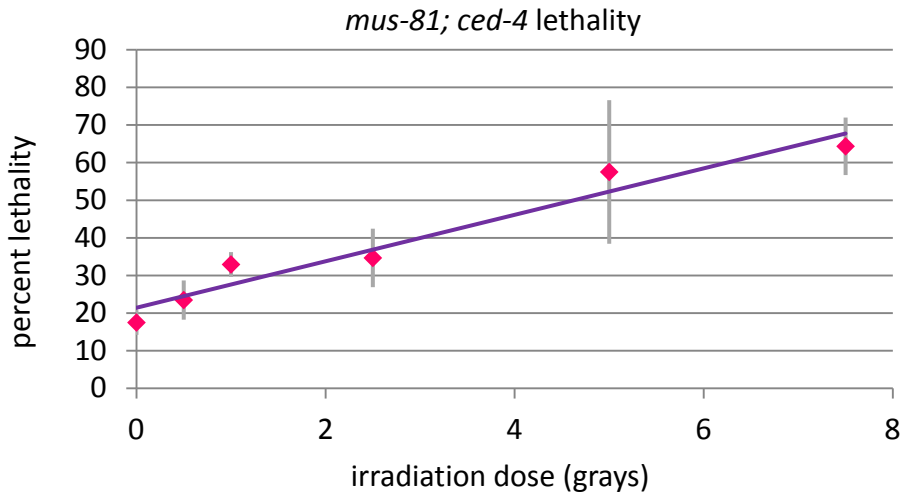

Figure 9. Embryonic lethality in irradiated animals is decoupled from MUS-81-dependence between 1 gray and 2.5 grays. (a) Embryonic lethality was calculated by the formula (total number of dead eggs) / (total number of eggs laid). Eggs were scored from 0 to 48 hours after exposure to radiation. (b) Graph depicts the linear relationship between embryonic lethality and irradiation dose in *mus-81; ced-4* mutants; error bars indicate standard error of the mean. Linear regression is shown in blue, with a slope of 6.17 and an $R^2 = 0.949$.

Figure 10.

Lethality calculated from 0-48 hours post-irradiation

	% lethality	SEM	average brood	SEM	broods
WT (0 Gy)	0.33	0.14	177.8	3.2	5
WT (7.5 Gy)	9.30	4.97	109.0	21.2	3
mus-81 (0 Gy)	7.80	1.53	90.8	8.3	5
mus-81 (7.5 Gy)	27.46	5.13	77.0	17.6	3
spo-11 (0 Gy)	95.82	1.70	136.0	2.1	4
spo-11 (7.5 Gy)	64.32	9.80	87.0	6.9	4
mus-81; spo-11 (0 Gy)	100.00	0.00	0.0	0.0	4
mus-81; spo-11 (7.5 Gy)	100.00	0.00	0.1	0.0	3

Figure 10. Radiation does not rescue embryonic lethality in *mus-81*; *spo-11* mutants. Embryonic lethality was calculated by the formula (total number of dead eggs) / (total number of eggs laid). Eggs were scored from 0 to 48 hours after exposure to radiation.

Figure 11a.

	Percent of oocytes with the indicated number of DAPI-staining bodies									
	average	**5**	**6**	**7**	**8**	**9**	**10**	**11**	**12**	**N (mothers)**
WT (0 Gy)	5.9	4	42	0	0	0	0	0	0	46 (15)
WT (7.5 Gy)	6.0	1	24	0	0	0	0	0	0	25 (12)
spo-11 (0 Gy)	11.9	0	0	0	0	0	0	3	36	39 (11)
spo-11 (7.5 Gy)	7.8	2	14	3	2	1	2	3	4	31 (11)
mus-81 (0 Gy)	5.9	3	26	0	0	0	0	0	0	29 (9)
mus-81 (7.5 Gy)	6.0	2	29	1	0	0	0	0	0	32 (10)
xpf-1 (0 Gy)	6.0	1	19	1	0	0	0	0	0	21 (8)
xpf-1 (7.5 Gy)	6.0	2	22	1	0	0	0	0	0	25 (9)
spo-11; mus-81-1 (0 Gy)	11.9	0	0	0	0	0	0	2	23	25 (12)
spo-11; mus-81 (7.5 Gy)	8.9	0	8	8	6	6	6	6	8	48 (15)
spo-11; xpf-1 (0 Gy)	11.9	0	0	0	0	0	3	5	69	77 (18)
spo-11; xpf-1 (7.5 Gy)	8.9	0	11	10	15	12	22	12	4	86 (25)

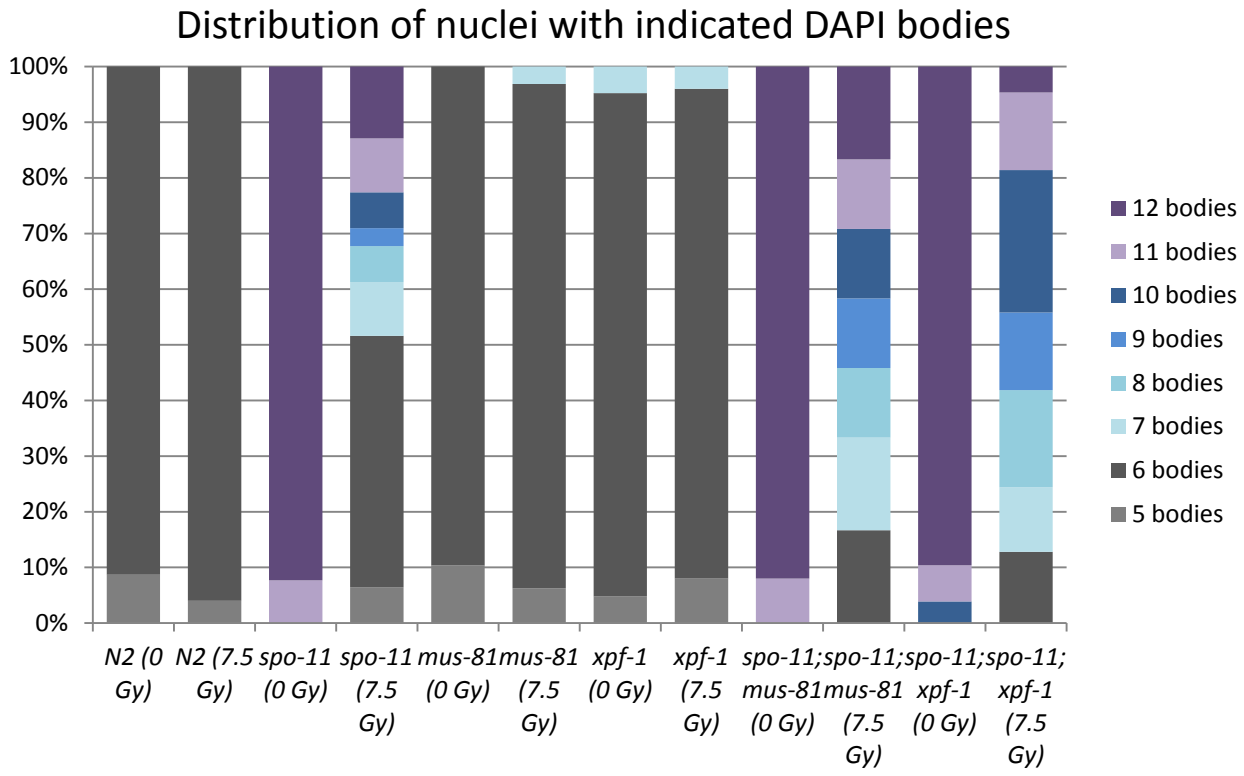

Figure 11b.

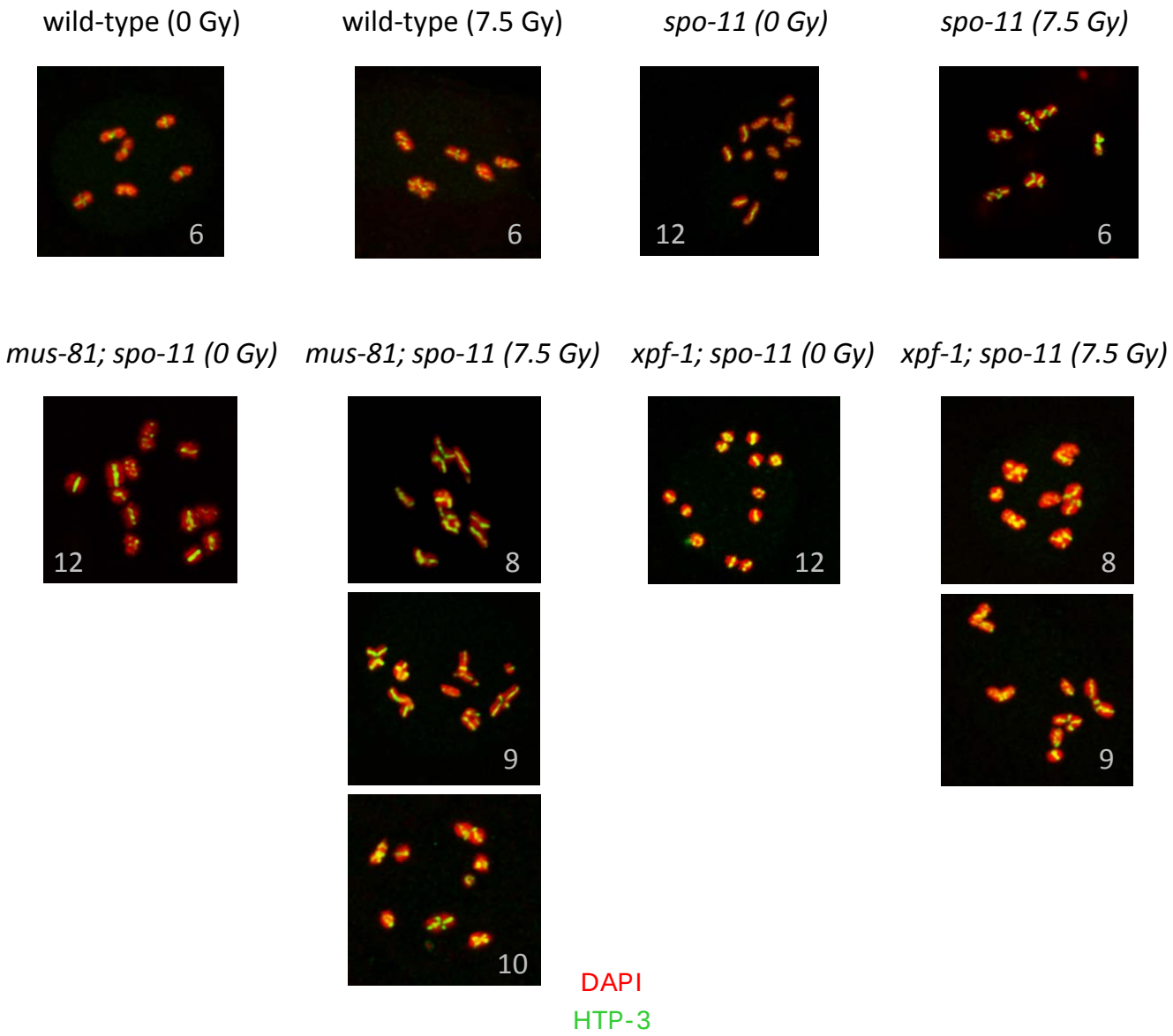

Figure 11. MUS-81 and XPF-1 are required for some radiation-induced chiasmata as inferred by number of DAPI bodies. (a) Quantification of DAPI-stained bodies in diakinesis nuclei. Table shows the average number of DAPI bodies, distribution of nuclei with indicated numbers of DAPI bodies, and N values of nuclei scored and animals scored. Stacked histogram represents distribution of nuclei with indicated numbers of DAPI bodies; key is shown to the right. (b) Projections of Z-stacks shown for representative diakinesis nuclei stained with HTP-3 antibody (green) and DAPI (red). The number of DAPI bodies for each nucleus is indicated; some DAPI bodies appear to overlap in the projection but can be distinguished as separate bodies in the Z-stack.

Figure 12a.

	Percent of oocytes with the indicated number of DAPI-staining bodies									
	average	**5**	**6**	**7**	**8**	**9**	**10**	**11**	**12**	**N (mothers)**
WT (0 Gy)	5.9	4	42	0	0	0	0	0	0	46 (15)
WT (7.5 Gy)	6.0	1	24	0	0	0	0	0	0	25 (14)
cosa-1 (0 Gy)	11.9	0	0	0	0	0	0	3	41	44 (10)
cosa-1 (7.5 Gy)	11.9	0	0	0	0	0	2	5	59	66 (23)

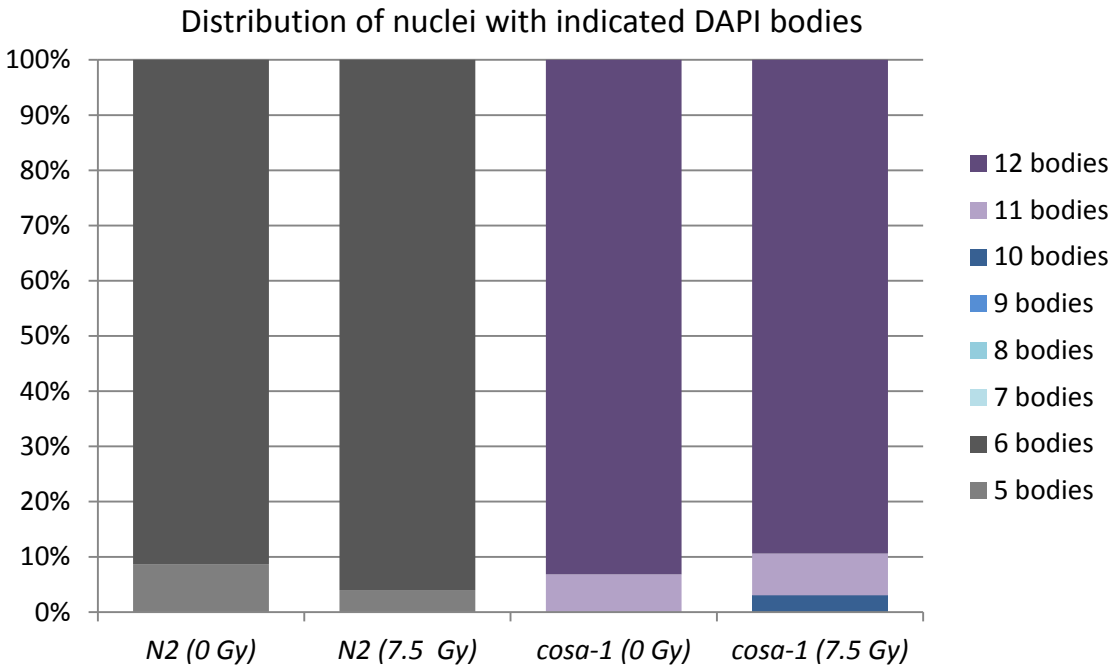

Figure 12b.

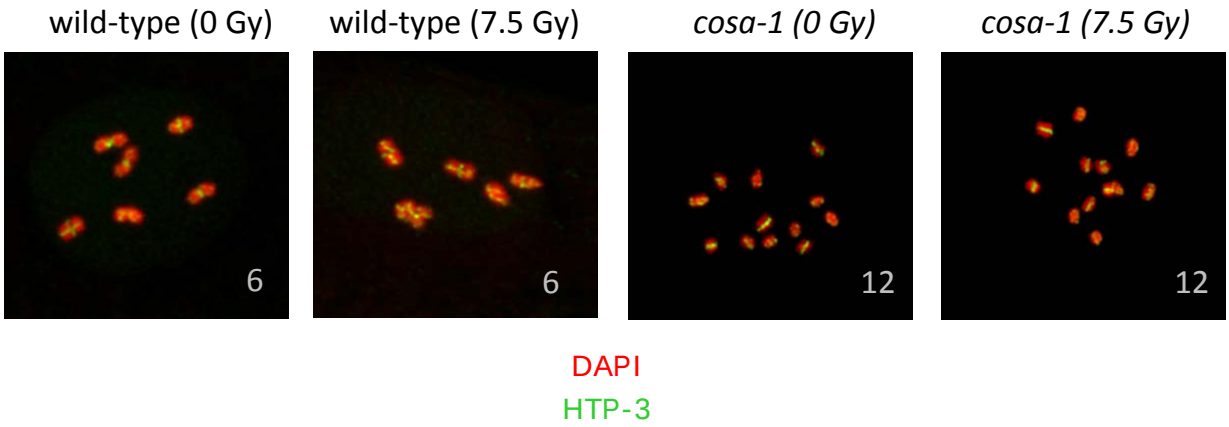

Figure 12. COSA-1 is required for chiasmata formation in irradiated animals. (a) Quantification of DAPI-stained bodies in diakinesis nuclei. Table shows the average number of DAPI bodies, distribution of nuclei with indicated numbers of DAPI bodies, and N of nuclei scored and animals scored. Stacked histogram represents distribution of nuclei with indicated numbers of DAPI bodies; key is shown to the right. (b) Projections of Z-stacks shown for representative diakinesis nuclei stained with HTP-3 antibody (green) and DAPI (red). The number of DAPI bodies for each nucleus is indicated.

Figure 13a.

Chr. X geno.	dose (Gy)	recomb	SEM	chromosomes with indicated number of crossovers: raw values 4	3	2	1	0	N (mothers)	frequencies 4	3	2	1	0
WT	0	0.46	0.04	0	0	0	168	200	368 (10)	0.00	0.00	0.00	0.46	0.55
gen-1		0.49	0.04	0	0	0	94	96	190 (4)	0.00	0.00	0.00	0.49	0.51
WT	7.5	0.87	0.01	0	5	36	69	70	180 (4)	0.00	0.03	0.20	0.38	0.39
gen-1		0.83	0.02	1	8	22	87	74	192 (4)	0.01	0.04	0.11	0.45	0.39

p values between N2 at the same dose

Figure 13. GEN-1 is not required for radiation-induced crossovers on Chromosome X. (a) Crossover frequency for *gen-1* mutants using six genetic markers on Chromosome X. Shown are map distance (with standard error of the mean); chromosomes that received either four, three, two, one, or no crossovers; and N values for meiotic products assayed and, in parentheses, meioses assayed. Frequencies were calculated by the formula (number of crossovers in each class)/(total meiotic products assayed). Asterisks indicate statistical significance of chromosome class distribution between *gen-1* mutants and wild-type animals: *P<0.05, **P<0.01, ***P<0.001, and ****P<0.0001 by the Fisher's exact test. (b) Crossover frequencies in each interval assayed. For each genotype, crossover frequencies (numbers in the colored boxes) were calculated by the formula (number of crossovers in each class)/(total meiotic products assayed). Box colors indicate the relative recombination frequency compared to untreated wild-type animals; key is shown to the right. The histogram of multiple-crossover chromosomes has each class of crossovers represented by the color in the key shown to the right.

Figure 13b.

genotype	dose (Gy)	Chr. X A to B	B to C	C to D	D to E	E to F	recomb	SEM
N2	0	0.07	0.07	0.13	0.09	0.10	0.46	0.04
gen-1		0.10	0.08	0.08	0.12	0.11	0.49	0.04
N2	7.5	0.23	0.24	0.21	0.12	0.07	0.87	0.01
gen-1		0.19	0.19	0.13	0.14	0.19	0.83	0.02

relative recombination frequency
4.50+
3.50-4.49
2.50-3.49
1.50-2.49
.50-1.49
0-.49

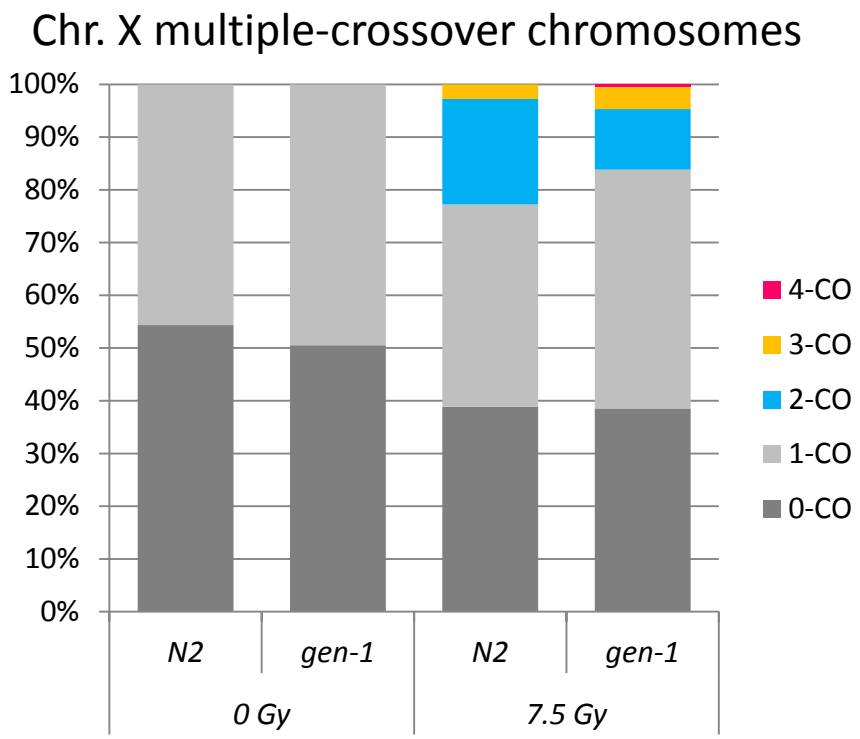

Figure 14a.

Chr. X genotype	dose (Gy)	recomb	SEM	chromosomes with indicated number of crossovers: raw values 4	3	2	1	0	N (mothers)	frequencies 4	3	2	1	0
WT	0	0.46	0.04	0	0	0	168	200	368 (10)	0.00	0.00	0.00	0.46	0.55
him-6	*	0.37	0.02	0	0	0	90	150	240 (5)	0.00	0.00	0.00	0.38	0.63
WT	7.5	0.87	0.01	0	5	36	69	70	180 (4)	0.00	0.03	0.20	0.38	0.39
him-6	****	0.63	0.05	0	0	17	119	103	239 (5)	0.00	0.00	0.07	0.50	0.43

p values between N2 at the same dose

Figure 14. HIM-6 is required for some radiation-induced crossovers on Chromosome X. (a) Crossover frequency for *him-6* mutants using six genetic markers on Chromosome X. Shown are map distance (with standard error of the mean); chromosomes that received either four, three, two, one, or no crossovers; and N values for meiotic products assayed and, in parentheses, meioses assayed. Frequencies were calculated by the formula (number of crossovers in each class)/(total meiotic products assayed). Asterisks indicate statistical significance of chromosome class distribution between *him-6* mutants and wild-type animals: *P<0.05, **P<0.01, ***P<0.001, and ****P<0.0001 by the Fisher's exact test. (b) Crossover frequencies in each interval assayed. For each genotype, crossover frequencies (numbers in the colored boxes) were calculated by the formula (number of crossovers in each class)/(total meiotic products assayed). Box colors indicate the relative recombination frequency compared to untreated wild-type animals; key is shown to the right. The histogram of multiple-crossover chromosomes has each class of crossovers represented by the color in the key shown to the right.

Figure 14b.

Chr. X genotype	dose (Gy)	Chr. X A to B	B to C	C to D	D to E	E to F	recomb	SEM
WT	0	0.07	0.07	0.13	0.09	0.10	0.46	0.04
him-6		0.05	0.05	0.07	0.11	0.10	0.37	0.02
WT	7.5	0.23	0.24	0.21	0.12	0.07	0.87	0.01
him-6		0.13	0.10	0.07	0.13	0.20	0.63	0.05

relative recombination frequency
4.50+
3.50-4.49
2.50-3.49
1.50-2.49
.50-1.49
0-.49

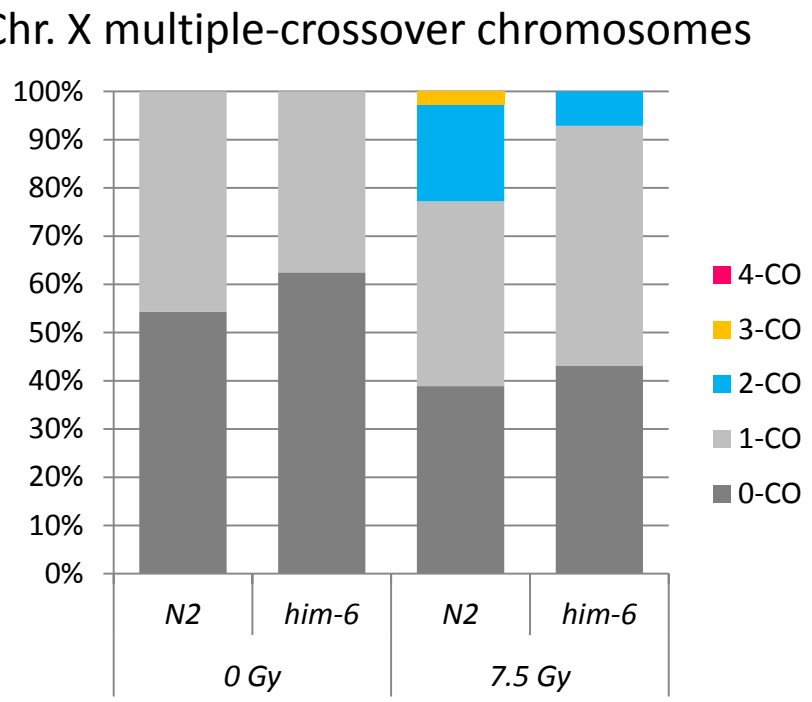

Figure 15.

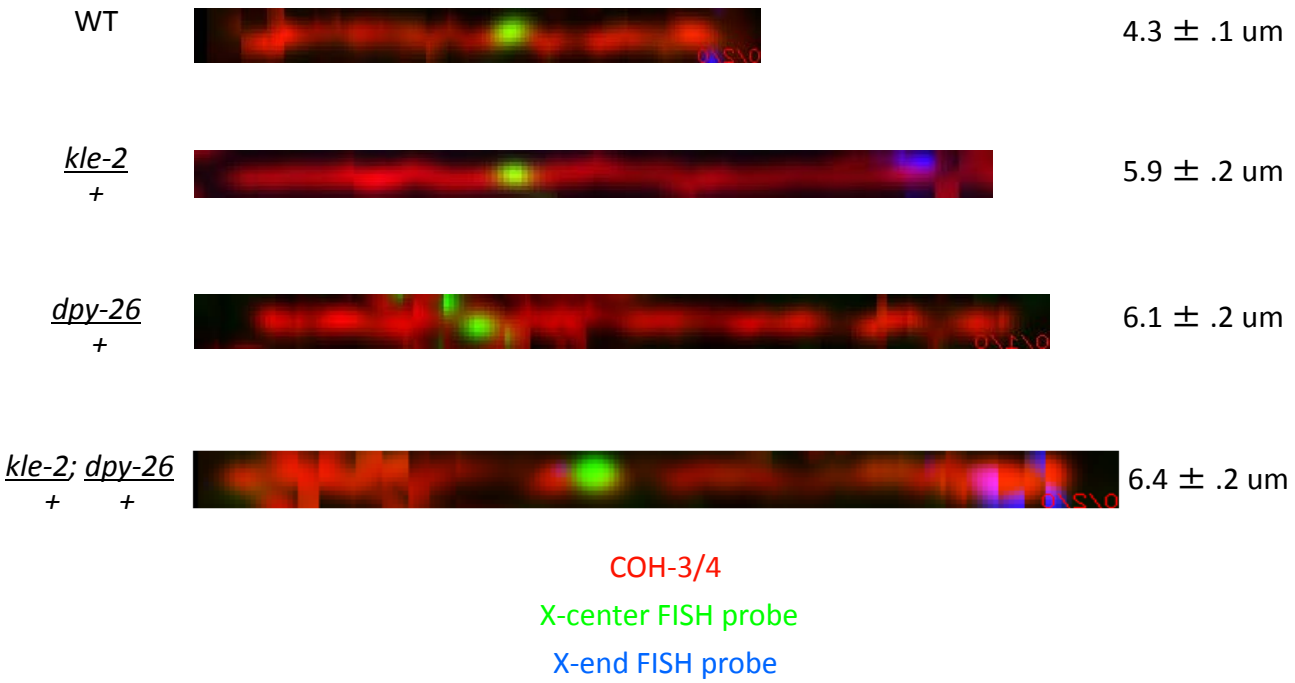

Figure 15. Axis length is extended in animals depleted of condensin. Computationally straightened X chromosome axes are displayed horizontally, labeled for axis protein COH-3/4 (red), a center X FISH probe (green), and a right end X FISH probe (blue). The scale bar represents 1 micron.

Figure 16a.

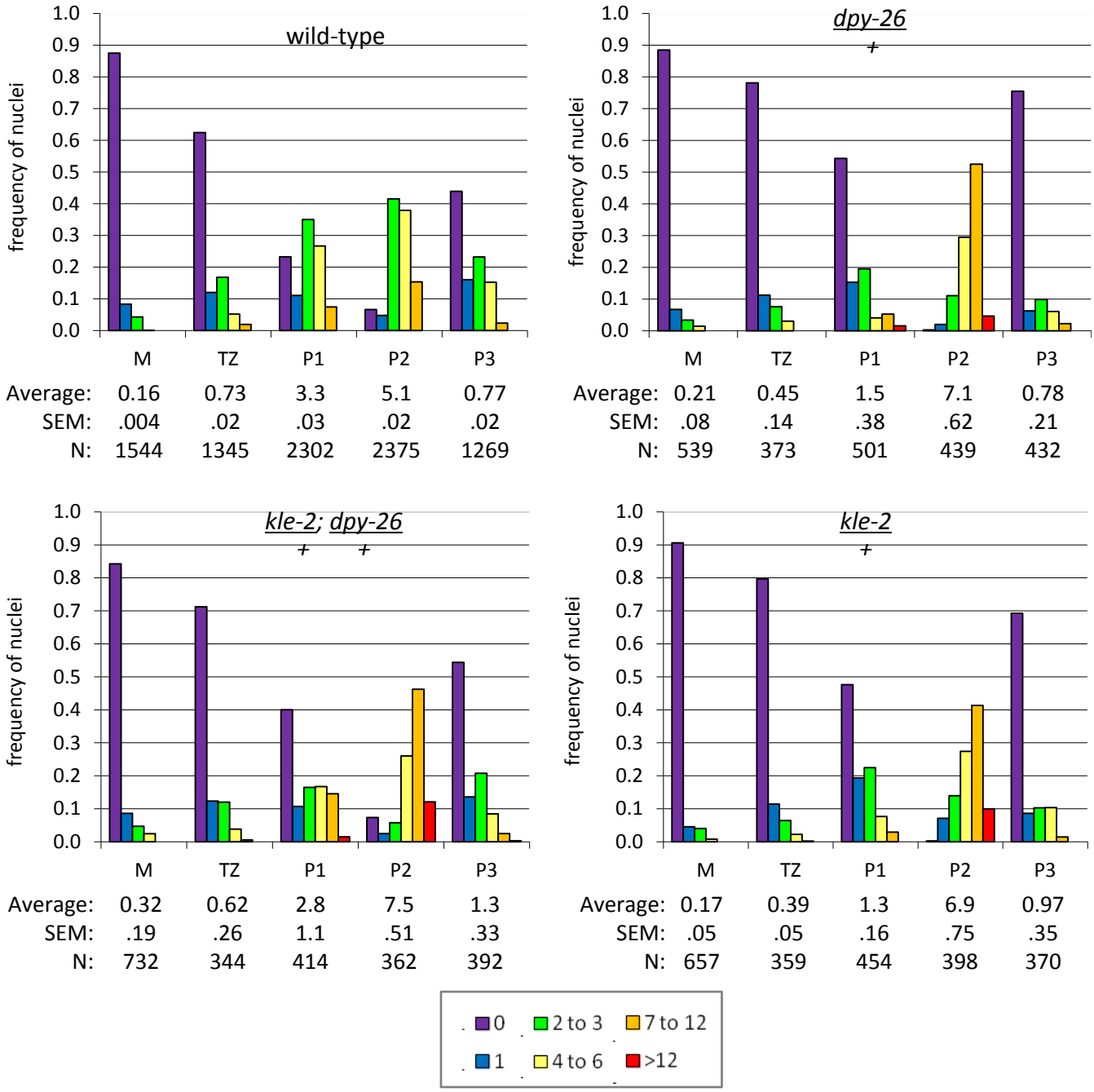

Figure 16a. More DSBs form in animals depleted of condensin. Histograms show quantification of RAD-51 foci in *dpy-26/+*, *kle-2/+*, and *kle-2/+; dpy-26/+* mutants. Each column color represents a class of nuclei with the indicated number of foci, a shown in the key on the bottom. The y-axis shows the frequency of nuclei in each class, the x-axis shows the meiotic stage: mitotic region (M), transition zone (TZ), early pachytene (P1), mid-pachytene (P2), and late pachytene (P3). The average number of RAD-51 foci per nucleus, standard error the mean, and number of nuclei scored are shown below each stage.

Figure 16b.

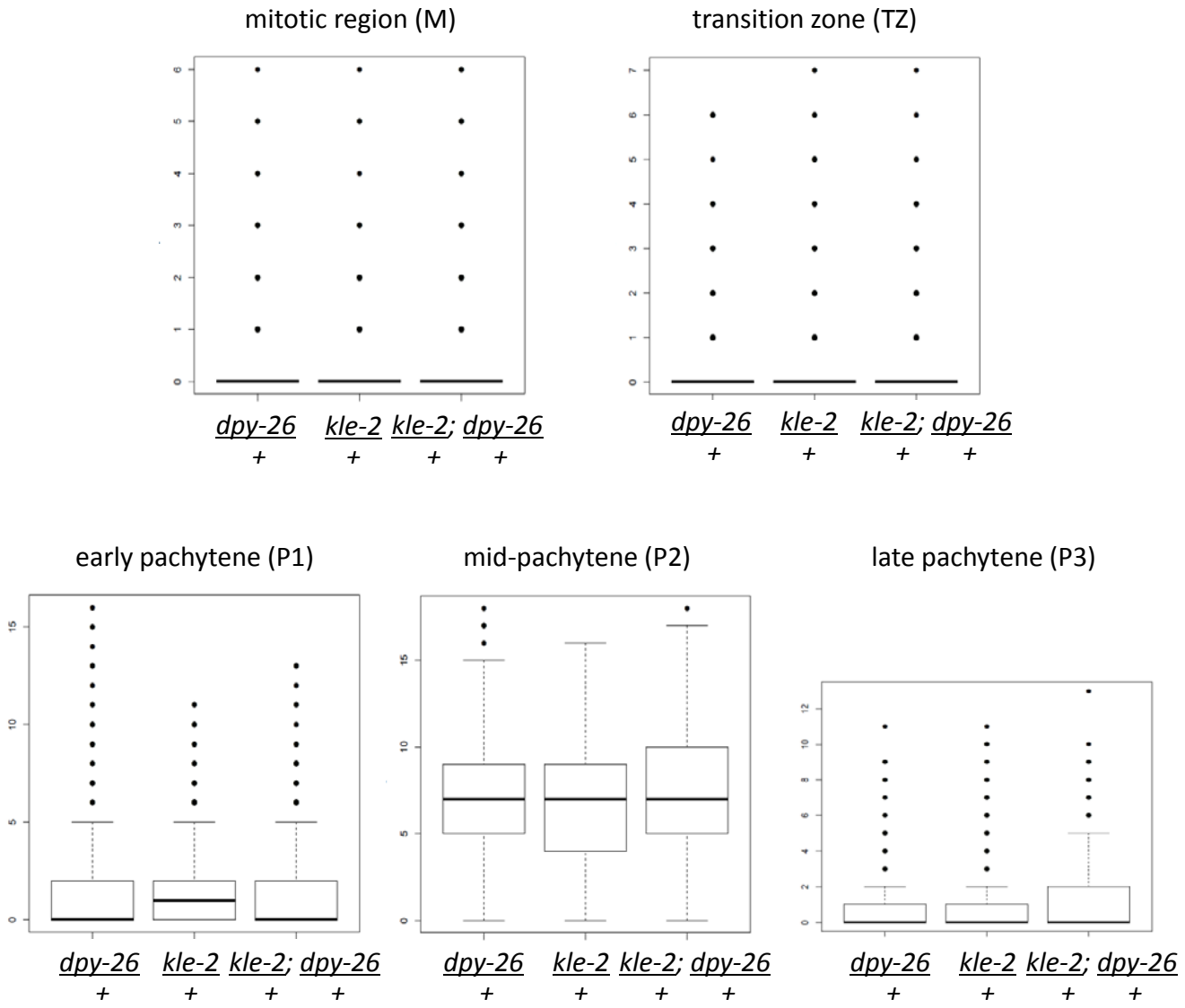

Figure 16b. More DSBs form in animals depleted of condensin. Whisker plots show the distribution of RAD-51 foci in five germline regions of *dpy-26/+*, *kle-2/+*, and *kle-2/+; dpy-26/+* mutants. The y-axis shows the number of RAD-51 foci in each nucleus. The whiskers represent the top and bottom quartile of data points, with the box represent the two middle quartiles; the dark line in the box is the median.

Figure 17a.

	average	Nuclei with the indicated number of GFP::COSA-1 foci					N
		3	4	5	6	7	
WT	5.60	0	2	4	63	2	75
dpy-26/+	5.41	0	4	15	148	3	112
kle-2/+	5.75	0	2	31	187	7	232
kle-2/+; dpy-26/+	5.85	0	10	57	352	13	432

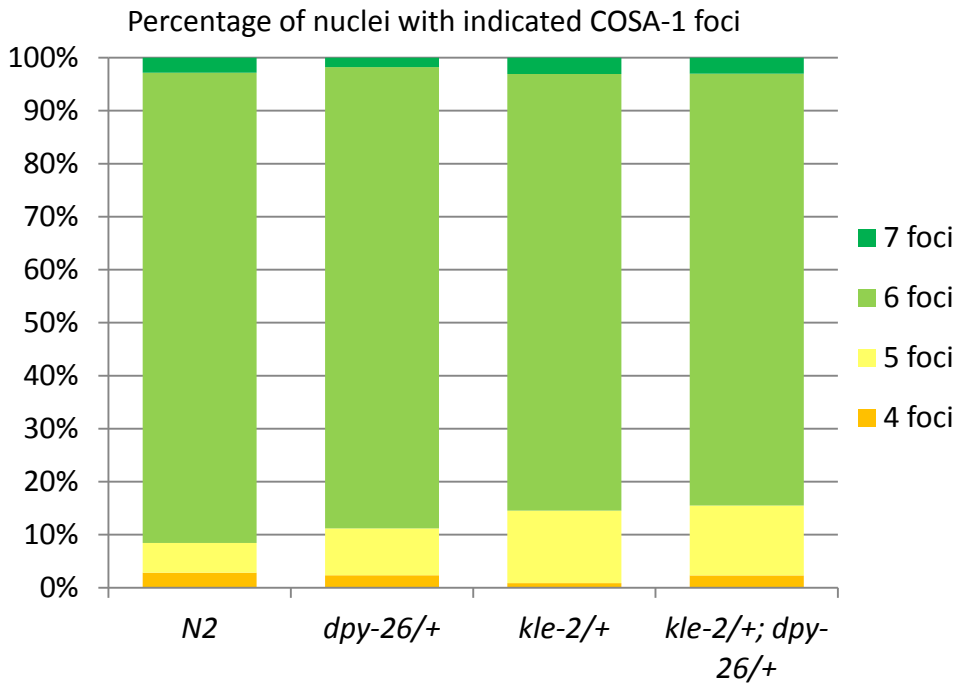

Figure 17b.

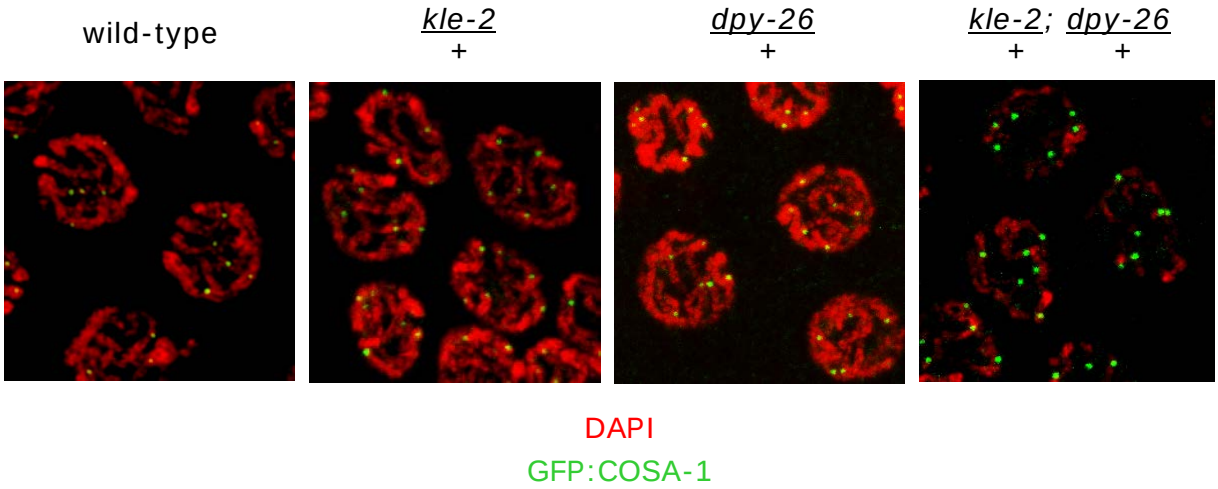

Figure 17. COSA-1 foci do not increase in animals depleted of condensin. (a) Quantification of GFP::COSA-1foci in late-pachytene nuclei. Table shows the average number of foci, distribution of nuclei with indicated numbers of foci, and N of nuclei scored. Stacked histogram represents distribution of nuclei with indicated numbers of GFP::COSA-1 foci; key is shown to the right. (b) Projections of Z-stacks shown for representative diakinesis nuclei stained with GFP antibody (green) and DAPI (red).

Figure 18a.

Chr. X genotype	recomb	SEM	chromosomes with indicated number of crossovers: raw values 4	3	2	1	0	N (mothers)	frequencies 4	3	2	1	0
WT	0.46	0.04	0	0	0	168	200	368 (10)	0.00	0.00	0.00	0.46	0.55
dpy-26	0.79	0.08	1	5	44	100	112	262 (5)	0.00	0.02	0.17	0.38	0.43
dpy-26/+	0.62	0.14	0	1	20	156	153	330 (4)	0.00	0.00	0.06	0.47	0.46
cosa-1/+	0.43	0.01	0	0	2	204	270	476 (5)	0.00	0.00	0.00	0.43	0.57
cosa-1/+; dpy-26/+	0.52	0.04	0	1	26	179	239	445 (5)	0.00	0.00	0.06	0.40	0.54

Figure 18. COSA-1 is required for some crossovers on Chromosome X in condensin I mutants. (a) Crossover frequency for condensin single and double mutants using six genetic markers on Chromosome X. Shown are map distance (with standard error of the mean); chromosomes that received either four, three, two, one, or no crossovers; and N values for meiotic products assayed and, in parentheses, meioses assayed. Frequencies were calculated by the formula (number of crossovers in each class)/(total meiotic products assayed). (b) Crossover frequencies in each interval assayed. For each genotype, crossover frequencies (numbers in the colored boxes) were calculated by the formula (number of crossovers in each class)/(total meiotic products assayed). Box colors indicate the relative recombination frequency compared to untreated wild-type animals; key is shown to the right. The histogram of multiple-crossover chromosomes has each class of crossovers represented by the color in the key shown to the right.

Figure 18b.

	Chr. X						
	A to B	**B to C**	**C to D**	**D to E**	**E to F**	**recomb**	**SEM**
WT	0.07	0.07	0.13	0.09	0.10	0.46	0.04
dpy-26	0.14	0.12	0.13	0.17	0.23	0.79	0.08
dpy-26/+	0.08	0.09	0.09	0.15	0.21	0.62	0.14
cosa-1/+	0.09	0.09	0.09	0.07	0.09	0.43	0.01
cosa-1/+; dpy-26/+	0.08	0.08	0.09	0.12	0.15	0.52	0.04

relative recombination frequency

4.50+
3.50-4.49
2.50-3.49
1.50-2.49
.50-1.49
0-.49

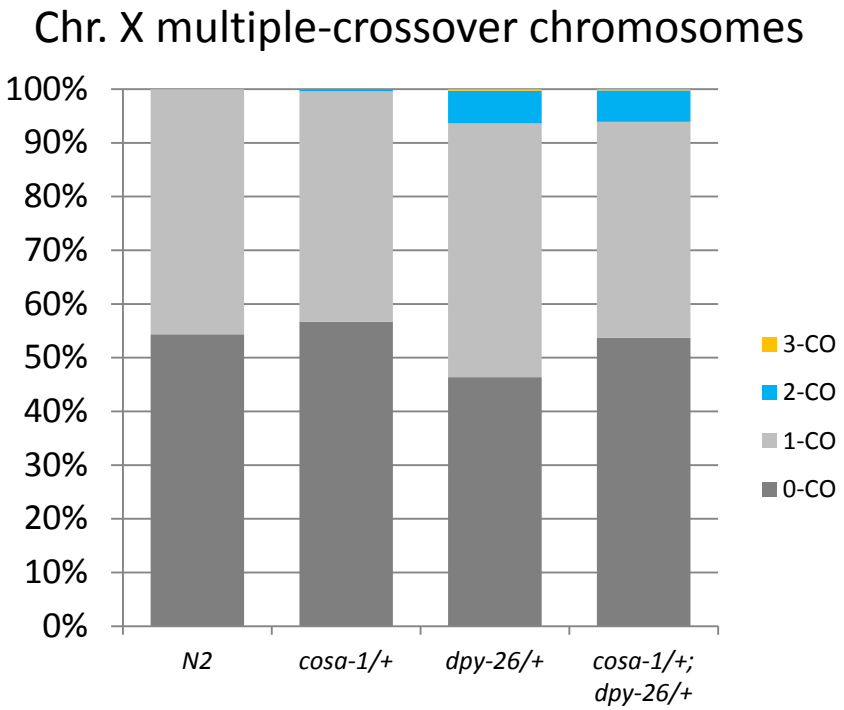

Figure 19a.

	Oocytes with the indicated number of DAPI-staining bodies										
	average	**4**	**5**	**6**	**7**	**8**	**9**	**10**	**11**	**12**	**N**
WT	5.9	0	9	91	0	0	0	0	0	0	46
dpy-26	6.2	0	4	12	10	0	0	0	0	0	26
cosa-1	11.8	0	0	0	0	0	0	0	14	44	58
dpy-26; cosa-1	10.6	0	0	0	0	1	3	6	9	6	25

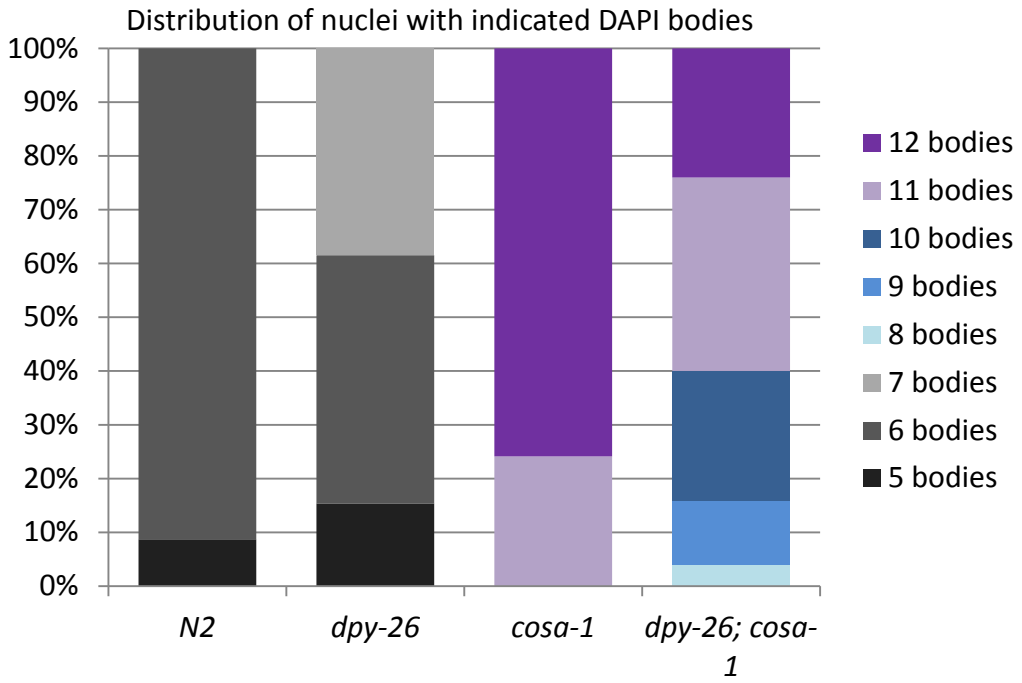

Figure 19b.

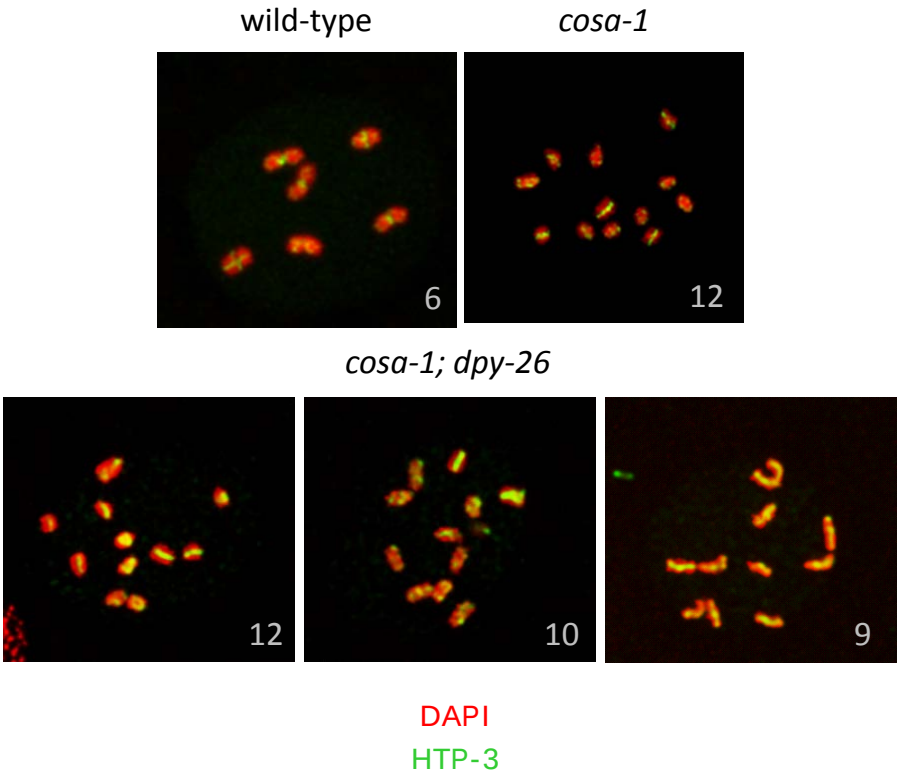

Figure 19. COSA-1 is required for chiasmata formation in condensin-depleted animals. (a) Quantification of DAPI-stained bodies in diakinesis nuclei. Table shows the average number of DAPI bodies, distribution of nuclei with indicated numbers of DAPI bodies, and N of nuclei scored and animals scored. Stacked histogram represents distribution of nuclei with indicated numbers of DAPI bodies; key is shown to the right. (b) Projections of Z-stacks shown for representative diakinesis nuclei stained with HTP-3 antibody (green) and DAPI (red). The number of DAPI bodies for each nucleus is indicated. Nuclei from wild-type animals and *cosa-1* mutants are repeated from Figure 11 for ease of comparison.

Figure 20a.

Chr. X genotype		recomb	SEM	chromosomes with indicated number of crossovers: raw values 3	2	1	0	N (mothers)	frequencies 3	2	1	0
WT		0.46	0.04	0	0	168	200	368 (10)	0.00	0.00	0.46	0.55
mus-81		0.47	0.04	0	3	144	125	272 (6)	0.00	0.01	0.53	0.46
dpy-26/+		0.62	0.14	1	20	156	153	330 (4)	0.00	0.06	0.47	0.46
mus-81; dpy-26/+		0.60	0.05	2	45	295	348	690 (9)	0.00	0.07	0.43	0.50
kle-2/+		0.55	0.23	1	11	81	99	192 (5)	0.01	0.06	0.42	0.52
mus-81; kle-2/+		0.64	0.03	1	36	148	162	347 (2)	0.00	0.10	0.43	0.47
kle-2/+; dpy-26/+	****	0.91	0.05	7	80	169	128	384 (4)	0.02	0.21	0.44	0.33
mus-81; kle-2/+; dpy-26/+		0.64	0.03	0	36	303	246	585 (9)	0.00	0.06	0.52	0.42
mix-1/+	***	0.73	0.30	3	16	70	61	150 (2)	0.02	0.11	0.47	0.41
mus-81; mix-1/+		0.52	0.07	0	7	81	94	182 (2)	0.00	0.04	0.45	0.52

p values between condensin mutant and *mus-81* in condensin mutant background

Figure 20. MUS-81 is required for crossovers on Chromosome X in animals depleted of both condensins. (a) Crossover frequency for condensin single and double mutants using six genetic markers on Chromosome X. Shown are map distance (with standard error of the mean); chromosomes that received either four, three, two, one, or no crossovers; and N values for meiotic products assayed and, in parentheses, meioses assayed. Frequencies were calculated by the formula (number of crossovers in each class)/(total meiotic products assayed). Asterisks indicate statistical significance of chromosome class distribution between condensin mutants and condensin mutants with a mutation in *mus-81*: *$P<0.05$, **$P<0.01$, ***$P<0.001$, and ****$P<0.0001$ by the Fisher's exact test. (b) Crossover frequencies in each interval assayed. For each genotype, crossover frequencies (numbers in the colored boxes) were calculated by the formula (number of crossovers in each class)/(total meiotic products assayed). Box colors indicate the relative recombination frequency compared to untreated wild-type animals; key is shown to the right. The histogram of multiple-crossover chromosomes has each class of crossovers represented by the color in the key shown to the right. Dashed orange line represents the percentage of chromosomes receiving no crossovers in untreated wild-type animals.

Figure 20b.

Chr. X

	A to B	B to C	C to D	D to E	E to F	recomb	SEM
WT	0.07	0.07	0.13	0.09	0.10	0.46	0.04
mus-81	0.10	0.11	0.09	0.10	0.08	0.47	0.04
dpy-26/+	0.08	0.09	0.09	0.15	0.21	0.62	0.14
mus-81; dpy-26/+	0.10	0.11	0.15	0.13	0.12	0.60	0.05
kle-2/+	0.16	0.09	0.08	0.10	0.13	0.55	0.23
mus-81; kle-2/+	0.19	0.16	0.09	0.09	0.12	0.64	0.03
kle-2/+; dpy-26/+	0.17	0.12	0.18	0.21	0.23	0.91	0.05
mus-81; kle-2/+; dpy-26/+	0.11	0.16	0.11	0.11	0.15	0.64	0.03
mix-1/+	0.21	0.17	0.09	0.14	0.12	0.73	0.30
mus-81; mix-1/+	0.13	0.09	0.14	0.09	0.08	0.52	0.07

relative recombination frequency

- 4.50+
- 3.50-4.49
- 2.50-3.49
- 1.50-2.49
- .50-1.49
- 0-.49

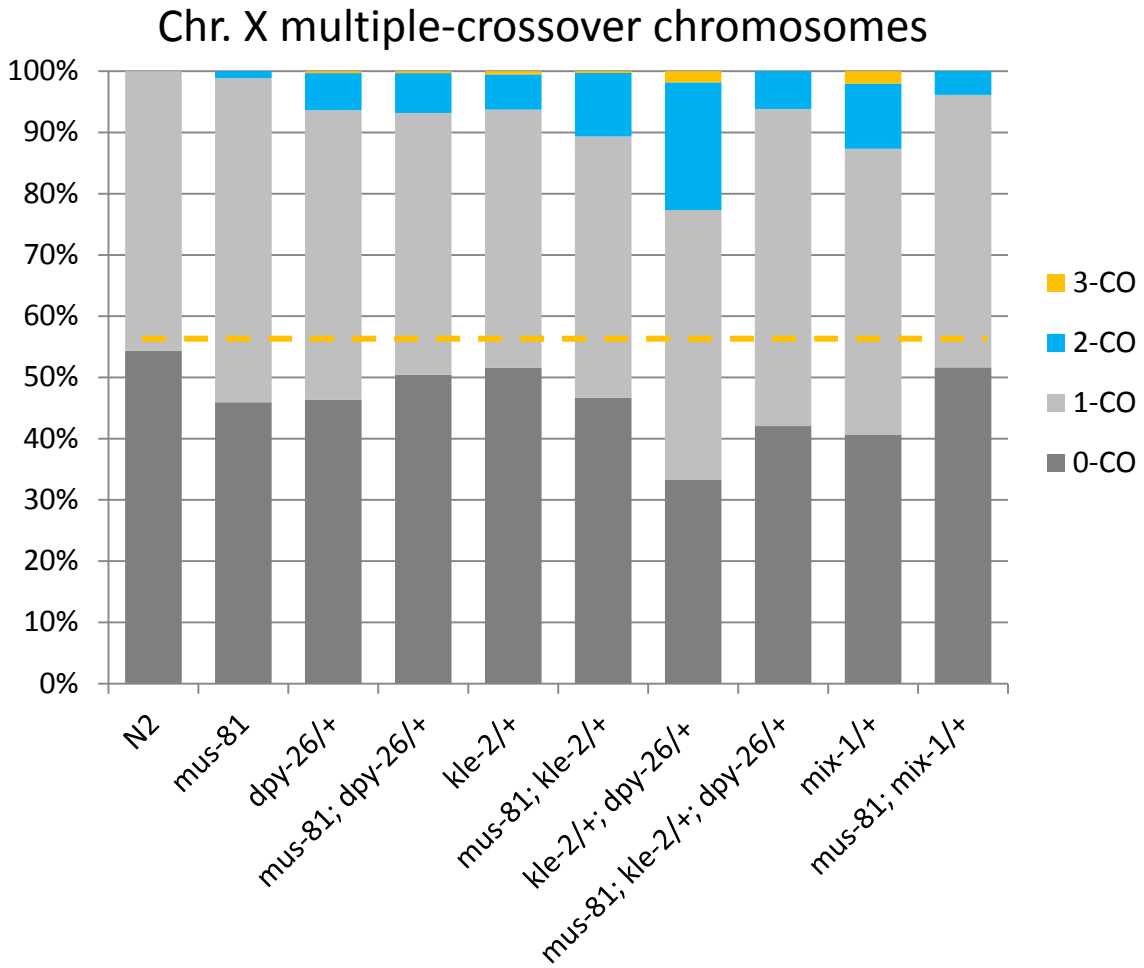

Figure 21a.

Chr. X genotype		recomb	SEM	raw values 3-CO	2-CO	1-CO	0-CO	N	frequencies 3-CO	2-CO	1-CO	0-CO
WT		0.46	0.04	0	0	168	200	368 (10)	0.00	0.00	0.46	0.55
xpf-1		0.43	0.03	0	0	68	89	157 (5)	0.00	0.00	0.43	0.57
dpy-26/+		0.62	0.14	1	20	156	153	330 (4)	0.00	0.06	0.47	0.46
xpf-1; dpy-26/+		0.59	0.04	1	7	95	87	190 (2)	0.01	0.04	0.50	0.46
kle-2/+; dpy-26/+	****	0.91	0.05	7	80	169	128	384 (4)	0.02	0.21	0.44	0.33
xpf-1; kle-2/+; dpy-26/+		0.60	0.06	1	10	91	88	190 (4)	0.01	0.05	0.48	0.46

p values between condensin mutant background and *mus-81* in the condensin mutant background

Figure 21. XPF-1 is required for crossovers on Chromosome X in animals depleted of both condensins. (a) Crossover frequency for condensin single and double mutants using six genetic markers on Chromosome X. Shown are map distance (with standard error of the mean); chromosomes that received either four, three, two, one, or no crossovers; and N values for meiotic products assayed and, in parentheses, meioses assayed. Frequencies were calculated by the formula (number of crossovers in each class)/(total meiotic products assayed). Asterisks indicate statistical significance of chromosome class distribution between condensin mutants and condensin mutants with a mutation in *xpf-1*: *$P<0.05$, **$P<0.01$, ***$P<0.001$, and ****$P<0.0001$ by the Fisher's exact test. (b) Crossover frequencies in each interval assayed. For each genotype, crossover frequencies (numbers in the colored boxes) were calculated by the formula (number of crossovers in each class)/(total meiotic products assayed). Box colors indicate the relative recombination frequency compared to untreated wild-type animals; key is shown to the right. The histogram of multiple-crossover chromosomes has each class of crossovers represented by the color in the key shown to the right. Dashed orange line represents the percentage of chromosomes receiving no crossovers in untreated wild-type animals.

Figure 21b.

	Chr. X						
	A to B	**B to C**	**C to D**	**D to E**	**E to F**	**recomb**	**SEM**
WT	0.07	0.07	0.13	0.09	0.10	0.46	0.04
xpf-1	0.09	0.08	0.07	0.11	0.08	0.43	0.03
dpy-26/+	0.08	0.09	0.09	0.15	0.21	0.62	0.14
xpf-1; dpy-26/+	0.11	0.09	0.10	0.15	0.14	0.59	0.04
kle-2/+; dpy-26/+	0.17	0.12	0.18	0.21	0.23	0.91	0.05
xpf-1; kle-2/+; dpy-26/+	0.11	0.07	0.20	0.09	0.14	0.60	0.06

relative recombination frequency

4.50+
3.50-4.49
2.50-3.49
1.50-2.49
.50-1.49
0-.49

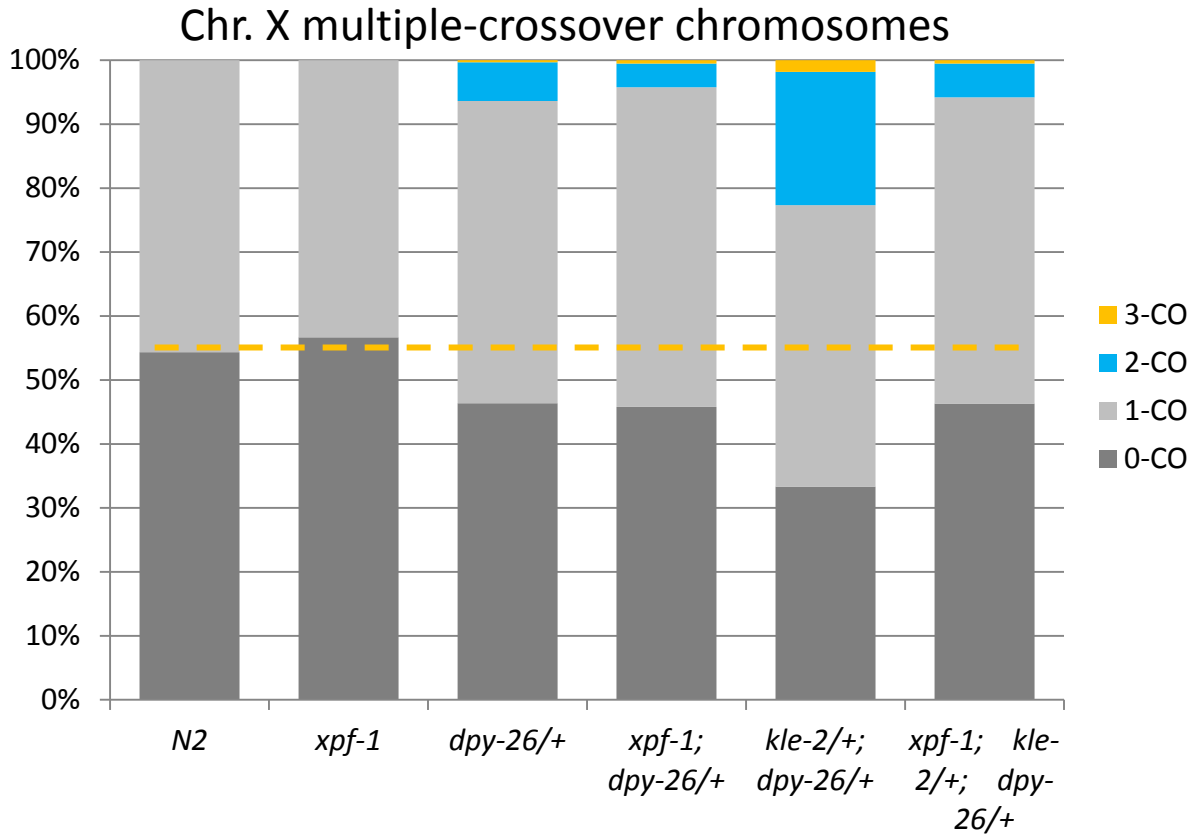

Figure 22a.

Chr. X genotype	dose (Gy)	recomb	SEM	chromosomes with indicated number of crossovers: raw values 4	3	2	1	0	N (mothers)	frequencies 4	3	2	1	0
WT	0	0.46	0.04	0	0	0	168	200	368 (10)	0.00	0.00	0.00	0.46	0.55
mus-81		0.47	0.04	0	0	3	144	125	272 (6)	0.00	0.00	0.01	0.53	0.46
dpy-26/+		0.62	0.14	0	1	20	156	153	330 (4)	0.00	0.00	0.06	0.47	0.46
mus-81; dpy-26/+		0.60	0.05	0	2	45	295	348	690 (9)	0.00	0.00	0.07	0.43	0.50
WT	1 *	0.58	0.06	0	1	7	39	49	96 (4)	0.00	0.01	0.07	0.31	0.49
mus-81		0.56	0.04	0	0	8	92	92	192 (7)	0.00	0.00	0.04	0.48	0.48
dpy-26/+		0.77	0.06	0	4	10	57	45	116 (3)	0.00	0.03	0.09	0.49	0.39
mus-81; dpy-26/+		0.58	0.04	0	0	3	50	43	96 (2)	0.00	0.00	0.03	0.52	0.45
WT	7.5 ***	0.87	0.01	0	5	36	69	70	180 (5)	0.00	0.03	0.20	0.38	0.39
mus-81		0.49	0.01	0	0	3	87	100	190 (4)	0.00	0.00	0.02	0.46	0.53
dpy-26/+		0.94	0.10	2	12	66	96	112	288 (6)	0.01	0.04	0.23	0.33	0.39
mus-81; dpy-26/+		0.43	0.05	0	0	4	47	78	129 (2)	0.00	0.00	0.03	0.37	0.60

p values between *dpy-26/+* and *mus-81; dpy-26/+*

Figure 22. A requirement for MUS-81 can be invoked by combining insults that do not independently cause a requirement on Chromosome X. (a) Crossover frequency for irradiated *mus-81, dpy-26/+,* and *mus-81; dpy-26/+* mutants using six genetic markers on Chromosome X. Shown are map distance (with standard error of the mean); chromosomes that received either four, three, two, one, or no crossovers; and N values for meiotic products assayed and, in parentheses, meioses assayed. Frequencies were calculated by the formula (number of crossovers in each class)/(total meiotic products assayed). Asterisks indicate statistical significance of chromosome class distribution between condensin I mutants and condensin I mutants with a mutation in *mus-81*: *P<0.05, **P<0.01, ***P<0.001, and ****P<0.0001 by the Fisher's exact test. (b) Crossover frequencies in each interval assayed. For each genotype, crossover frequencies (numbers in the colored boxes) were calculated by the formula (number of crossovers in each class)/(total meiotic products assayed). Box colors indicate the relative recombination frequency compared to untreated wild-type animals; key is shown to the right. The histogram of multiple-crossover chromosomes has each class of crossovers represented by the color in the key shown to the right. Dashed orange line represents the percentage of chromosomes receiving no crossovers in untreated wild-type animals.

Figure 22b.

Chr. X

genotype	dose (Gy)	A to B	B to C	C to D	D to E	E to F	recomb	SEM
WT	0	0.07	0.07	0.13	0.09	0.10	0.46	0.04
mus-81		0.10	0.11	0.09	0.10	0.08	0.47	0.04
dpy-26/+		0.08	0.09	0.09	0.15	0.21	0.62	0.14
mus-81; dpy-26/+		0.10	0.11	0.15	0.13	0.12	0.60	0.05
WT	1	0.08	0.08	0.16	0.16	0.10	0.58	0.06
mus-81		0.09	0.17	0.16	0.07	0.07	0.56	0.04
dpy-26/+		0.15	0.12	0.10	0.22	0.19	0.77	0.06
mus-81; dpy-26/+		0.14	0.07	0.08	0.13	0.17	0.58	0.04
WT	7.5	0.23	0.24	0.21	0.12	0.07	0.87	0.01
mus-81		0.10	0.07	0.11	0.11	0.11	0.49	0.01
dpy-26/+		0.25	0.17	0.19	0.15	0.18	0.94	0.10
mus-81; dpy-26/+		0.08	0.05	0.06	0.08	0.16	0.43	0.05

relative recombination frequency

- 4.50+
- 3.50-4.49
- 2.50-3.49
- 1.50-2.49
- .50-1.49
- 0-.49

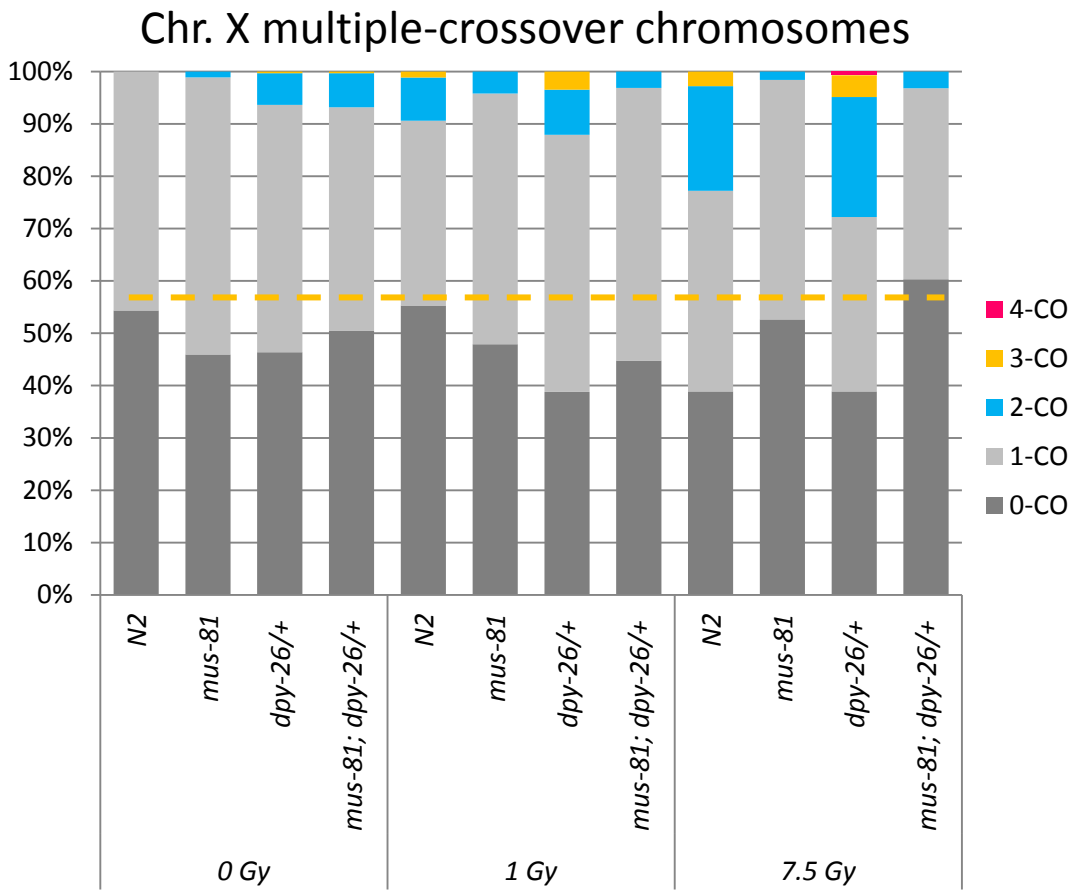

Figure 23a.

Chr. X genotype	dose (Gy)	recomb	SEM	chromosomes with indicated number of crossovers: raw values 4	3	2	1	0	N (mothers)	frequencies 4	3	2	1	0
WT	0	0.46	0.04	0	0	0	168	200	368 (10)	0.00	0.00	0.00	0.46	0.55
xpf-1		0.43	0.03	0	0	0	68	89	157 (5)	0.00	0.00	0.00	0.43	0.57
dpy-26/+		0.62	0.14	0	1	20	156	153	330 (4)	0.00	0.00	0.06	0.47	0.46
xpf-1; dpy-26/+		0.59	0.04	0	1	7	95	87	190 (2)	0.00	0.01	0.04	0.50	0.46
WT	1 ***	0.58	0.06	0	1	7	39	49	96 (4)	0.00	0.01	0.07	0.31	0.49
xpf-1		0.44	0.14	0	0	0	42	53	95 (2)	0.00	0.00	0.00	0.44	0.56
dpy-26/+		0.77	0.06	0	4	10	57	45	116 (3)	0.00	0.03	0.09	0.49	0.39
xpf-1; dpy-26/+		0.42	0.03	0	0	1	59	83	143 (2)	0.00	0.00	0.01	0.41	0.59
WT	7.5 **	0.87	0.01	0	5	36	69	70	180 (5)	0.00	0.03	0.20	0.38	0.39
xpf-1		0.48	0.06	0	0	0	81	87	168 (5)	0.00	0.00	0.00	0.48	0.52
dpy-26/+		0.94	0.10	2	12	66	96	112	288 (6)	0.01	0.04	0.23	0.33	0.39
xpf-1; dpy-26/+		0.42	0.08	0	0	0	40	56	96 (2)	0.00	0.00	0.00	0.42	0.58

p values between *dpy-26/+* and *xpf-1; dpy-26/+*

Figure 23. A requirement for XPF-1 can be invoked by combining insults that do not independently cause a requirement on Chromosome X. (a) Crossover frequency for irradiated *xpf-1, dpy-26/+,* and *xpf-1; dpy-26/+* mutants using six genetic markers on Chromosome X. Shown are map distance (with standard error of the mean); chromosomes that received either four, three, two, one, or no crossovers; and N values for meiotic products assayed and, in parentheses, meioses assayed. Frequencies were calculated by the formula (number of crossovers in each class)/(total meiotic products assayed). Asterisks indicate statistical significance of chromosome class distribution between condensin I mutants and condensin I mutants with a mutation in *xpf-1*: *P<0.05, **P<0.01, ***P<0.001, and ****P<0.0001 by the Fisher's exact test. (b) Crossover frequencies in each interval assayed. For each genotype, crossover frequencies (numbers in the colored boxes) were calculated by the formula (number of crossovers in each class)/(total meiotic products assayed). Box colors indicate the relative recombination frequency compared to untreated wild-type animals; key is shown to the right. The histogram of multiple-crossover chromosomes has each class of crossovers represented by the color in the key shown to the right. Dashed orange line represents the percentage of chromosomes receiving no crossovers in untreated wild-type animals.

Figure 23b.

Chr. X genotype	dose (Gy)	A to B	B to C	C to D	D to E	E to F	recomb	SEM
WT	0	0.07	0.07	0.13	0.09	0.10	0.46	0.04
xpf-1		0.09	0.08	0.07	0.11	0.08	0.43	0.03
dpy-26/+		0.08	0.09	0.09	0.15	0.21	0.62	0.14
xpf-1; dpy-26/+		0.11	0.09	0.10	0.15	0.14	0.59	0.04
WT	1	0.08	0.08	0.16	0.16	0.10	0.58	0.06
xpf-1		0.04	0.11	0.12	0.07	0.11	0.44	0.14
dpy-26/+		0.15	0.12	0.10	0.22	0.19	0.77	0.06
xpf-1; dpy-26/+		0.07	0.05	0.07	0.12	0.12	0.42	0.03
WT	7.5	0.23	0.24	0.21	0.12	0.07	0.87	0.01
xpf-1		0.08	0.08	0.11	0.13	0.08	0.48	0.06
dpy-26/+		0.25	0.17	0.19	0.15	0.18	0.94	0.10
xpf-1; dpy-26/+		0.08	0.08	0.04	0.10	0.10	0.42	0.08

relative recombination frequency

4.50+
3.50-4.49
2.50-3.49
1.50-2.49
.50-1.49
0-.49

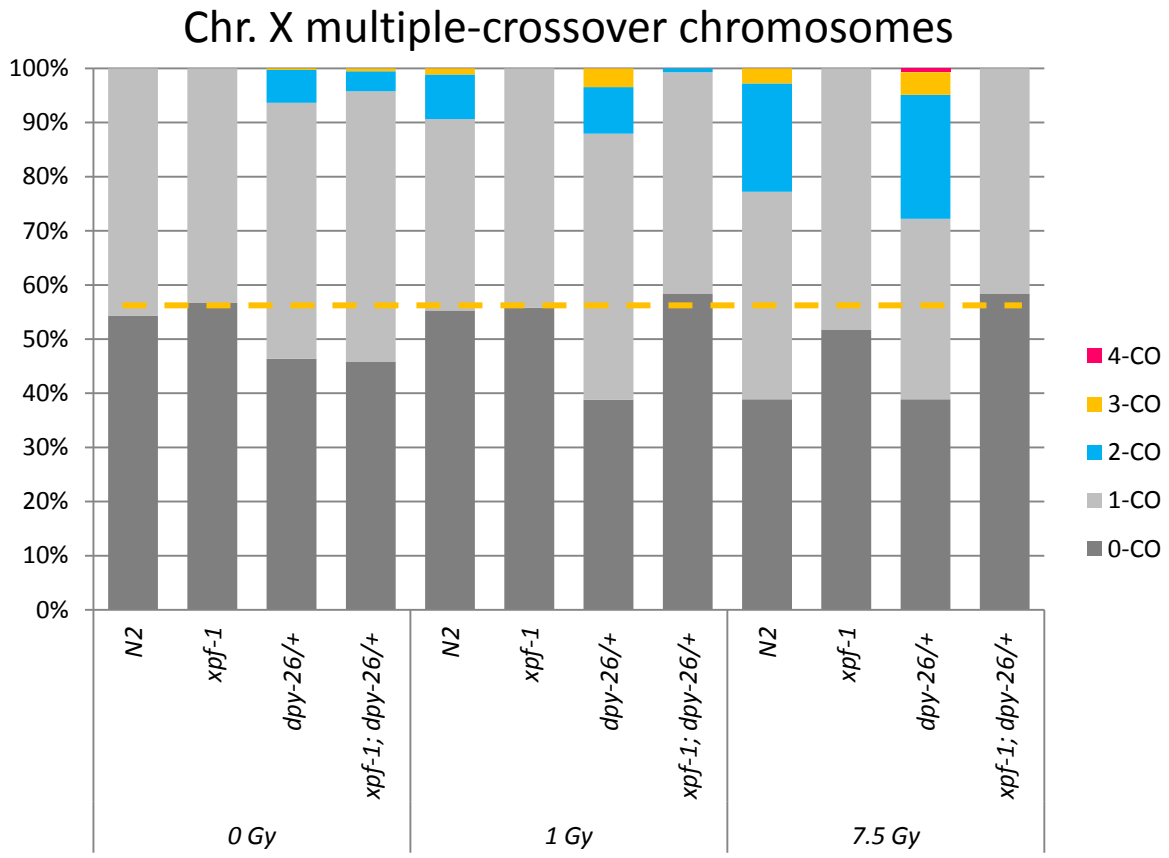

Figure 24a.

Chr. II genotype	dose (Gy)	recomb	SEM	chromosomes with indicated number of crossovers: raw values 4	3	2	1	0	N (mothers)	frequencies 4	3	2	1	0
WT	0	0.51	0.06	0	0	1	95	96	192 (4)	0.00	0.00	0.01	0.49	0.50
xpf-1		0.46	0.08	0	0	0	109	129	238 (6)	0.00	0.00	0.00	0.46	0.54
dpy-26/+		0.56	0.08	0	0	9	62	71	142 (2)	0.00	0.00	0.06	0.44	0.50
xpf-1; dpy-26/+		0.60	0.13	0	3	9	53	77	142 (2)	0.00	0.02	0.06	0.37	0.54
WT	1 *	0.56	0.06	0	0	6	41	47	94 (4)	0.00	0.00	0.06	0.44	0.50
xpf-1		0.43	0.03	0	0	0	82	110	192 (2)	0.00	0.00	0.00	0.43	0.57
dpy-26/+		0.61	0.19	0	3	4	40	47	94 (2)	0.00	0.03	0.04	0.43	0.50
xpf-1; dpy-26/+		0.49	0.01	0	0	0	47	49	96 (2)	0.00	0.00	0.00	0.49	0.51
WT	7.5 *	0.95	0.12	1	1	24	36	34	96 (4)	0.01	0.01	0.25	0.38	0.35
xpf-1		0.46	0.06	0	0	0	79	94	173 (2)	0.00	0.00	0.00	0.46	0.54
dpy-26/+		0.80	0.11	1	9	35	149	138	332 (4)	0.00	0.03	0.11	0.45	0.42
xpf-1; dpy-26/+		0.49	0.06	0	0	0	68	71	139 (2)	0.00	0.00	0.00	0.49	0.51

p values between *dpy-26/+* and *xpf-1; dpy-26/+*

Figure 24. A requirement for XPF-1 can be invoked by combining insults that do not independently cause a requirement on Chromosome II. (a) Crossover frequency for irradiated *xpf-1, dpy-26/+,* and *xpf-1; dpy-26/+* mutants using six genetic markers on Chromosome II. Shown are map distance (with standard error of the mean); chromosomes that received either four, three, two, one, or no crossovers; and N values for meiotic products assayed and, in parentheses, meioses assayed. Frequencies were calculated by the formula (number of crossovers in each class)/(total meiotic products assayed). Asterisks indicate statistical significance of chromosome class distribution between condensin I mutants and condensin I mutants with a mutation in *xpf-1*: *P<0.05, **P<0.01, ***P<0.001, and ****P<0.0001 by the Fisher's exact test. (b) Crossover frequencies in each interval assayed. For each genotype, crossover frequencies (numbers in the colored boxes) were calculated by the formula (number of crossovers in each class)/(total meiotic products assayed). Box colors indicate the relative recombination frequency compared to untreated wild-type animals; key is shown to the right. The histogram of multiple-crossover chromosomes has each class of crossovers represented by the color in the key shown to the right. Dashed orange line represents the percentage of chromosomes receiving no crossovers in untreated wild-type animals.

Figure 24b.

Chr. II genotype	dose (Gy)	A to B	B to C	C to D	D to E	E to F	recomb	SEM
WT	0	0.08	0.15	0.07	0.11	0.10	0.51	0.06
xpf-1		0.06	0.10	0.09	0.11	0.09	0.46	0.08
dpy-26/+		0.15	0.13	0.06	0.08	0.15	0.56	0.08
xpf-1; dpy-26/+		0.10	0.09	0.08	0.14	0.19	0.60	0.13
WT	1	0.10	0.17	0.14	0.13	0.03	0.56	0.06
xpf-1		0.10	0.08	0.06	0.08	0.09	0.43	0.03
dpy-26/+		0.06	0.15	0.14	0.10	0.16	0.61	0.19
xpf-1; dpy-26/+		0.08	0.10	0.07	0.09	0.14	0.49	0.01
WT	7.5	0.21	0.13	0.25	0.15	0.22	0.95	0.12
xpf-1		0.08	0.09	0.12	0.12	0.04	0.46	0.06
dpy-26/+		0.22	0.15	0.11	0.16	0.16	0.80	0.11
xpf-1; dpy-26/+		0.11	0.18	0.02	0.07	0.11	0.49	0.06

relative recombination frequency

4.50+
3.50-4.49
2.50-3.49
1.50-2.49
.50-1.49
0-.49

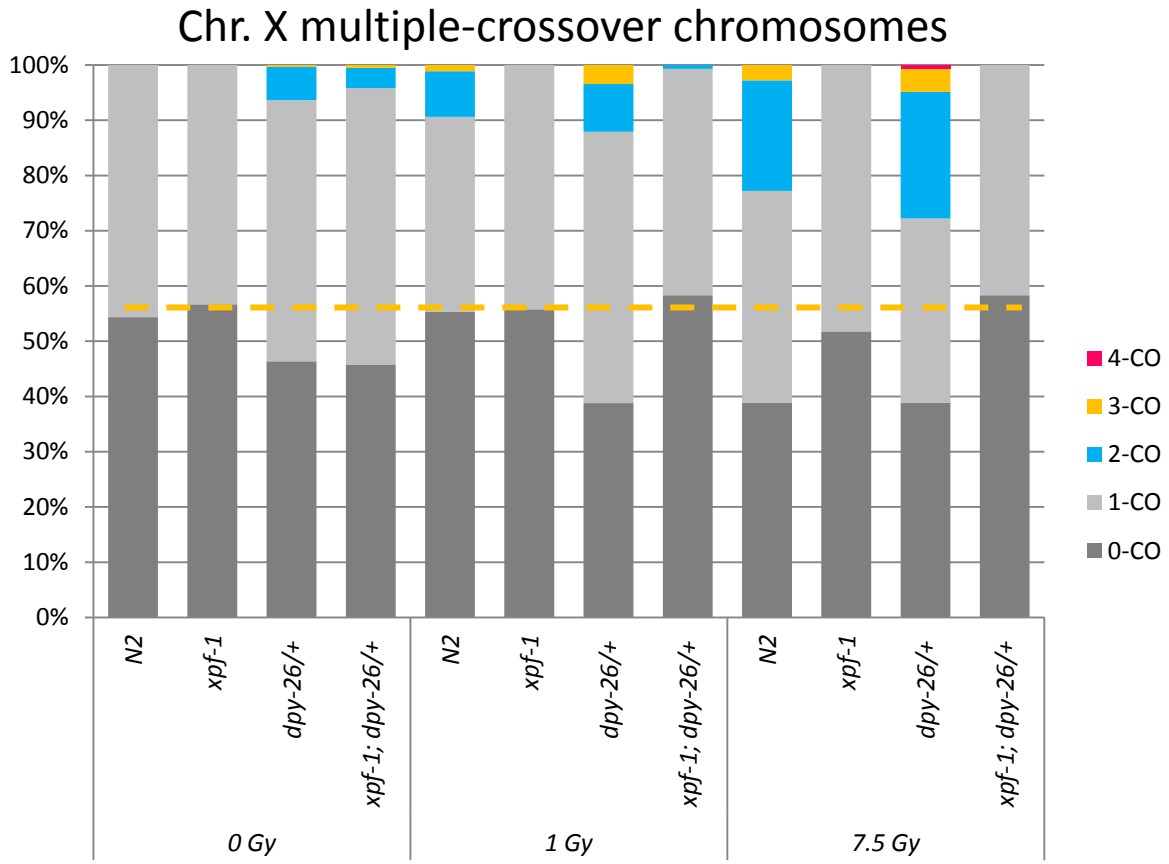

Figure 25a.

Chr. X genotype	dose (Gy)	recomb	SEM	chromosomes with indicated number of crossovers: raw values 4	3	2	1	0	N (mothers)	frequencies 4	3	2	1	0
WT	0	0.46	0.04	0	0	0	168	200	368 (10)	0.00	0.00	0.00	0.46	0.55
mus-81	0	0.47	0.04	0	0	3	144	125	272 (6)	0.00	0.00	0.01	0.53	0.46
dpy-28 (y283)	0	0.50	0.04	0	0	0	38	40	78 (2)	0.00	0.00	0.00	0.49	0.51
mus-81; dpy-28 (y283)	0	0.52	0.04	0	0	0	98	94	192 (2)	0.00	0.00	0.00	0.51	0.49
WT	1	0.58	0.06	0	1	7	39	49	96 (4)	0.00	0.01	0.07	0.31	0.49
mus-81	1	0.56	0.04	0	0	8	92	92	192 (7)	0.00	0.00	0.04	0.48	0.48
dpy-28 (y283)	1	0.62	0.03	0	1	15	83	89	188 (2)	0.00	0.01	0.08	0.44	0.47
mus-81; dpy-28 (y283)	1	0.59	0.07	0	0	15	104	97	216 (4)	0.00	0.00	0.07	0.48	0.45
WT	7.5	0.87	0.01	0	5	36	69	70	180 (5)	0.00	0.03	0.20	0.38	0.39
mus-81	7.5	0.49	0.01	0	0	3	87	100	190 (4)	0.00	0.00	0.02	0.46	0.53
dpy-28 (y283)	7.5	0.86	0.01	0	4	13	43	34	94 (2)	0.00	0.04	0.14	0.46	0.36
mus-81; dpy-28 (y283)	7.5	0.62	0.07	0	1	8	84	75	168 (4)	0.00	0.01	0.05	0.50	0.45

p values between *dpy-28 (y283)* and *mus-81; dpy-28 (y283)*

Figure 25. Depleting condensin without increasing DSB number suppresses the requirement for MUS-81 in irradiated animals. (a) Crossover frequency for irradiated *mus-81, dpy-28 (y283),* and *mus-81; dpy-26 (y283)* mutants using six genetic markers on Chromosome X. Shown are map distance (with standard error of the mean); chromosomes that received either four, three, two, one, or no crossovers; and N values for meiotic products assayed and, in parentheses, meioses assayed. Frequencies were calculated by the formula (number of crossovers in each class)/(total meiotic products assayed). Asterisks indicate statistical significance of chromosome class distribution between condensin I mutants and condensin I mutants with a mutation in *mus-81*: **P*<0.05, ***P*<0.01, ****P*<0.001, and *****P*<0.0001 by the Fisher's exact test. (b) Crossover frequencies in each interval assayed. For each genotype, crossover frequencies (numbers in the colored boxes) were calculated by the formula (number of crossovers in each class)/(total meiotic products assayed). Box colors indicate the relative recombination frequency compared to untreated wild-type animals; key is shown to the right. The histogram of multiple-crossover chromosomes has each class of crossovers represented by the color in the key shown to the right. Dashed orange line represents the percentage of chromosomes receiving no crossovers in untreated wild-type animals.

Figure 25b.

Chr. X genotype	dose (Gy)	A to B	B to C	C to D	D to E	E to F	recomb	SEM
WT	0	0.07	0.07	0.13	0.09	0.10	0.46	0.04
mus-81		0.10	0.11	0.09	0.10	0.08	0.47	0.04
dpy-28 (y283)		0.03	0.05	0.05	0.18	0.18	0.50	0.04
mus-81; dpy-28 (y283)		0.07	0.07	0.05	0.17	0.17	0.52	0.04
WT	1	0.08	0.08	0.16	0.16	0.10	0.58	0.06
mus-81		0.09	0.17	0.16	0.07	0.07	0.56	0.04
dpy-28 (y283)		0.09	0.05	0.13	0.17	0.17	0.62	0.03
mus-81; dpy-28 (y283)		0.12	0.12	0.06	0.14	0.13	0.59	0.07
WT	7.5	0.23	0.24	0.21	0.12	0.07	0.87	0.01
mus-81		0.10	0.07	0.11	0.11	0.11	0.49	0.01
dpy-28 (y283)		0.16	0.13	0.18	0.14	0.25	0.86	0.01
mus-81; dpy-28 (y283)		0.16	0.16	0.07	0.17	0.11	0.62	0.07

relative recombination frequency

4.50+
3.50-4.49
2.50-3.49
1.50-2.49
.50-1.49
0-.49

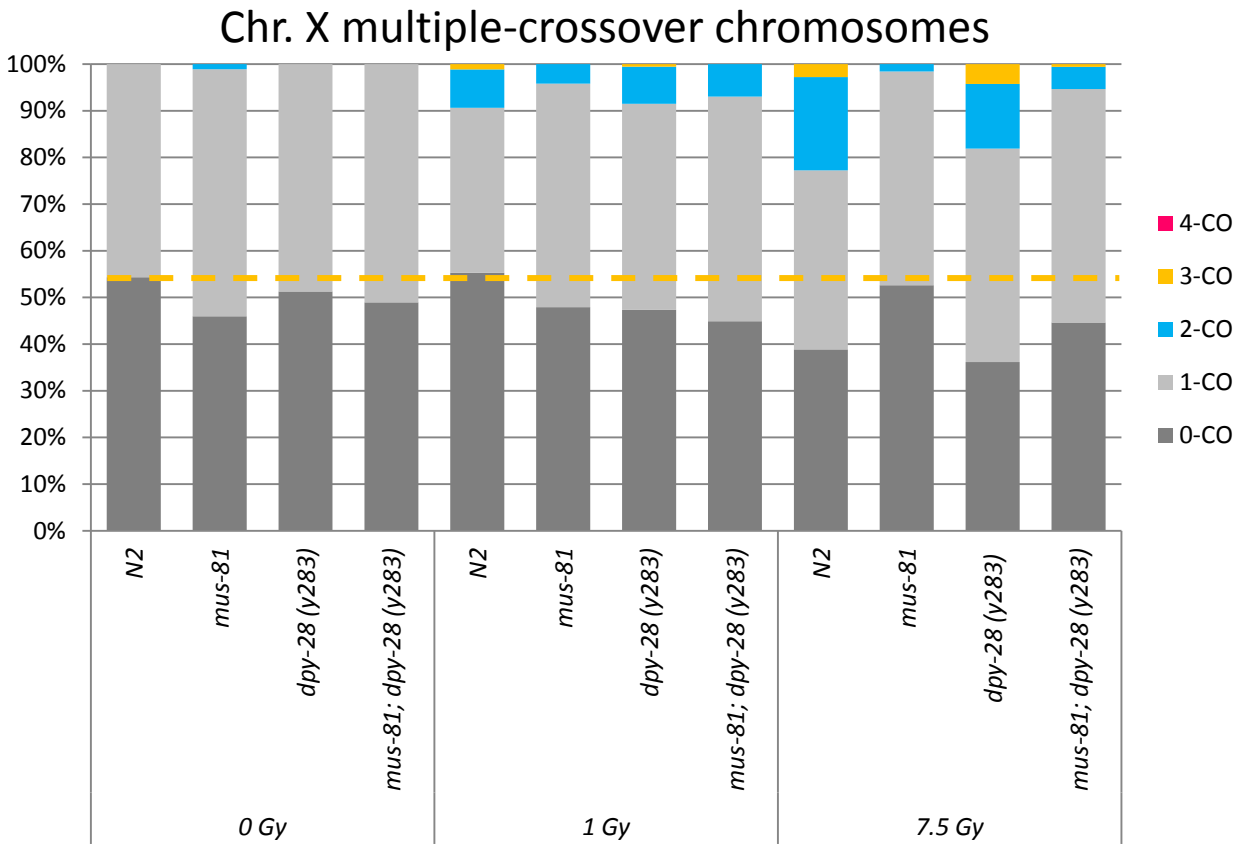

Materials and Methods

C. elegans strains and maintenance

Strains were maintained at 20° C as described in BRENNER 1974. Experiments were conducted at 20° C. Homozygous mutant animals were derived either from homozygous strains or from heterozygous balanced strains by selecting animals that lacked the dominant balancer-linked marker (Rol or GFP). Heterozygous mutant animals were obtained by crossing N2 males into the balanced heterozygous strain and selecting animals lacking a dominant balancer-linked marker. In cases where a visual marker was not present, animals were genotyped by PCR. Males were generated through heat-shock: L4 hermaphrodites were incubated at 37° C for one hour, cloned onto individual plates, and allowed to lay for three to five days; resulting males were then crossed back into the original strain and maintained through crosses.

Table 1: Strains used in this study

AV596	*cosa-1(tm3298) / qC1[qIs26] III*
AV630	*meIs8II*
AV733	*meIs8 II; dpy-28(s939)III / hT2 [qIs48] (I;III)*
CB4856	Hawaiian wild-type
CV211	*xpf-1(e1487)/mIn1[mIs14] II; him-6(ok412) IV / DnT1(IV;V)*
CV294	*mus-81(tm1937) slx-1(tm2644) I / hT2 [qIs48] (I;III)*
FX1937	*mus-81(tm1937) I*
MT2547	*ced-4(n1162) III*
N2	Bristol wild-type
SP365	*unc-4(e120) mix-1(mn29) / mnC1 II*
TG1540	*gen-1(tm2940) III*
TG1660	*xpf-1(tm2842) II*
TG1890	*mus-81 (tm1837) I / hT2 [qIs48] (I;III) ; xpf-1 (tm2842) II*
TY3784	*dpy-28(y283) III / hT2 [qIs48] (I;III)*
TY4342	*spo-11(me44) IV / nT1[qIs51] (IV:V)*
TY5117	*mix-1 (mn29) / mnC1 II*
TY5161	*dpy-26(n199) IV / nT1[qIs51] (IV:V)*
TY5542	*meIs8 II; dpy-26(n199) IV / nT1[qIs51] (IV:V)*
TY5543	*mus-81(tm1937) I; dpy-26(n199) IV / nT1[qIs51] (IV:V)*
TY5552	*meIs8 II; kle-2(ok1151) III / hT2 [qIs48] (I;III)*
TY5553	*mus-81 (tm1937) I /hT2 [qIs48] (I;III); kle-2(ok1151) III / hT2 [qIs48] (I;III)*
TY5554	*mus-81 (tm1937) I /hT2 [qIs48] (I;III); dpy-28(y283) III / hT2 [qIs48] (I;III)*
TY5554	*mus-81 (tm1937) I /hT2[qIs48] (I:III); dpy-28(y283) III / hT2[qIs48] (I:III)*
TY5555	*cosa-1 (tm3298) /qC1[qIs26] III; dpy-26 (n199) IV / nT1 [qIs51] (IV, V)*
TY5556	*mus-81 (tm1937) I; mix-1 (mn29) / mnC1 II*

TY5645	*mus-81(tm1937) I; spo-11(me44)IV / nT1[qIs51] (IV:V)*
TY5722	*xpf-1(tm2842) II; kle-2(ok1151) III / hT2 [qIs48] (I;III)*
TY5724	*mus-81 (tm1837) I; ced-4(n1162) III*
TY5732	*xpf-1(tm2842) II; dpy-26(n199) IV / nT1[qIs51] (IV:V)*
VC193	*him-6 (ok412) IV*
VC768	*kle-2(ok1151) III / hT2 [qIs48] (I;III)*

<u>balancers</u>
DnT1 [unc-?(n754) let-?(m435)](IV;V)
hT2 [bli-4(e937) let-?(qIs48] (I;III)
mIn1 [dpy-10(e128) mIs14] II
mnC1 [dpy-10(e128) unc-54(e444)] II
nT1 [let-?(m435) qIs51](IV:V)
qC1 [dpy-19(e1259) glp-1(q339)] III

<u>transgenes</u>
meIs8 [unc-119(+) pie-1promoter::gfp::cosa-1] II
mIs14 [myo-2::GFP; pes-10::GFP] – pharynx-specific GFP was used as a marker
qIs26 [lag-2::GFP + rol-6(su1006)] – rolling was used as a marker
qIs48 [Pmyo-2::GFP; Ppes-10::GFP; Pges-1::GFP] – pharynx-specific GFP was used as a marker
qIs51 [myo-2::GFP; pes-10::GFP; F22B7.9::GFP] – pharynx-specific GFP was used as a marker

Genetic crosses to generate mutants for crossover assay

See Table 2 for all strains used in crosses.

Hybrid homozygous mutant F2 hermaphrodites were obtained by crossing indicated mutant males into CB4856 hermaphrodites. From this parental cross, heterozygous hybrid F1 males were chosen using the following criteria: if the mutation in the parental strain was being maintained over a balanced chromosome, males lacking the marker on the balancer were used; if the mutation in the parental strain was in a homozygous strain, any F1 male was used. These F1 males were then mated with indicated mutant hermaphrodites. Resulting F2 hermaphrodites were individually mated with CB4856 males, and all parents were transferred every day to a fresh plate. After six days, F2 hermaphrodites were sacrificed for genotyping by PCR to identify individuals with the desired genotype. We also required that F2 hermaphrodites were heterozygous for two markers on Chromosome X (since the cross construction would have allowed no recombination from the Bristol X chromosome before the F2 generation) or for all six markers on Chromosome II (indicating an animal who received a parental Bristol chromosome or a chromosome where the obligatory crossover fell outside the marker range). F3 progeny from F2 hermaphrodites with the desired genotype were then picked into lysis buffer and frozen for use in the crossover assay.

Hybrid trans-heterozygous mutant F2 hermaphrodites were obtained by crossing indicated mutant males into CB4856 hermaphrodites. From the parental cross, heterozygous hybrid F1 males were identified by lack of a dominant marker on the paternal balancer chromosome. These F1 males were then mated with indicated mutant hermaphrodites. Resulting F2 hermaphrodites (lacking the dominant marker on the maternal balancer) were individually mated with CB4856 males and genotype using the same scheme as above. F3 progeny from F2 hermaphrodites with the desired genotype were then picked into lysis buffer and frozen for use in the crossover assay.

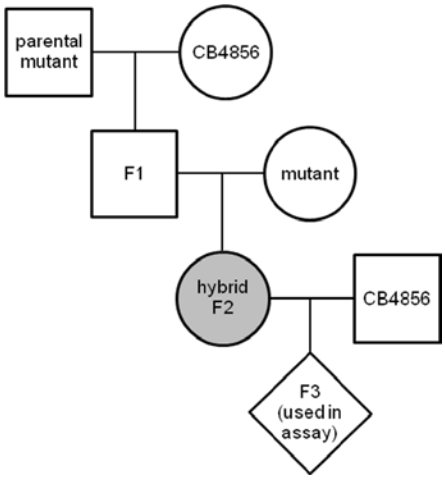

Methods Figure 1. Schematic of the genetic strategy for obtaining F3 progeny used in the crossover assay, to analyze recombination in the F2 hermaphrodite (shown in gray). Squares indicates males; circles indicate hermaphrodites.

Hybrid heterozygous mutant F1 hermaphrodites were obtained by crossing indicated mutant males into CB4856 hermaphrodites. Heterozygous hybrid F1 hermaphrodites (chosen using the same criteria as above) were then mated with CB4856 males and genotyped using the same scheme as above. F2 progeny from hermaphrodites with the desired genotype were then picked into lysis buffer and frozen for use in the crossover assay.

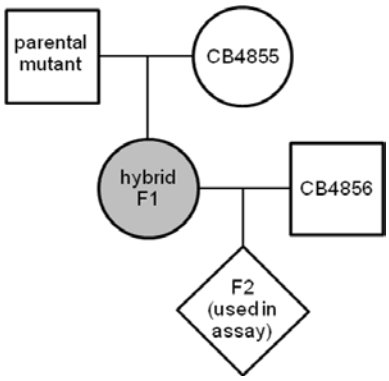

Methods Figure 2. Schematic of the genetic strategy for obtaining F2 progeny used in the crossover assay, to analyze recombination in the F1 hermaphrodite (shown in gray). Squares indicates males; circles indicate hermaphrodites.

Hybrid wild-type F2 hermaphrodites (containing one Bristol chromosome and one Hawaiian chromosome) were obtained by crossing CB4856 males into N2 hermaphrodites. F2 hybrids were mated to CB4856 males and genotyped as described above. F3 progeny were picked into lysis buffer and frozen for use in the crossover assay.

Table 2. Parental strain used in crosses to build hybrid animals for crossover assay

Shorthand genotypes are give to reflect the important mutations and balancers

genotype assayed	male in first cross	hermaphrodite in second cross
mus-81(tm1937)	FX1937 *mus-81*	FX1937 *mus-81*
xpf-1(tm2842)	TG1660 *xpf-1*	TG1660 *xpf-1*
mus-81(tm1937); xpf-1(tm2842)	TG1890 *mus-81/hT2; xpf-1*	TG1890 *mus-81/hT2; xpf-1*
mus-81(tm1937); ced-4(n1162)	TY5724 *mus-81;ced-4*	TY5724 *mus-81;ced-4*
dpy-26(n199) /+	TY5161 *dpy-26/nT1*	--
kle-2(ok1151) /+	VC768 *kle-2/hT2*	--
kle-2(ok1151) /+; dpy-26(n199) /+	VC768 *kle-2/hT2*	TY5161 *dpy-26/nT1*
cosa-1(tm3298)/+	AV596 *cosa-1/qC1*	--
cosa-1(tm3298)/+; dpy-26(n199) /+	TY5555 *cosa-1/qC1; dpy-26/nT1*	TY5555 *cosa-1/qC1; dpy-26/nT1*
mus-81(tm1937); dpy-26(n199) /+	TY5543 *mus-81; dpy-26/nT1*	TY5543 *mus-81; dpy-26/nT1*
mus-81(tm1937); kle-2(ok1151) /+	TY5553 *mus-81; kle-2/hT2*	TY5553 *mus-81; kle-2/hT2*
mus-81(tm1937); kle-2(ok1151) /+; dpy-26(n199) /+	TY5553 *mus-81; kle-2/hT2*	TY5543 *mus-81; dpy-26/nT1*
mix-1(mn29)/+	TY5117 *mix-1/mnC1*	--
mus-81(tm1937); mix-1(mn29)/+	TY5556 *mus-81; mix-1/mnC1*	TY5556 *mus-81; mix-1/mnC1*
xpf-1(tm2842); dpy-26(n199) /+	TY5732 *xpf-1; dpy-26/nT1*	TY5732 *xpf-1; dpy-26/nT1*
xpf-1(tm2842); kle-2(ok1151) /+	TY5722 *xpf-1; kle-2/hT2*	TY5722 *xpf-1; kle-2/hT2*
xpf-1(tm2842); kle-2(ok1151) /+; dpy-26(n199) /+	TY5722 *xpf-1; kle-2/hT2*	TY5732 *xpf-1; dpy-26/nT1*
dpy-28 (y283)	TY3784 *dpy-28/hT2*	TY3784 *dpy-28/hT2*
mus-81(tm1937); dpy-28 (y283)	TY5554 (*mus-81; dpy-28/hT2*	TY5554 *mus-81; dpy-28/hT2*
him-6(ok412)	VC193 *him-6*	VC193 *him-6*
gen-1(tm2940)	TG1540 *gen-1*	TG1540 *gen-1*
mus-81 (tm1937) slx-1(tm2644)	CV294 *mus-81 slx-1/hT2*	CV294 *mus-81 slx-1/hT2*
xpf-1(tm2842); him-6(ok412)	CV211 *xpf-1/mIn1; him-6/DnT1*	CV211 *xpf-1/mIn1; him-6/DnT1*

Snip-SNP crossover assay

Analysis of crossovers was performed by PCR on single-worm lysates using six SNP markers and indicated restriction digestions for either Chromosome X or Chromosome II. Primer sequences, restriction endonucleases, and map position for each marker are listed in Table 3.

Table 3. snip-SNP markers used in crossover assay

	map position	primer sequence (5' to 3')	restriction enzyme	N2 fragments (bp)	CB4856 fragments (bp)
Chr II A	-17.9	CGGAGATAGTCTCGTGGTACTG CAGTCATGCTCCAAACATTCTC	DraI	336, 93	288, 93, 48
Chr II B	-14.5	TCCATCTTCGCAATCAGATTTC AACGTACTGCTTCCCATGCTC	AluI	368	203, 165
Chr II C	-6	GAAAGTGTGGATGAAGGCGAGG AGGACCGATAATTTGTGACTGG	DraI	753	206, 548
Chr II D	3.3	TTCTCACAACTTCTTTTCCAAG TTCACTATTTCCCTCGCTGG	TaqaI	572, 112, 15	382, 190, 112, 15
Chr II E	13.6	TAGGAAAGTTGTGTCCACCTGG TGATGACTCCTTCTTCAGCTGC	HinfI	449	288, 160
Chr II F	20.9	GATTCGGAATGGGTGTTG TCTTGAATGCGTGGTGTG	TaqaI	482	340, 142
Chr X A	-19	GGTATCCGATCCCTTCAACAAG TGGCAAAACACATCCCTGTG	BspHI	208, 156	364
Chr X B	-15.6	CTTTAGACGTTGGATGTTCCTG CTATAAAACCCAAATCTGTGGC	NciI	532	255, 276
Chr X C	-11.1	TCGTGGCACCATAAAAGTG GATTCAGATCAAACAGAGGTGG	DraI	243	128, 115
Chr X D	-0.51	TGTAGGAACCGTTTGTTTCTTC GGGGTATAATGAACCAACCTG	ApoI	261, 48	150, 111, 48
Chr X E	10.1	GGCTCTGAGAAACCAACAAG TGTTTGCGATGACGTGTCAG	BfuCI	318, 149	467
Chr X F	20.8	CGAGCAGAGATGCAGAGTTCTCAACTG CGACCTGAAAGATGTGAGGTTCCTTATC	HaeIII	280, 300	580

Exposure to ionizing radiation

Hermaphrodites at the indicated stages were irradiated on agar plates at the indicated doses with a sealed ^{137}Cs source. Doses are given in grays; 1 gray is equivalent to 100 rads. For each experiment, unirradiated control animals were treated identically to irradiated animals with the omission of exposure to radiation.

To measure crossover formation, F2 hermaphrodites were generated as described above and exposed to radiation at the L4-stage. After exposure, hermaphrodites were mated with CB4856 males. After twelve hours, all parents were transferred to new plates and allowed to lay embryos for 24 hours, after which, F2 hermaphrodites were sacrificed for genotyping. F3 progeny of mothers with the desired genotype from this 24-hour interval were assayed as described above. Exposure and

collection of F3s differed slightly from methods previously reported in Mets and Meyer 2009, as did our crossover counts at the 7.5 gray dose. By reproducing the method in Mets and Meyer 2009, we demonstrate that the difference in crossover number is caused by the different method and not by other factors (Methods Figure 3).

To quantify DAPI-stained bodies at diakinesis, L4-stage hermaphrodites were irradiated and dissected 18 hours post-irradiation as described below. STAMPER *et al.* 2013 previously reported complete rescue of DAPI body number in *spo-11* mutants exposed to 10 grays of radiation. At 7.5 grays, we observed partial but not complete rescue. By reproducing the methods and dose in STAMPER *et al.* 2013, we demonstrate that the difference is caused by dose and age of animal at exposure, instead of other factors (Methods Figure 4).

To assess embryonic lethality, L4-stage hermaphrodites were irradiated and cloned onto individual plates. After twelve hours, animals were transferred to fresh plates and eggs were counted as described below.

Quantification of embryonic lethality

L4 hermaphrodites were picked onto individual plates and transferred to new plates every 24 hours for up to six days or until fertilized embryos were no longer observed. Eggs were counted immediately after animals had been transferred, and surviving adult progeny were counted three days later. For quantification of lethality in irradiated animals, L4 hermaphrodites were exposed to radiation, picked onto individual plates, and transferred to new plates every 24 hours for two days; all lethality counts in irradiated animals are 0-48 hours post-exposure.

Germline dissection and immunostaining

Hermaphrodites were cut at the vulva to extrude the gonads in egg buffer (25 mM HEPES pH 7.4, 118 mM NaCl, 48 mM KCl, 0.2 mM $CaCl_2$, 0.2 mM $MgCl_2$) containing 0.1% Tween-20 on coverslips. For fixation, egg buffer containing paraformaldehyde was added to sample for a final concentration of 0.8% paraformaldehyde samples were sandwiched with a Superfrost Plus slide. After five minutes, slides were frozen n in liquid nitrogen. Coverslips were cracked off and slides were immersed in 95% ethanol at room temperature for at least five minutes. Slides were then washed three times for five minutes in phosphate-buffered saline containing 0.5% Triton-X (PBSt). Samples were incubated in a humid chamber overnight at room temperature with primary antibody solutions diluted in PBSt with 3% bovine serum albumin (BSA) and 1mM EDTA (see Table 4 for primary antibody concentrations and secondary antibodies used). After washing three times for five minutes in PBSt, samples were incubated in a humid chamber for two hours at room temperature in secondary antibody (Molecular Probes) diluted 1:200 in PBSt with 3% BSA and 1mM EDTA. Slides were washed three times for five minutes, mounted with SloFade with 2 mg/ml DAPI solution, and sealed with nail polish.

Table 4. Antibodies used for immunostaining

primary antibody	concentration	reference	secondary antibody
RAD-51	1:125	ALPI *et al.* 2003	anti-rabbit Alexa488
HTP-3	1:250	MACQUEEN *et al.* 2005	anti-guinea pig Alexa 594
GFP	1:200	Invitrogen	anti-chicken Alexa488
COH-3/4	1:100,000	SEVERSON *et al.* 2009	anti-rabbit Alexa633

Quantification of diakinesis DAPI bodies

DAPI bodies were counted in diakinesis oocytes in the -3, -2, and -1 positions relative to the spermatheca on a Leica TCS SP2 AOBS confocal microscope (Leica SP2). Images of DAPI were collected on a Leica SP2 in stacks taken every 0.25 microns and projections were made using ImageJ. Images of DAPI and HTP-3 were collected on a Leica SP2 in stacks taken every 0.08 microns and deconvolved with Huygens Pro (Scientific Volume Imaging) software. Projections were made using Priism (CHEN *et al.* 1996).

Quantification of GFP:COSA-1 foci in late pachytene nuclei

GFP was detected by immunofluoresence as described above. Images were collected on a Leica SP2 in stacks taken every 0.25 microns, and projections were made using ImageJ. In these projections, foci were counted in the last five rows of pachytene nuclei.

Chromosome axis length measurements

Whole-mount germlines were labeled by FISH as in (METS and MEYER 2009)with two oligonucleotide probes to X (right end sequence: 5'-GACTCCATCCACCAGCACTGCTTCG AGTACGACAGAAAGCACTTC-3' and center sequence 5'-TTCGCTTAGAGCGATTCCTT ACCCTTAAATGGGCGCCGG-3', then stained with COH-3/4 antibodies followed by secondary antibodies. Images were collected on a Leica SP2 and deconvolved with Huygens Pro software. Chromosomes were traced in 3D along the COH-3/4 –stained axis and straightened computationally in Priism.

Acknowledgements

We thank A. Severson for COH-3/4 antibody, A. Dernburg for HTP-3 antibody, and A. Gartner for RAD-51 antibody; A. Villeneuve, the *Caenorhabditis* Genetics Center, and the National Bioresource Project for strains; E. Ralston, D. Libuda, and A. Villeneuve for discussion; and B. Wheeler for invaluable comments on the manuscript.

This work is supported by a National Science Foundation Predoctoral Fellowship to T.W.L. and a Miller Institute Senior Fellowship B.J.M, who is also a member of the Howard Hughes Medical Institute.

Methods Figure 3a.

Chr. X genotype	recomb	SEM	chromosomes with indicated number of crossovers: raw values 4	3	2	1	0	N (mothers)	frequencies 4	3	2	1	0
WT untreated	0.46	0.04	0	0	0	168	200	368 (10)	0.00	0.00	0.00	0.46	0.55
WT (7.5 Gy) IR on plate	0.56	0.02	0	2	15	46	81	144 (5)	0.00	0.01	0.10	0.32	0.56
WT (7.5 Gy) IR in liquid	0.55	0.01	0	1	11	54	78	144 (6)	0.00	0.01	0.08	0.38	0.54

Methods Figure 3. Comparison to method used in Mets and Meyer 2009 to evaluate crossovers in irradiated animals. (a) Crossover frequency for irradiated wild-type animals using six genetic markers on Chromosome X. Animals were exposed to radiation either on agar plates or in liquid culture in plastic microfuge tubes. Shown are map distance (with standard error of the mean); chromosomes that received either four, three, two, one, or no crossovers; and N values for meiotic products assayed and, in parentheses, meioses assayed. Frequencies were calculated by the formula (number of crossovers in each class)/(total meiotic products assayed). Crossover frequencies in each interval assayed. For each genotype, crossover frequencies (numbers in the colored boxes) were calculated by the formula (number of crossovers in each class)/(total meiotic products assayed). Box colors indicate the relative recombination frequency compared to untreated wild-type animals; key is shown to the right. The histogram of multiple-crossover chromosomes has each class of crossovers represented by the color in the key shown to the right.

Methods Figure
3b.

	Chr. X						
	A to B	B to C	C to D	D to E	E to F	recomb	SEM
WT untreated	0.07	0.07	0.13	0.09	0.10	0.46	0.04
WT (7.5 Gy) IR on plate	0.18	0.15	0.04	0.12	0.07	0.56	0.02
WT (7.5 Gy) IR in liquid	0.18	0.09	0.08	0.08	0.12	0.55	0.01

relative recombination frequency

4.50+
3.50-4.49
2.50-3.49
1.50-2.49
.50-1.49
0-.49

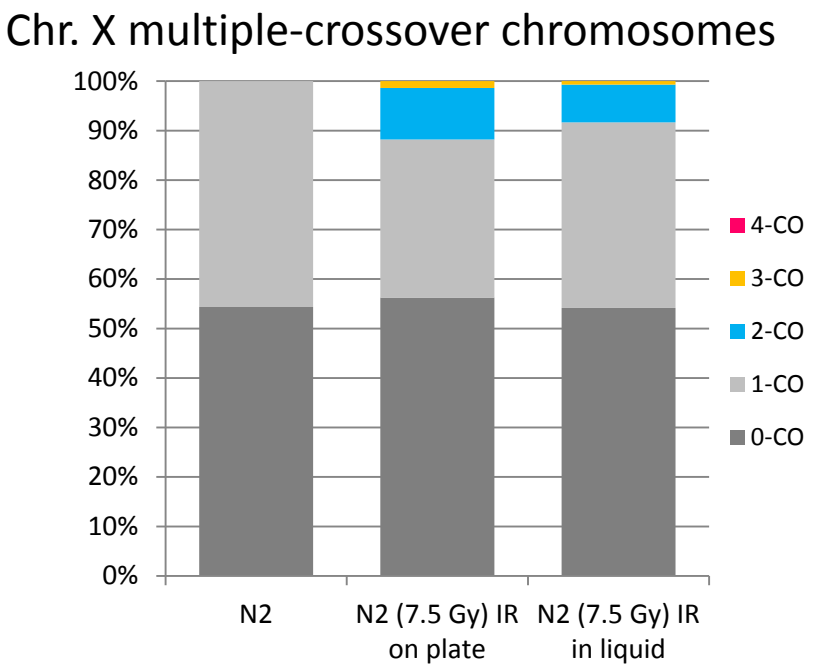

Methods Figure 4.

	average	4	5	6	7	8	9	10	11	12	N (mothers)
		Percent of oocytes with the indicated number of DAPI-staining bodies									
WT (0 Gy)	5.9	0	4	42	0	0	0	0	0	0	46 (15)
WT (7.5 Gy)	6.0	3	33	1	0	0	0	0	0	0	37 (15)
spo-11 (0 Gy)	11.9	0	0	0	0	0	0	0	3	28	31 (7)
spo-11 (10 Gy)	6.0	0	2	91	2	1	0	0	0	0	96 (20)

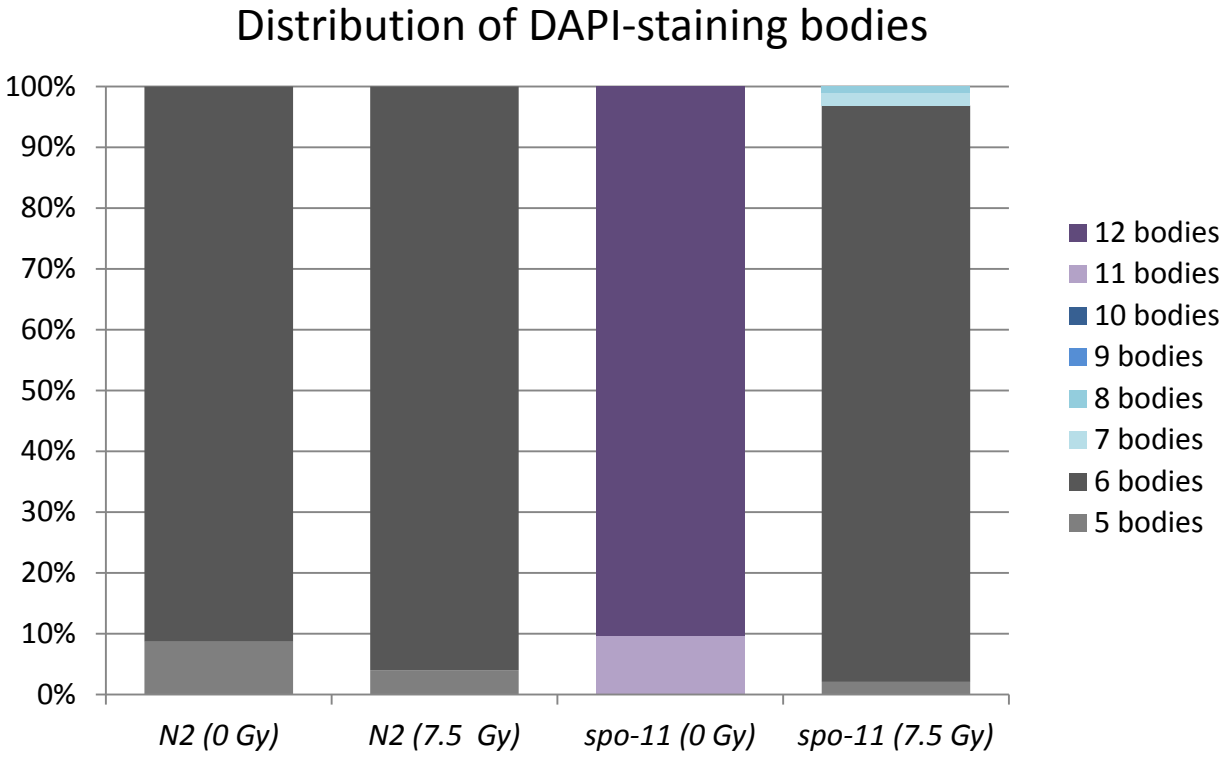

Methods Figure 4. Comparison to method used in STAMPER *et al*. 2013 to evaluate DAPI-staining bodies in diakinesis nuclei of irradiated animals. Quantification of DAPI-stained bodies in diakinesis nuclei. Animals were exposed to radiation as young adults and dissected for analysis 18 hours after exposure. Table shows the average number of DAPI bodies, distribution of nuclei with indicated numbers of DAPI bodies, and N of nuclei scored and animals scored. Stacked histogram represents distribution of nuclei with indicated numbers of DAPI bodies; key is shown to the right.

References

AGOSTINHO A., MEIER B., SONNEVILLE R., JAGUT M., WOGLAR A., BLOW J., JANTSCH V., GARTNER A., 2013 Combinatorial regulation of meiotic holliday junction resolution in *C. elegans* by HIM-6 (BLM) helicase, SLX-4, and the SLX-1, MUS-81 and XPF-1 nucleases. PLoS Genet. **9**: e1003591.

ALPI A., PASIERBEK P., GARTNER A., LOIDL J., 2003 Genetic and cytological characterization of the recombination protein RAD-51 in *Caenorhabditis elegans*. Chromosoma **112**: 6–16.

BAILLY A. P., FREEMAN A., HALL J., AHMED S., GARTNER A., 2010 The *Caenorhabditis elegans* Homolog of Gen1 / Yen1 Resolvases Links DNA Damage Signaling to DNA Double-Strand Break Repair. PLoS Genet. **6**.

BENNETT C. B., LEWIS A. L., BALDWIN K. K., RESNICK M. A., 1993 Lethality induced by a single site-specific double-strand break in a dispensable yeast plasmid. Proc. Natl. Acad. Sci. U. S. A. **90**: 5613–7.

BHALLA N., DERNBURG A. F., 2005 A conserved checkpoint monitors meiotic chromosome synapsis in *Caenorhabditis elegans*. Science **310**: 1683–6.

BHALLA N., DERNBURG A. F., 2008 Prelude to a division. Annu. Rev. Cell Dev. Biol. **24**: 397–424.

BODDY M. N., GAILLARD P. H., MCDONALD W. H., SHANAHAN P., YATES J. R., RUSSELL P., 2001 Mus81-Eme1 are essential components of a Holliday junction resolvase. Cell **107**: 537–48.

BRENNER S., 1974 The Genetics of *Caenorhabditis elegans*. Genetics **77**: 71–94.

CHEN H., HUGHES D. D., CHAN T. A., SEDAT J. W., AGARD D. A., 1996 IVE (Image Visualization Environment): a software platform for all three-dimensional microscopy applications. J. Struct. Biol. **116**: 56–60.

CICCIA A., MCDONALD N., WEST S. C., 2008 Structural and functional relationships of the XPF/MUS81 family of proteins. Annu. Rev. Biochem. **77**: 259–87.

COUTEAU F., ZETKA M., 2011 DNA damage during meiosis induces chromatin remodeling and synaptonemal complex disassembly. Dev. Cell **20**: 353–63.

CROMIE G. a, HYPPA R. W., TAYLOR A. F., ZAKHARYEVICH K., HUNTER N., SMITH G. R., 2006 Single Holliday junctions are intermediates of meiotic recombination. Cell **127**: 1167–78.

CSANKOVSZKI G., COLLETTE K., SPAHL K., CAREY J., SNYDER M., PETTY E., PATEL U., TABUCHI T., LIU H., MCLEOD I., THOMPSON J., SARKESHIK A., SARKESIK A., YATES J., MEYER B. J., HAGSTROM K., 2009 Three distinct condensin complexes control *C. elegans* chromosome dynamics. Curr. Biol. **19**: 9–19.

DERNBURG A. F., MCDONALD K., MOULDER G., BARSTEAD R., DRESSER M., VILLENEUVE A. M., 1998 Meiotic recombination in *C. elegans* initiates by a conserved mechanism and is dispensable for homologous chromosome synapsis. Cell **94**: 387–98.

ELLIS H. M., HORVITZ H. R., 1986 Genetic Control of Programmed Cell Death in the Nematode *C. elegans*. Cell **44**: 817–829.

GARTNER A., MILSTEIN S., AHMED S., HODGKIN J., HENGARTNER M. O., 2000 A Conserved Checkpoint Pathway Mediates DNA Damage – Induced Apoptosis and Cell Cycle Arrest in *C. elegans*. Mol. Cell **5**: 435–443.

HAMMARLUND M., DAVIS M. W., NGUYEN H., DAYTON D., JORGENSEN E. M., 2005 Heterozygous insertions alter crossover distribution but allow crossover interference in *Caenorhabditis elegans*. Genetics **171**: 1047–56.

HEYER W.-D., EHMSEN K. T., LIU J., 2010 Regulation of homologous recombination in eukaryotes. Annu. Rev. Genet. **44**: 113–39.

HILLERS K. J., VILLENEUVE A. M., 2003 Chromosome-Wide Control of Meiotic Crossing over in *C. elegans*. Curr. Biol. **13**: 1641–1647.

HO C. K., MAZÓN G., LAM A. F., SYMINGTON L. S., 2010 Mus81 and Yen1 promote reciprocal exchange during mitotic recombination to maintain genome integrity in budding yeast. Mol. Cell **40**: 988–1000.

HODGKIN J., 1983 Male Phenotypes and Mating Efficiency in *Caenorhabditis elegans*. Genetics **103**: 43–64.

HOLLIDAY R., 1964 The Induction of Mitotic Recombination By Mitomycin C in *Ustilago* and *Saccharomyces*. Genetics **50**: 323–35.

HOLLOWAY J. K., SUN X., YOKOO R., VILLENEUVE A. M., COHEN P. E., 2014 Mammalian CNTD1 is critical for meiotic crossover maturation and deselection of excess precrossover sites. J. Cell Biol. **1**: 633–641.

HOU Y., FAN W., YAN L., LI R., LIAN Y., HUANG J., LI J., XU L., TANG F., XIE X. S., QIAO J., 2013 Genome analyses of single human oocytes. Cell **155**: 1492–506.

JESSOP L., LICHTEN M., 2008 Mus81/Mms4 endonuclease and Sgs1 helicase collaborate to ensure proper recombination intermediate metabolism during meiosis. Mol. Cell **31**: 313–23.

KEENEY S., GIROUX C. N., KLECKNER N., 1997 Meiosis-Specific DNA Double-Strand Breaks Are Catalyzed by Spo11 , a Member of a Widely Conserved Protein Family. Cell **88**: 375–384.

KOHL K. P., SEKELSKY J., 2013 Meiotic and mitotic recombination in meiosis. Genetics **194**: 327–34.

MACQUEEN A. J., PHILLIPS C. M., BHALLA N., WEISER P., VILLENEUVE A. M., DERNBURG A. F., 2005 Chromosome sites play dual roles to establish homologous synapsis during meiosis in *C. elegans*. Cell **123**: 1037–50.

MARTINEZ-PEREZ E., COLAIÁCOVO M. P., 2009 Distribution of meiotic recombination events: talking to your neighbors. Curr. Opin. Genet. Dev. **19**: 105–12.

MATOS J., BLANCO M. G., MASLEN S., SKEHEL J. M., WEST S. C., 2011 Regulatory control of the resolution of DNA recombination intermediates during meiosis and mitosis. Cell **147**: 158–72.

METS D. G., MEYER B. J., 2009 Condensins regulate meiotic DNA break distribution, thus crossover frequency, by controlling chromosome structure. Cell **139**: 73–86.

MUYT A. DE, JESSOP L., KOLAR E., SOURIRAJAN A., CHEN J., DAYANI Y., LICHTEN M., 2012 BLM helicase ortholog Sgs1 is a central regulator of meiotic recombination intermediate metabolism. Mol. Cell **46**: 43–53.

NABESHIMA K., VILLENEUVE A. M., HILLERS K. J., 2004 Chromosome-wide regulation of meiotic crossover formation in *Caenorhabditis elegans* requires properly assembled chromosome axes. Genetics **168**: 1275–92.

NEALE M. J., PAN J., KEENEY S., 2006 Endonucleolytic processing of covalent protein-linked double-strand breaks. Nature **436**: 1053–1057.

NOTTKE A. C., BEESE-SIMS S. E., PANTALENA L. F., REINKE V., SHI Y., COLAIÁCOVO M. P., 2011 SPR-5 is a histone H3K4 demethylase with a role in meiotic double-strand break repair. Proc. Natl. Acad. Sci. U. S. A. **108**: 12805–10.

O'NEIL N. J., MARTIN J. S., YOUDS J. L., WARD J. D., PETALCORIN M. I. R., ROSE A. M., BOULTON S. J., 2013 Joint molecule resolution requires the redundant activities of MUS-81 and XPF-1 during *Caenorhabditis elegans* meiosis. PLoS Genet. **9**: e1003582.

OH S. D., LAO J. P., TAYLOR A. F., SMITH G. R., HUNTER N., 2008 RecQ helicase, Sgs1, and XPF family endonuclease, Mus81-Mms4, resolve aberrant joint molecules during meiotic recombination. Mol. Cell **31**: 324–36.

PAGE S. L., HAWLEY R. S., 2003 Chromosome choreography: the meiotic ballet. Science **301**: 785–9.

PÂQUES F., HABER J. E., 1999 Multiple Pathways of Recombination Induced by Double-Strand Breaks in *Saccharomyces cerevisiae*. Microbiol. Mol. Biol. Rev. **63**: 349–404.

PLENEFISCH J. D., DELONG L., MEYER B. J., 1989 Genes That Implement the Hermaphrodite Mode of Dosage Compensation. Genetics **121**: 57–76.

ROSU S., LIBUDA D. E., VILLENEUVE A. M., 2011 Robust crossover assurance and regulated interhomolog access maintain meiotic crossover number. Science **334**: 1286–9.

SAITO T. T., LUI D. Y., KIM H.-M., MEYER K., COLAIÁCOVO M. P., 2013 Interplay between structure-specific endonucleases for crossover control during *Caenorhabditis elegans* meiosis. PLoS Genet. **9**: e1003586.

SAITO T. T., MOHIDEEN F., MEYER K., HARPER J. W., COLAIÁCOVO M. P., 2012 SLX-1 Is Required for Maintaining Genomic Integrity and Promoting Meiotic Noncrossovers in the *Caenorhabditis elegans* Germline (SE Plon, Ed.). PLoS Genet. **8**: e1002888.

SAITO T. T., YOUDS J. L., BOULTON S. J., COLAIÁCOVO M. P., 2009 *Caenorhabditis elegans* HIM-18/SLX-4 interacts with SLX-1 and XPF-1 and maintains genomic integrity in the germline by processing recombination intermediates. PLoS Genet. **5**: e1000735.

SCHVARZSTEIN M., PATTABIRAMAN D., LIBUDA D. E., RAMADUGU A., TAM A., MARTINEZ-PEREZ E., ROELENS B., ZAWADZKI K. A., YOKOO R., ROSU S., SEVERSON A. F., MEYER B. J., NABESHIMA K., VILLENEUVE A. M., 2014 DNA Helicase HIM-6/BLM Both Promotes MutS γ-Dependent Crossovers and Antagonizes MutS γ-Independent Inter-homolog Associations during *Caenorhabditis elegans* meiosis. Genetics.

SEKELSKY J. J., MCKIM K. S., CHIN G. M., HAWLEY R. S., 1995 The *Drosophila* Meiotic Recombination Gene mei-9 Encodes a Homologue of the Yeast Excision Repair Protein Rad1. Genetics **627**: 619–627.

SEVERSON A. F., LING L., ZUYLEN V. VAN, MEYER B. J., 2009 The axial element protein HTP-3 promotes cohesin loading and meiotic axis assembly in *C. elegans* to implement the meiotic program of chromosome segregation. Genes Dev. **23**: 1763–78.

STAMPER E. L., RODENBUSCH S. E., ROSU S., AHRINGER J., VILLENEUVE A. M., DERNBURG A. F., 2013 Identification of DSB-1, a protein required for initiation of meiotic recombination in *Caenorhabditis elegans*, illuminates a crossover assurance checkpoint. PLoS Genet. **9**: e1003679.

SUN H., TRECO D., SCHULTES N. P., SZOSTAK J. W., 1989 Double-strand breaks at an initiation site for meiotic gene conversion. Nature **338**: 87–90.

TEUSCHER F., BROCKMANN G. a, RUDOLPH P. E., SWALVE H. H., GUIARD V., 2000 Models for chromatid interference with applications to recombination data. Genetics **156**: 1449–60.

TSAI C. J., METS D. G., ALBRECHT M. R., NIX P., CHAN A., MEYER B. J., 2008 Meiotic crossover number and distribution are regulated by a dosage compensation protein that resembles a condensin subunit. Genes Dev. **22**: 194–211.

WICKY C., ALPI A., PASSANNANTE M., ROSE A., GARTNER A., MÜLLER F., MU F., 2004 Multiple Genetic Pathways Involving the *Caenorhabditis elegans* Bloom's Syndrome Genes him-6, rad-51, and top-3 Are Needed To Maintain Genome Stability in the Germ Line. Mol. Cell. Biol. **24**: 5016–5027.

WOOD A. J., SEVERSON A. F., MEYER B. J., 2010 Condensin and cohesin complexity: the expanding repertoire of functions. Nat. Rev. Genet. **11**: 391–404.

YOKOO R., ZAWADZKI K. A., NABESHIMA K., DRAKE M., ARUR S., VILLENEUVE A. M., 2012 COSA-1 reveals robust homeostasis and separable licensing and reinforcement steps governing meiotic crossovers. Cell **149**: 75–87.

YOUDS J. L., BOULTON S. J., 2011 The choice in meiosis - defining the factors that influence crossover or non-crossover formation. J. Cell Sci. **124**: 501–13.

YOUDS J. L., METS D. G., MCILWRAITH M. J., MARTIN J. S., WARD J. D., ONEIL N. J., ROSE A. M., WEST S. C., MEYER B. J., BOULTON S. J., 2010 RTEL-1 enforces meiotic crossover interference and homeostasis. Science **327**: 1254–8.

ZAKHARYEVICH K., TANG S., MA Y., HUNTER N., 2012 Delineation of Joint Molecule Resolution Pathways in Meiosis Identifies a Crossover-Specific Resolvase. Cell **149**: 334–347.

ZHAO H., MCPEEK M. S., SPEED T. P., 1995 Statistical analysis of chromatid interference. Genetics **139**: 1057–65.

ZICKLER D., KLECKNER N., 1999 Integrating Structure and Function. Annu. Rev. Genet. **33**: 603–754.

Appendix I

Each chromosome receives an obligate DSB in *rad-54* mutants

Appendix I.
Each chromosome receives an obligate DSB in *rad-54* mutants

The work in this appendix was performed by me and a former student in the Meyer lab, Dr. David Mets. Specifically, I dissected, stained and analyzed germline RAD-51 foci (Figure 1), and dissected and stained samples for HTP-3 and RAD-51 (Figure 2).

Introduction

Two scenarios could guarantee at least one break per chromosome to ensure the obligate crossover: the random formation of an excess number of DSBs, or an active mechanism that monitors break formation and prevents their random distribution. To see if DSBs were formed in an amount that would allow us to distinguish between these scenarios, we undertook an investigation of the total number of DSBs formed during meiosis.

RAD-51 is a single-stranded binding protein that is required for meiotic DSB repair in *C. elegans* (ALPI *et al.* 2003; OGAWA *et al.* 2014). By loading onto the 3' overhang left after DSB resection, it facilitates a homology search while making a convenient cytological marker for DSBs at this stage of repair. The *C. elegans* germline is arranged like a production-line, in which nuclei progress through the stages of meiosis as they move from the distal to the spermatheca (LEMMENS and TIJSTERMAN 2011). This allows for the examination of all meiotic prophase stages in a single animal and reflects a temporal progression through meiosis. In *C. elegans,* RAD-51 foci begin to appear in the transition zone (leptotene/zygotene), reach a peak number during mid-pachytene, and are almost entirely absent from chromosomes by the end of diakinesis (ALPI *et al.* 2003). However, DSB repair is an ongoing process in which RAD-51 only localizes to DSBs for a short period of time. Therefore, analyses of DSB formation using RAD-51 localization give an incomplete estimate of total breaks formed during meiosis.

In *S. cerevisiae*, mutations that prevent DSB repair after RAD-51 loading can allow for more accurate estimations of DSB formation. RAD-54 is a DEAD-like helicase required for homologous recombination (SHINOHARA *et al.* 2000). In *S. cerevisiae*, rad54 mutants cannot effectively repair DSBs, slowing the removal of Rad51 (SHINOHARA *et al.* 2000; SOLINGER and HEYER 2001). A previous graduate student in our lab developed an assay to measure DSB number using the *rad-54* genetic background to similarly arrest the removal of RAD-51 (METS and MEYER 2009). He demonstrated that *C. elegans rad-54* mutants have persistent RAD-51 foci that reach a plateau level of 11 foci per nucleus at mid-pachytene, and reasoned that this value should represent all DSBs that are repaired through a RAD-51 intermediate (METS and MEYER 2009). Since *C. elegans* has six chromosomes that each receives one crossover, half of the DSBs formed are destined to become crossovers. Mets and Meyer theorized that since *C. elegans* does not form an excess of DSBs during meiosis, an active mechanism must exist to ensure that each chromosome receives at least one DSB. In support of their theory that DSB formation is not random, they showed that significantly fewer chromosomes than expected receive no DSBs, and significantly more chromosomes than expected receive one DSB.

Studies since performed by other groups have detected a higher incidence of RAD-51 foci in *rad-54* mutants (NOTTKE *et al.* 2011; ROSU *et al.* 2011, and Roshni Kasad, personal communication). We revisited the assay and now report a revised estimate of 18 DSBs per nucleus in mid-pachytene, with an increase to 23 DSBs per nucleus in late pachytene. These data are in accordance with other studies.

Results and Discussion

We have used two alleles of *rad-54: ok615*, a deletion of part of an upstream gene and the first exon of *rad-54* and *tm1268*, a deletion of four exons in *rad-54*. In a close analysis of *rad-54* mutants, we observed shorter germlines, aberrant nuclear organization, and more than six DAPI-staining bodies in diakinesis nuclei, indicating a defect in chiasmata formation and presumably crossover resolution (data not shown). Differences in chromosomal structure because very apparent in diplotene and diakinesis nuclei, where we observed nuclei with pachytene-like chromosomes mixed with those that had a diplotene- or diakinesis-like organization. These phenotypes are consistent with defects in DSB repair and in accordance with previous studies(ALPI *et al.* 2003). Assessing RAD-51 foci in both alleles of *rad-54*, we observed the following averages in each meiotic stage (these are combined averages for both alleles): 1.2 foci in the mitotic zone, 1.3 foci in the transition zone, 7.9 foci in early pachytene, 18.5 foci in mid-pachytene, and 22.7 foci in late pachytene (Figure 1). Though we did not count RAD-51 foci in diplotene and diakinesis, we did observe that in *rad-54* mutants, levels of RAD-51 remained very high (nearly indistinguishable from nuclei in late pachytene) instead of decreasing dramatically as they do in wild-type animals.

However, recent studies have shown that DSB formation in *C. elegans* is governed by a feedback mechanism that responds to whether all chromosomes have received a crossover-competent repair intermediate (ROSU *et al.* 2013; STAMPER *et al.* 2013). Thus, any mutation that impedes DSB repair or crossover resolution could also instigate the formation of more DSBs. This possibility could account for the reason that, in this new analysis, we see a continual increase in RAD-51 foci number throughout all pachytene stages, instead of observing a plateau of foci number as previously reported (METS and MEYER 2009). We reasoned that perturbation of the feedback loop in *rad-54* mutants may make RAD-51 foci number in late-pachytene (which is after the peak of foci number in wild-type animals) an inaccurate assessment of DSB number. To preclude this complication, we use our mid-pachytene averages as an estimate of total DSBs formed during the state of wild-type DSB competency. In both alleles, mid-pachytene nuclei had an average of 18.5 foci per nucleus, with a range spanning 3 to 43 foci (Figure 1). In a complementary analysis, we traced all individual chromosomes within one nucleus in *rad-54 (tm1268)* mutants to determine the average number of RAD-51 foci per chromosome (Figure 2). The per-chromosome average of 3.1 foci indicates that each nucleus receives 18.6 foci, which corresponds well with our whole-germline analyses of RAD-51 foci.

One aspect of crossover regulation is crossover assurance, which operates to ensure that each homolog recieves at least one crossover (SHINOHARA *et al.* 2008). Rosu and colleagues demonstrated the robust nature of crossover assurance using an assay that monitors the repair

outcome at a defined DSB site in the absence of other DSBs. When chromosomes receive only one DSB, it is heavily favored to become a crossover (ROSU *et al.* 2011). This led them to conclude that a crossover assurance mechanism in *C. elegans* can operate by ensuring that each chromosome receives at least one DSB. With an average of three DSBs per chromosome, random placement of DSBs would lead to many chromosomes that lack DSBs entirely – a Poisson distribution predicts that 5% of chromosomes will have no DSBs. Since each chromosome receives at least one DSB, it is unlikely that crossover assurance is accomplished by the formation of randomly placed breaks. This suggests that an active mechanism prevents random DSB distribution to assure at least one per chromosome, which supports two levels of crossover interference: before DSB formation (since DSBs are not placed randomly) and after DSB formation (because multiple breaks per chromosome still yield only one crossover).

Three recent studies have revealed another aspect of crossover assurance, which uses feedback loops to regulate DSB formation in response to crossover formation. In *C. elegans*, two meiotic proteins, DSB-1 and DSB-2, associate with chromatin to maintain a DSB-competent state (ROSU *et al.* 2013; STAMPER *et al.* 2013). Once all chromosomes have received a DSB (or perhaps a crossover-competent repair intermediate), DSB-1 and DSB-2 are removed from chromatin to signal an end to DSB initiation (ROSU *et al.* 2013; STAMPER *et al.* 2013). In *S. cerevisiae*, ZMM proteins, which are components of the synaptonemal complex, act to limit DSB formation in wild-type cells once homologous chromosomes have successfully engaged each other, whether by synapsis or through the formation of crossover-competent repair intermediates (THACKER *et al.* 2014). Therefore, cells may monitor crossover formation to ensure that sufficient numbers of DSBs are formed to guarantee at each chromosome receives one crossover; this corresponds with the active mechanism to control DSB formation proposed in METS AND MEYER 2009.

Materials and Methods

C. elegans strains and maintenance

Strains were maintained at 20° C as described in BRENNER 1974. Experiments were conducted at 20° C. Homozygous mutant animals were derived from heterozygous balanced strains by selecting animals that lacked the dominant balancer-linked marker (GFP).

N2	Bristol wild-type
VC531	r*ad-54 (ok615) tag-157(ok615) I/hT2[qIs48] (I;III)*
TY5352	*rad-54(tm1268) I/ hT2 [qIs48] (I;III)*

Immunofluoresence

Hermaphrodites were cut at the vulva to extrude the gonads in egg buffer (25 mM HEPES pH 7.4, 118 mM NaCl, 48 mM KCl, 0.2 mM $CaCl_2$, 0.2 mM $MgCl_2$) containing 0.1% Tween-20 on coverslips. For fixation, egg buffer containing paraformaldehyde was added to sample for a final concentration of 0.8% paraformaldehyde samples were sandwiched with a Superfrost Plus slide. After five minutes, slides were frozen n in liquid nitrogen. Coverslips were cracked off and slides

were immersed in 95% ethanol at room temperature for at least five minutes. Slides were then washed three times for five minutes in phosphate-buffered saline containing 0.5% Triton-X (PBSt). Samples were incubated in a humid chamber overnight at room temperature with primary antibody solutions diluted in PBSt with 3% bovine serum albumin (BSA) and 1mM EDTA (1:125 anti-RAD-51(Alpi et al 2003); 1:250 anti-HTP-3 (MacQueen et al 2005)). After washing three times for five minutes in PBSt, samples were incubated in a humid chamber for two hours at room temperature in secondary antibody (Molecular Probes) diluted 1:200 in PBSt with 3% BSA and 1mM EDTA (anti-rabbit Alexa-488, anti-rabbit Alexa 405, or anti-guinea pig Alexa 633 (Molecular Probes)). Slides were washed three times for five minutes, mounted with SloFade with 2 mg/ml DAPI solution, and sealed with nail polish.

Image collection and analysis

Images were acquired using a Leica TCS SP2 AOBS confocal microscope. Images shown are projections of Z-stacks acquired at 0.25 um intervals for Figure 1 and at 0.08 um intervals for Figure 2.

Quantification of RAD-51 foci was performed by viewing side-by-side individual Z-stacks spanning the entire germline. A RAD-51 focus was scored if it was seen in consecutive stacks and was within or very close to the DAPI stain for that nucleus. Only fully separated foci were scored – occasionally, a RAD-51 signal would form a short track through consecutive Z-stacks, and these were scored as a single focus. Meiotic prophase zones were defined as: 1. Mitotic region, encompassing nuclei from the distal tip to the transition zone; 2. Transition Zone, encompassing nuclei with clustered, cresent-shaped chromosome organization; 3. Pachytene encompassing nuclei between the transition zone and the beginning of diplotene/diakinesis (pachytene was further divided into equal sections of early, mid-, and late regions); and 4. Diplotene/Diakinesis, which encompasses a region from where nuclei have chromosomes that begin to desynapse until the spermatheaca (counts for this region are not included in this analysis).

Chromosome axis traces

Whole-mount germlines were labeled by FISH as in Mets et al. 2009 with two oligonucleotide probes to X (right end sequence: 5'-GACTCCATCCACCAGCACTGCTTCGAGTACGACAG AAAGCACTTC-3' and center sequence 5'-TTCGCTTAGAGCGATTCCTTACCCTTAAATG GGCGCCGG-3', then stained with RAD-51 and COH-3/4 antibodies followed by secondary antibodies. Images were collected on a Leica SP2 and deconvolved with Huygens Pro software. Chromosomes were traced in 3D along the COH-3/4 –stained axis and straightened computationally in Priism.

Appendix I
Figure 1.

	ok615 (2 animals)			*tm1268* (3 animals)			wild-type (8 animals)		
meitoic stage	**average foci/nucleus**	**SEM**	**N**	**average foci/nucleus**	**SEM**	**N**	**average foci/nucleus**	**SEM**	**N**
mitotic region	1.47	0.03	309	1.00	0.01	475	0.16	0.00	1182
transition zone	0.82	0.02	501	1.77	0.01	219	0.77	0.02	1213
early pachytene	7.49	0.37	204	8.36	0.16	278	3.31	0.03	2138
mid-pachytene	18.55	0.28	202	18.50	0.04	286	4.88	0.02	2205
late pachytene	21.18	0.02	501	24.26	0.01	219	1.43	0.02	1106

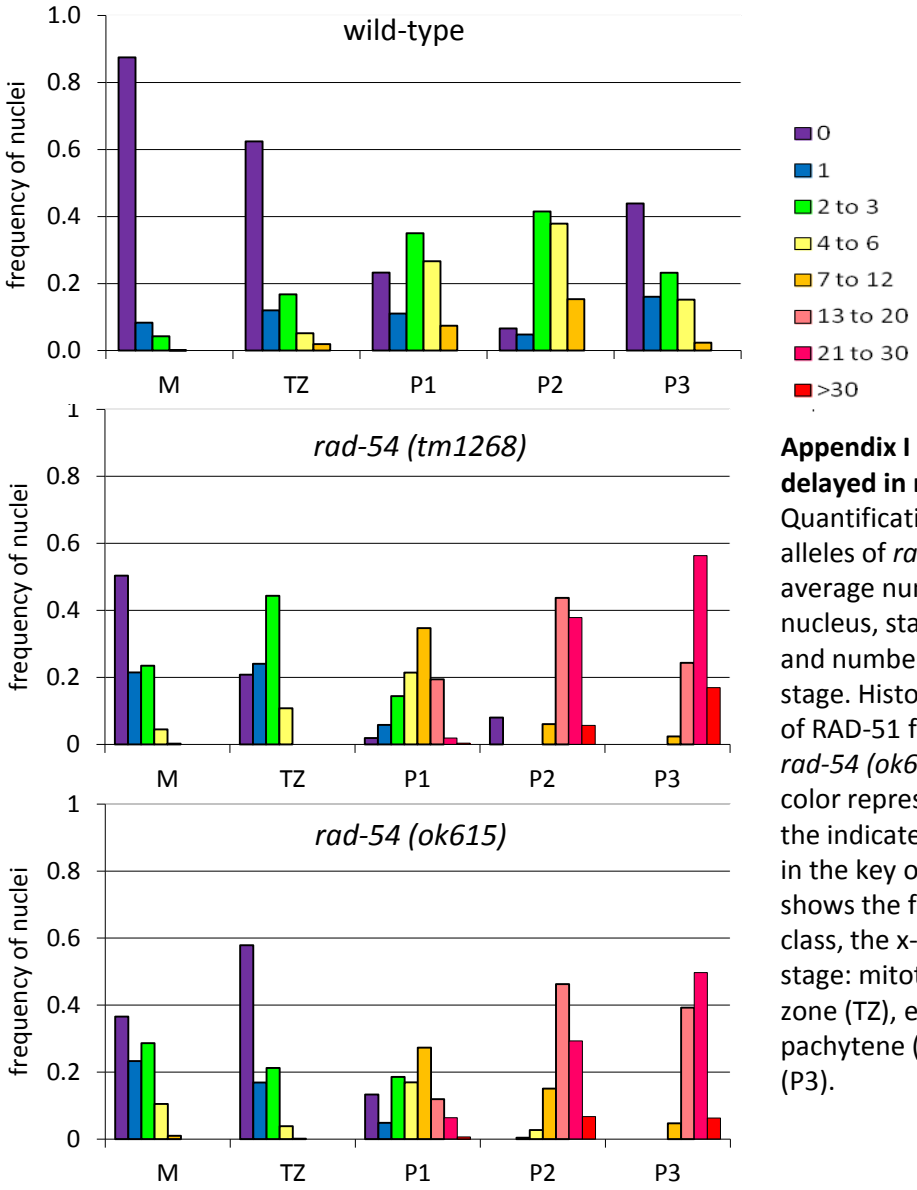

Appendix I Figure 1. DSB repair is delayed in rad-54 mutants. Quantification of RAD-51 foci in two alleles of *rad-54* mutants. Table shows average number of RAD-51 foci per nucleus, standard error of the mean, and number of nuclei assayed for each stage. Histograms show quantification of RAD-51 foci in *rad-54 (tm1268)* and *rad-54 (ok615)* mutants. Each column color represents a class of nuclei with the indicated number of foci, a shown in the key on the bottom. The y-axis shows the frequency of nuclei in each class, the x-axis shows the meiotic stage: mitotic region (M), transition zone (TZ), early pachytene (P1), mid-pachytene (P2), and late pachytene (P3).

Appendix I
Figure 2.

	chromosomes with indicated number of foci	
foci	**observed**	**expected**
0	0	10.2
1	35	31.0
2	58	47.3
3	52	48.1
4	31	36.7
5	15	22.4
6	18	11.4
7	6	5.0
8	0	1.9
9	0	0.6
total	215	

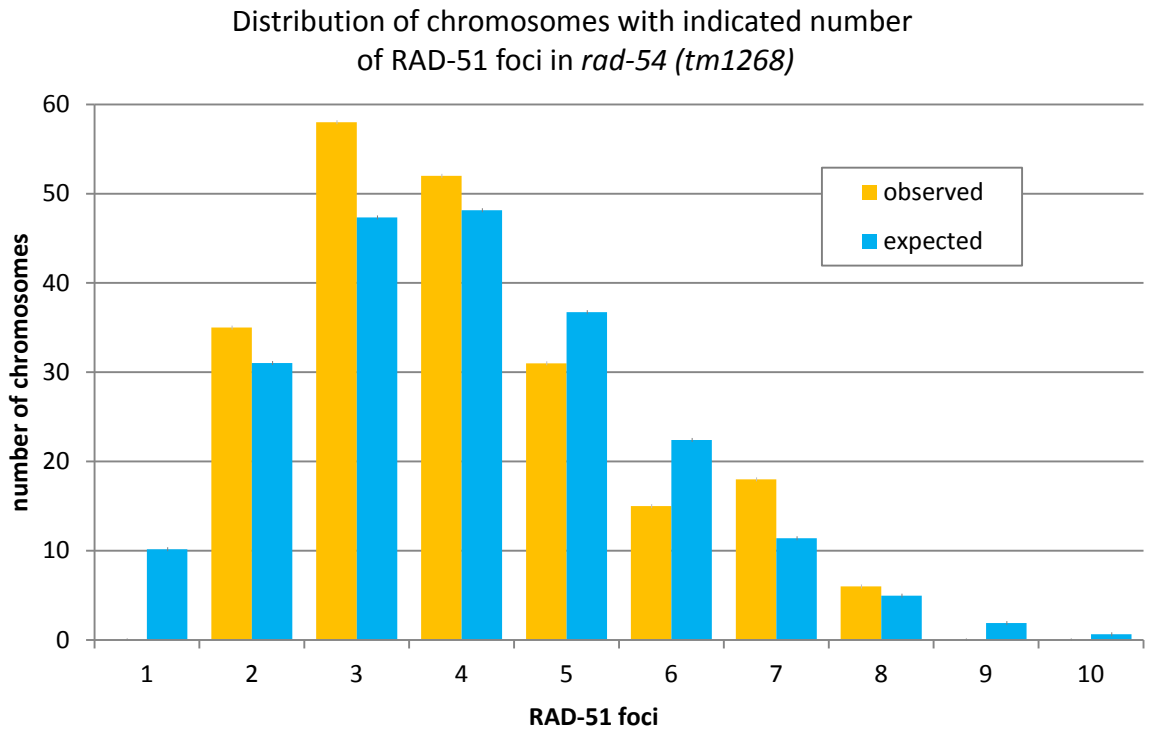

Appendix II Figure 2. When DSB repair is delayed, all chromosomes receive at least one DSB during mid-pachytene. Quantification of RAD-51 foci per chromosome in *rad-54 (tm1268)* mutants. Table shows the number of chromosomes with indicated numbers RAD-51 foci scored, and the number expected given the total number of chromosomes analyzed. Graph shows the distribution of observed and expected chromosome classes.

References

ALPI A., PASIERBEK P., GARTNER A., LOIDL J., 2003 Genetic and cytological characterization of the recombination protein RAD-51 in *Caenorhabditis elegans*. Chromosoma **112**: 6–16.

BRENNER S., 1974 The Genetics of *Caenorhabditis elegans*. Genetics **77**: 71–94.

LEMMENS B. B. L. G., TIJSTERMAN M., 2011 DNA double-strand break repair in *Caenorhabditis elegans*. Chromosoma **120**: 1–21.

METS D. G., MEYER B. J., 2009 Condensins regulate meiotic DNA break distribution, thus crossover frequency, by controlling chromosome structure. Cell **139**: 73–86.

NOTTKE A. C., BEESE-SIMS S. E., PANTALENA L. F., REINKE V., SHI Y., COLAIÁCOVO M. P., 2011 SPR-5 is a histone H3K4 demethylase with a role in meiotic double-strand break repair. Proc. Natl. Acad. Sci. U. S. A. **108**: 12805–10.

OGAWA T., YU X., SHINOHARA A., EGELMAN E. H., 2014 Similarity of the Yeast RAD51 Filament to the Bacterial RecA Filament. Science (80-.). **259**: 1896–1899.

ROSU S., LIBUDA D. E., VILLENEUVE A. M., 2011 Robust crossover assurance and regulated interhomolog access maintain meiotic crossover number. Science **334**: 1286–9.

ROSU S., ZAWADZKI K. A., STAMPER E. L., LIBUDA D. E., REESE A. L., DERNBURG A. F., VILLENEUVE A. M., 2013 The C. elegans DSB-2 protein reveals a regulatory network that controls competence for meiotic DSB formation and promotes crossover assurance. PLoS Genet. **9**: e1003674.

SHINOHARA M., GASIOR S. L., BISHOP D. K., SHINOHARA A., 2000 Tid1/Rdh54 promotes colocalization of Rad51 and Dmc1 during meiotic recombination. Proc. Natl. Acad. Sci. **97**: 10814–10819.

SHINOHARA M., OH S. D., HUNTER N., SHINOHARA A., 2008 Crossover assurance and crossover interference are distinctly regulated by the ZMM proteins during yeast meiosis. Nat. Genet. **40**: 299–309.

SOLINGER J. A., HEYER W. D., 2001 Rad54 protein stimulates the postsynaptic phase of Rad51 protein-mediated DNA strand exchange. Proc. Natl. Acad. Sci. U. S. A. **98**: 8447–53.

STAMPER E. L., RODENBUSCH S. E., ROSU S., AHRINGER J., VILLENEUVE A. M., DERNBURG A. F., 2013 Identification of DSB-1, a protein required for initiation of meiotic recombination in *Caenorhabditis elegans*, illuminates a crossover assurance checkpoint. PLoS Genet. **9**: e1003679.

THACKER D., MOHIBULLAH N., ZHU X., KEENEY S., 2014 Homologue engagement controls meiotic DNA break number and distribution. Nature **510**: 241–246.

Appendix II

SUMO depletion affects meiotic chromosome structure without affecting DSBs or crossovers

Appendix II
SUMO depletion affects meiotic chromosome structure without affecting DSBs or crossovers

Introduction

The small ubiquitin-related modifier (SUMO) protein is a post-translational covalent modification involved in many cellular processes, including protein stability, transport, and cell-cycle progression. Sumoylation, the covalent attachment of SUMO to a target protein, is regulated by an enzymatic process that resembles ubiquitination (GEISS-FRIEDLANDER and MELCHIOR 2007). With the activity of a SUMO-specific protease, sumoylation is a reversible process – proteins regulated by this modification have *in vivo* populations that fluctuate between their sumoylated and unmodified forms. Although higher eukaryotes have multiple SUMO paralogs, *C. elegans* has one SUMO homolog, SMO-1 (MELCHIOR 2000; JONES *et al.* 2002; GLYNN *et al.* 2004).

Sumoylation is important for proper meiotic development across a wide-range of taxa (WATTS and HOFFMANN 2011). In *S. cervisiae*, several components of the synaptonemal complex are sumoylated or recognize SUMO-modification on other proteins. One component of the synaptonemal complex, Zip3, is a SUMO E3 ligase thought to sumoylate Red1, a component of chromosome axes (and a lateral element of the synaptonemal complex). Syumoylated Red1, in turn, allows for proper loading and polymerization of Zip1, the central element of the synaptonemal complex (HOOKER and ROEDER 2006; CHENG *et al.* 2006). Similarly, in *S. pombe*, sumoylation is required for linear element formation, an analogous structure that to the synaptonemal complex: mutants with aberrant sumoylation do not form linear elements and have significantly fewer crossovers (SPIREK *et al.* 2010). The association between sumoylation and the synaptonemal complex is also true in *C. elegans,* where the homolog to Zip3 is ZHP-3, a pro-crossover molecule. ZHP-3 acts to coordinate crossover formation with remodeling of the synaptonemal complex during diakinesis, perhaps in coordination with SUMO (BHALLA *et al.* 2008).

Here, we report meiotic defects in animals with reduced concentrations of the SUMO peptide. We see that *smo-1(RNAi)* mutants have longer chromosome axes than wild-type animals, but this increase in axis length does not correlate with an increase in DSB number or crossover formation.

Results and Discussion

To investigate the role of sumoylation during meiosis, we depleted SUMO by RNAi against the *C. elegans* SUMO peptide, SMO-1, and analyzed chromosome axis length, DSB formation, and crossovers. Germlines in *smo-1(RNAi)* mutants were slightly disordered, with a few nuclei exhibiting transition zone morphology (representation the leptotene-zygotene stage of meiosis) in the region of the germline where nuclei should be in pachytene (data not shown). This defect might be a reflection of delayed entry into pachytene for some nuclei. However, by diakinesis, all nuclei look normal; the

delayed nuclei could have eventually transitioned into pachytene or they could have been culled through apoptosis.

Axis length in *smo-1 (RNAi)* mutants is nearly 50% longer than axes in wild-type animals (6.3 um in *smo-1* mutants and 4.3 um in wild-type animals, $p < 1e-11$) (Figure 1). We observe a wider range of axis lengths in *smo-1 (RNAi)* mutants than we observed in wild-type animals (a spread of 5.9 um in *smo-1* mutants, versus 3 um in wild-type). This might be caused by variable penetrence of the RNAi condition; alternatively, it could be a consequence of sumoylation affecting multiple interacting components of chromosome axes.

In animals depleted of condensin, axis length is correlated with the formation of extra DSBs (METS and MEYER 2009). To determine whether this was also true in *smo-1(RNAi)* mutants, we performed immunofluoresence against RAD-51, a cytological marker for DSBs (ALPI *et al.* 2003). In wild-type animals, RAD-51 foci appear during leptotene-zygotene, reach a peak during pachytene with an average of 4.9 foci per nucleus, and disappear by the end of diplotene (Figure 2). Despite their drastic increase in axis length, *smo-1(RNAi)* mutants did not have significantly different numbers of RAD-51 foci during mid-pachytene. Although we did not see more DSBs forming during pachytene, we did observed differences in the mitotic region and earlier stages of meiosis. *smo-1(RNAi)* mutants had a slight increase in RAD-51 foci in the mitotic region of the germline, as well as in the transition zone, where nuclei are in the leptotene and zygotene stages of meiosis. This indicates that when SMO-1 is depleted, DSBs formation begins slightly earlier during meiosis. The presence of more DSBs in the mitotic region could indicate a defect in the repair of DSBs that arise during replication. However, since this assay only captures the subset of DSBs present at the time of sample fixation, it might miss some effects of SMO-1 depletion on DSB formation or the timing of their repair.

In accordance with the lack of an DSB increase in *smo-1(RNAi)* mutants, we observed no crossover increase in this background (Figure 3). Although crossover classes did not significantly differ between wild-type animals and *smo-1(RNAi)* mutants, we did observe a few chromosomes with two crossovers, which could indicate a slight disruption of crossover regulation. Additionally, crossover distribution in *smo-1(RNAi)* mutants was altered very slightly when compared to that in wild-type animals, with more crossovers forming on the right end of Chromosome X (Figure 3).

In summary, depleting the SUMO peptide drastically increases axis length without creating more DSBs or crossovers. We find it interesting that depleting SMO-1 can have a large effect on chromosome axes without concomitantly increasing DSB number. This increase in axis length must be effected in a different manner that the increase observed in animals depleted of condensin, which correlates with an increase in DSBs and crossovers. However, the lack of in DSBs and also crossovers in *smo-1*mutants supports the hypothesis that increasing the numbers of DSBs can result in more crossovers (METS and MEYER 2009).

Materials and Methods

C. elegans strains and maintenance

Strains were maintained at 20° C as described in BRENNER 1974. Experiments were conducted at 20° C. Males were generated by heat-shocking at 37° C for one hour and maintained via crosses.

N2	Bristol wild-type
CB4856	Hawaiian wild-type

RNA interference

Bacteria carrying an Ahringer feeding library plasmid expressing double strand RNA to *smo-1* were grown overnight at 37° C in Luria broth with 50 ug/ml ampicillin (KAMATH and AHRINGER 2003). The inducing agent isopropyl-B-D-thiogalactopyranoside (IPTG) was added after about twelve hours to a final concentration of 4mM, and cultures were grown for an additional two hours. Cultures were spun down and plated onto agar plates containing 1mM IPTG and 1ug/ml carbinocillin, then incubated at 25° C for twelve hours. For germline dissections, wild-type young adult hermaphrodites were added to *smo-1* RNAi plates and kept at 20° C. After laying embryos for twelve hours, parents were removed. Once progeny reached young adult stage, they were dissected as described below. For the crossover assay, wild-type young adult males were mated with CB4856 L4 stage hermaphrodites on *smo-1* RNAi plates. L4 stage hybrid F1 progeny were then crossed with CB4856 young adult males on *smo-1* RNAi plates.

Genetic crosses to generate mutants for crossover assay

After six days, F1 hermaphrodites (resulting from the cross described above) were sacrificed for genotyping by PCR to identify individuals that were heterozygous for two markers on Chromosome X (since the cross construction would have allowed no recombination from the Bristol X chromosome before the F1 generation). F2 males from hermaphrodites with the desired genotype were then picked into lysis buffer and frozen for use in the crossover assay.

Hybrid wild-type F1 hermaphrodites (containing one Bristol chromosome and one Hawaiian chromosome) were obtained by crossing CB4856 males into N2 hermaphrodites. F1 hybrids were mated to CB4856 males and genotyped as described above. F2 males from F1 hermaphrodite with the desired genotype were picked into lysis buffer and frozen for use in the crossover assay.

Snip-SNP crossover assay

Analysis of crossovers was performed by PCR on single-worm lysates using six SNP markers and indicated restriction digestions. Primer sequences, restriction endonucleases, and map position for each marker are listed in Table 1.

Table 1. snip-SNP markers used in crossover assay

	map position	primer sequence (5' to 3')	restriction enzyme	N2 fragments (bp)	CB4856 fragments (bp)

Chr X A	-19	GGTATCCGATCCCTTCAACAAG TGGCAAAACACATCCCTGTG	BspHI	208, 156	364
Chr X C	-11.1	TCGTGGCACCATAAAAGTG GATTCAGATCAAACAGAGGTGG	DraI	243	128, 115
Chr X E	10.1	GGCTCTGAGAAACCAACAAG TGTTTGCGATGACGTGTCAG	BfuCI	318, 149	467
Chr X F	20.8	CGAGCAGAGATGCAGAGTTCTCAACTG CGACCTGAAAGATGTGAGGTTCCTTATC	HaeIII	280, 300	580

Germline dissection and immunofluoresence

Hermaphrodites were cut at the vulva to extrude the gonads in egg buffer (25 mM HEPES pH 7.4, 118 mM NaCl, 48 mM KCl, 0.2 mM $CaCl_2$, 0.2 mM $MgCl_2$) containing 0.1% Tween-20 on coverslips. For fixation, egg buffer containing paraformaldehyde was added to sample for a final concentration of 0.8% paraformaldehyde samples were sandwiched with a Superfrost Plus slide. After five minutes, slides were frozen n in liquid nitrogen. Coverslips were cracked off and slides were immersed in 95% ethanol at room temperature for at least five minutes. Slides were then washed three times for five minutes in phosphate-buffered saline containing 0.5% Triton-X (PBSt). Samples were incubated in a humid chamber overnight at room temperature with primary antibody solutions diluted in PBSt with 3% bovine serum albumin (BSA) and 1mM EDTA (1:125 anti-RAD-51(Alpi et al 2003); 1:250 anti-HTP-3 (MacQueen et al 2005)). After washing three times for five minutes in PBSt, samples were incubated in a humid chamber for two hours at room temperature in secondary antibody (Molecular Probes) diluted 1:200 in PBSt with 3% BSA and 1mM EDTA (anti-rabbit Alexa-488, anti-rabbit Alexa 405, or anti-guinea pig Alexa 633 (Molecular Probes)). Slides were washed three times for five minutes, mounted with SloFade with 2 mg/ml DAPI solution, and sealed with nail polish.

Image collection and analysis

Images were acquired using a Leica TCS SP2 AOBS confocal microscope. Images shown are projections of Z-stacks acquired at 0.08 um intervals for Figure 1 and 0.25 um intervals for Figure 2.

Quantification of RAD-51 foci was performed by viewing side-by-side individual Z-stacks spanning the entire germline. A RAD-51 focus was scored if it was seen in consecutive stacks and was within or very close to the DAPI stain for that nucleus. Only fully separated foci were scored – occasionally, a RAD-51 signal would form a short track through consecutive Z-stacks, and these were scored as a single focus. Meiotic prophase zones were defined as: 1. Mitotic region, encompassing nuclei from the distal tip to the transition zone; 2. Transition Zone, encompassing nuclei with clustered, cresent-shaped chromosome organization; 3. Pachytene encompassing nuclei between the transition zone and the beginning of diplotene/diakinesis (pachytene was further divided into equal sections of early, mid-, and late regions); and 4. Diplotene/Diakinesis, which encompasses a region from where nuclei have chromosomes that begin to desynapse until the spermatheaca (counts for this region are not included in this analysis).

Chromosome axis traces

Whole-mount germlines were labeled by FISH as in Mets et al. 2009 with two oligonucleotide probes to X (right end sequence: 5'-GACTCCATCCACCAGCACTGCTTCGAGTACGACAG AAAGCACTTC-3' and center sequence 5'-TTCGCTTAGAGCGATTCCTTACCCTTAAATG GGCGCCGG-3', then stained with RAD-51 and COH-3/4 antibodies followed by secondary antibodies. Images were collected on a Leica SP2 and deconvolved with Huygens Pro software. Chromosomes were traced in 3D along the COH-3/4 –stained axis and straightened computationally in Priism.

Appendix II
Figure 1.

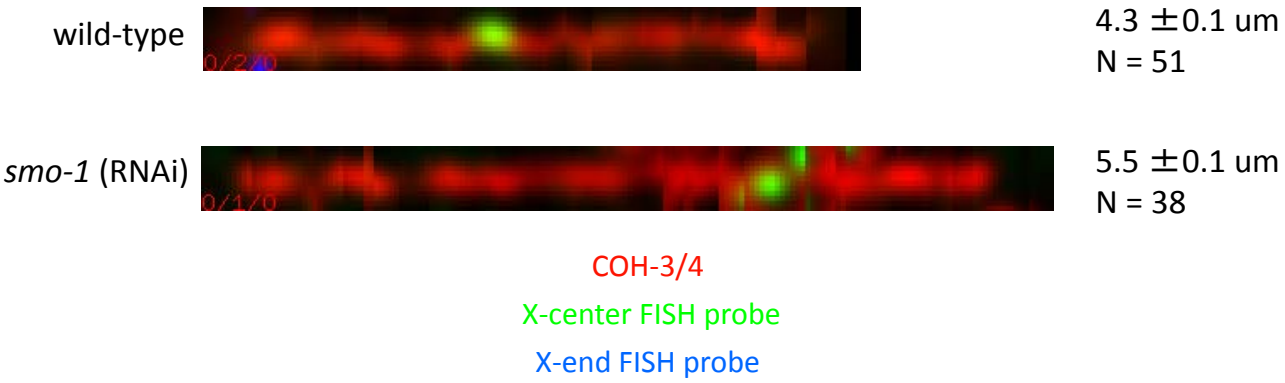

Appendix II Figure 1. Axis length is extended in animals depleted of the SUMO peptide. Computationally straightened X chromosome axes are displayed horizontally, labeled for axis protein COH-3/4 (red), a center X FISH probe (green), and a right end X FISH probe (blue). The scale bar represents 1 micron.

Appendix II
Figure 2.

meitoic stage	wild-type (8 animals) average foci/nucleus	SEM	N	*smo-1* (RNAi) (3 animals) average foci/nucleus	SEM	N
mitotic region	0.16	0.00	1182	1.01	0.03	463
transition zone	0.77	0.02	1213	1.41	0.04	466
early pachytene	3.31	0.03	2138	3.25	0.14	244
mid-pachytene	4.88	0.02	2205	4.38	0.19	191
late pachytene	1.43	0.02	1106	2.64	0.16	162

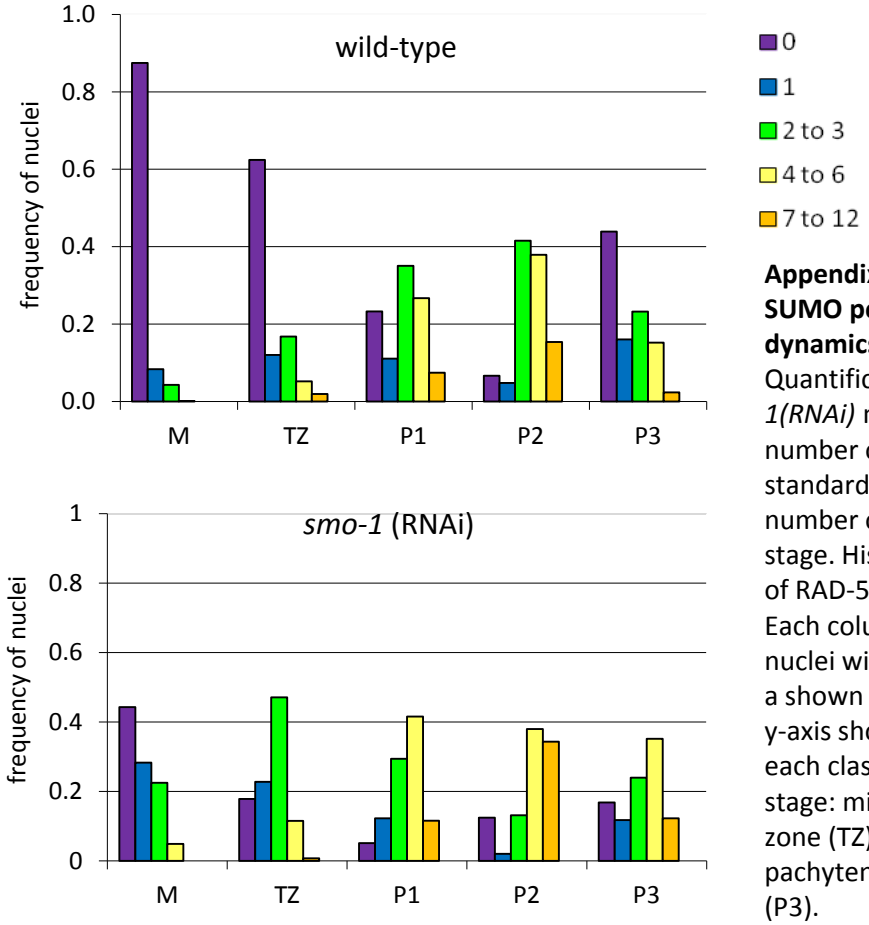

Appendix II Figure 2. Depletion of the SUMO peptide does not affect DSB dynamics during pachytene. Quantification of RAD-51 foci in *smo-1(RNAi)* mutants. Table shows average number of RAD-51 foci per nucleus, standard error of the mean, and number of nuclei assayed for each stage. Histograms show quantification of RAD-51 foci in *smo-1(RNAi)* mutants. Each column color represents a class of nuclei with the indicated number of foci, a shown in the key on the bottom. The y-axis shows the frequency of nuclei in each class, the x-axis shows the meiotic stage: mitotic region (M), transition zone (TZ), early pachytene (P1), mid-pachytene (P2), and late pachytene (P3).

Appendix II
Figure 3a.

Chr. X genotype	recomb	3-CO	2-CO	1-CO	0-CO	N	3-CO	2-CO	1-CO	0-CO
WT	0.52	0	0	45	51	96	0.00	0.00	0.52	0.59
smo-1 (RNAi)	0.53	0	2	49	45	96	0.00	0.02	0.51	0.47

Appendix II
Figure 3b.

Chr. X genotype	A to C	C to E	E to F	recomb
WT	0.15	0.26	0.12	0.52
smo-1 (RNAi)	0.11	0.23	0.19	0.53

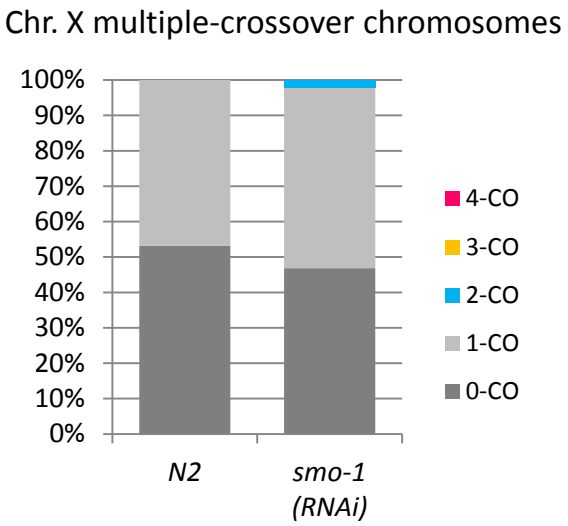

Appendix II Figure 3. Depletion of the SUMO peptide does not affect crossovers on Chromosome X. (a) Crossover frequency for *smo-1(RNAi)* mutants using four genetic markers on Chromosome X. Shown are map distance; chromosomes that received either two, one, or no crossovers; and N values for meiotic products assayed. Frequencies were calculated by the formula (number of crossovers in each class)/(total meiotic products assayed). Asterisks indicate statistical significance of chromosome class distribution between *smo-1* mutants and wild-type animals: **P*<0.05, ***P*<0.01, ****P*<0.001, and *****P*<0.0001 by the Fisher's exact test. (b) Two visual representations of crossovers formed: crossover frequencies for each interval assayed and a stacked histogram of chromosomes that received the indicated number of crossovers. For each genotype, crossover frequencies (numbers in the colored boxes) were calculated by the formula (number of crossovers in each class)/(total meiotic products assayed). Box colors indicate the relative recombination frequency compared to untreated wild-type animals; key is shown to the right. The histogram of multiple-crossover chromosomes has each class of crossovers represented by the color in the key shown to the right.

References

ALPI A., PASIERBEK P., GARTNER A., LOIDL J., 2003 Genetic and cytological characterization of the recombination protein RAD-51 in *Caenorhabditis elegans*. Chromosoma **112**: 6–16.

BHALLA N., WYNNE D. J., JANTSCH V., DERNBURG A. F., 2008 ZHP-3 acts at crossovers to couple meiotic recombination with synaptonemal complex disassembly and bivalent formation in *C. elegans*. PLoS Genet. **4**: e1000235.

BRENNER S., 1974 The Genetics of *Caenorhabditis elegans*. Genetics **77**: 71–94.

CHENG C.-H., LO Y.-H., LIANG S.-S., TI S.-C., LIN F.-M., YEH C.-H., HUANG H.-Y., WANG T.-F., 2006 SUMO modifications control assembly of synaptonemal complex and polycomplex in meiosis of *Saccharomyces cerevisiae*. Genes Dev. **20**: 2067–81.

GEISS-FRIEDLANDER R., MELCHIOR F., 2007 Concepts in sumoylation: a decade on. Nat. Rev. Mol. Cell Biol. **8**: 947–56.

GLYNN E. F., MEGEE P. C., YU H.-G., MISTROT C., UNAL E., KOSHLAND D. E., DERISI J. L., GERTON J. L., 2004 Genome-wide mapping of the cohesin complex in the yeast *Saccharomyces cerevisiae*. PLoS Biol. **2**: E259.

HOOKER G. W., ROEDER G. S., 2006 Report A Role for SUMO in Meiotic Chromosome Synapsis. Curr. Biol. **16**: 1238–1243.

JONES D., CROWE E., STEVENS T. A., CANDIDO E. P. M., 2002 Functional and phylogenetic analysis of the ubiquitylation system in *Caenorhabditis elegans*: ubiquitin-conjugating enzymes, ubiquitin-activating enzymes, and ubiquitin-like proteins. Genome Biol. **3**: RESEARCH0002.

KAMATH R. S., AHRINGER J., 2003 Genome-wide RNAi screening in Caenorhabditis elegans. Methods **30**: 313–321.

MELCHIOR F., 2000 SUMO--nonclassical ubiquitin. Annu. Rev. Cell Dev. Biol. **16**: 591–626.

METS D. G., MEYER B. J., 2009 Condensins regulate meiotic DNA break distribution, thus crossover frequency, by controlling chromosome structure. Cell **139**: 73–86.

SPIREK M., ESTREICHER A., CSASZAR E., WELLS J., MCFARLANE R. J., WATTS F. Z., LOIDL J., 2010 SUMOylation is required for normal development of linear elements and wild-type meiotic recombination in *Schizosaccharomyces pombe*. Chromosoma **119**: 59–72.

WATTS F. Z., HOFFMANN E., 2011 SUMO meets meiosis: an encounter at the synaptonemal complex: SUMO chains and sumoylated proteins suggest that heterogeneous and complex interactions lie at the centre of the synaptonemal complex. Bioessays **33**: 529–37.